THE IMPORTANCE OF A COASTAL EMBAYMENT FOR MIGRATING HUMPBACK WHALE MOTHER-CALF GROUPS: CHARACTERISING MOVEMENT PATTERNS USING GEOSPATIAL METHODS

Alexandra Jones

A thesis submitted to fulfil the requirements for the degree of

Doctor of Philosophy

School of Geosciences
Faculty of Science
The University of Sydney

2023

STATEMENT OF ORIGINALITY

This is to certify that to the best of my knowledge, the content of this thesis is my own work. This thesis has not been submitted for any degree or other purposes.

I certify that the intellectual content of this thesis is the product of my own work and that all the assistance received in preparing this thesis and sources have been acknowledged.

Alexandra Jones, 13 March 2023

ACKNOWLEDGEMENTS

This thesis would not have come together over the last five years without the help and support of many people. Firstly, I would like to thank my primary supervisor, Eleanor Bruce. This PhD has been a rollercoaster and I'm not sure I would be here submitting without your continued support, encouragement, and practical advice. I couldn't have asked for a better mentor and role model. Thank you to Doug Cato for always finding the time to share your breadth of whale knowledge with me, and to Kevin Davies for your insights into remote sensing and technical expertise.

I would like to thank the volunteers who assisted during long fieldwork periods and without whom this thesis could not have happened. This includes Alessandra Cani, Andrea Mendez-Bye, David Lorieux, Duncan Morton, Euan Smith, Evie Hyland, Gaby Genty, Kelly Coffin, Kennadie Haigh, Lisa McComb, Matt Clements, Nathan Angelakis, and Nicci Kennedy. With special thanks to Natasha Garner for assisting in all three field seasons and becoming a great friend. My favourite moments from this PhD have been in the field and I have all of you to thank for that. I also need to thank Scott Sheehan, Jeremy Randle, and Eric Kniest for their technical field support. Thank you to Glenn Maybury and the rest of the staff at Dolphin Watch Cruises for being so accommodating.

I am particularly thankful to my friends (the already Dr's and soon to be Dr's) who have been fellow PhD students over the last few years, including Claire Rowe, Elizabeth Duncan, Hannah Della-Bosca, Jamie Simpson, Kia Ferrell, Nicola Perry, and Rich Grainger. Your friendship, mutual understanding, and laughter has been a great support through this PhD.

I also need to thank Iver Cairns and the rest of my CUAVA colleagues for support over the years and introducing me to a world of drones and CubeSats. Thank you to friends and colleagues in the School of Geosciences. To Tommy Fellowes for your friendship and daily check-ins, especially in the last month. To Tom Savage and Bill Pritchard for support in ensuring I was able to complete my final field season. And to Tom Hubble for providing me the opportunity of a lifetime spending six weeks on the RV Investigator. An experience I will never forget!

I would like to thank my parents, Helen and Phil, and sister, Kate, for their constant support. I'm glad you now all know what a cetacean is. And finally, to my partner Matt. Thank you for your unwavering support and always being there for me (and being a fellow whale nerd).

ABSTRACT

Humpback whale populations that migrate along Australian coastlines each year have rapidly increased in population size since modern whaling. This population growth has been associated with increased presence and activity of humpback whales in coastal embayments along the Australian coastlines, particularly mother-calf groups who use the sheltered waters to conserve energy. However, growing numbers in nearshore areas also increases the potential for disturbance from Defence, recreational and commercial activities. The disturbance of resting mothers and calves may have longer term implications for calf growth during key development stages. Jervis Bay is a coastal embayment in which increased numbers of mother-calf groups have been observed in the last two decades and is also an area of significant anthropogenic activity. This thesis aims to assess the significance of Jervis Bay to humpback whale groups using novel survey methods. The movement patterns in the Bay are characterised and compared with that observed for humpback whales migrating south offshore. During the peak timing for humpback whales passing Jervis Bay in 2018, 2019, and 2021, land-based, boat-based, and unoccupied aerial vehicle (UAV) survey methods were conducted. Results showed that a disproportionately high percentage of groups entering the Bay contained a calf and that travel of mother-calf groups in the Bay was significantly slower and less directed than movements of these groups offshore. Resting and nurturing behaviour was observed in aerial footage. These findings support the argument for identifying Jervis Bay as a resting ground for mother-calf humpback whale groups of the east Australia (substock E1) population. With improved understanding of their behaviour and movement in the Bay, there is a need to monitor and manage increased anthropogenic activities during the southern migration season.

Post-processing methods and thermal infrared sensors to improve current whale detection methods were evaluated. Detection of marine animals using UAV-captured images is impacted by attenuation of visible light as it passes through the water column. Correction methods, used widely in remote sensing studies to enhance the detection of underwater substrate and benthic habitats, can be applied to improve the detection of submerged animals. A modified version of Lyzenga's water column correction was applied to UAV images over humpback whale groups. Using RGB sensors, commonly used

in marine wildlife surveys, the performance of three depth-invariant band pairs (i.e., red/green, red/blue, green/blue) were examined for improving visibility, contrast, and edge definition. Findings demonstrate the optimal band pair combination will be dependent on the depth of the whale.

Thermal infrared images can enhance the contrast between a whale and their surrounds, particularly in low light conditions, to improve detection rates. The whale detection capabilities of three UAV-mounted sensors with synchronous visual and thermal capture were reviewed. Thermal sensor resolution had a significant impact on the detection of the direct whale cues (i.e. the body on the surface), with only the higher resolution sensors detecting a contrast. However, the lowest resolution sensor was able to detect the thermal gradient of a whale's footprint on the surface after the whales were observed in visual images. Although these sensors were not a viable option to replace visual sensors for whale detection, they can be used in simultaneous data capture to enhance whale detection rates and extend the availability of observation time.

Unlike thermal detection from a UAV, thermal detection systems from near-horizontal platforms (i.e., ship or shore) can provide continuous observation. Methods for improving thermal imaging systems for round-the-clock detection of cetaceans were investigated. A field study to assess the thermal capabilities of three different sensors for detecting bottlenose dolphins was conducted to review the influence of sensor resolution, detector temperature, and spectral range on detection rates. Cetacean cues at distances $\sim$ 1km were clearly detected from a very high resolution (1280 x 1024) cryogenically cooled sensor in calm, clear conditions.

Jervis Bay, a semi-enclosed embayment, provides a resting ground for humpback whale mother-calf groups on the southern migration pathway. Critical resting and nurturing behaviours were observed prior to their 3,500 km migration to the Antarctic feeding grounds. Recognition of the importance of key marine habitats for migrating cetacean species highlights the need to understand and monitor for the potential impacts of increased anthropogenic activity and development of our oceans, including offshore mining, shipping, and naval operations. Emergent sensor technology and remote sensing

approaches can provide novel, accurate and resource effective methods for cetacean monitoring.

AUTHORSHIP ATTRIBUTION STATEMENT

List of co-authors:

Eleanor Bruce (EB)
Doug Cato (DC)
Kevin P. Davies (KD)
Tomonori Hu (TH)
KC Wong (KW)
Scott Sheehan (SS)
Mark Bishop (MB)

This thesis is based on the following four papers:

Paper 1 (Chapter 2): Jones, A., Bruce, E., Cato, D. H. (2023). Characterising resting patterns of mother-calf humpback whale groups in a semi-enclosed embayment along the Australian east coast migration pathway, *Scientific Reports, 13,* 14702. https://doi.org/10.1038/s41598-023-41856-1

I co-designed this study in collaboration with my co-authors. I collected and analysed the data and wrote the manuscript. All co-authors provided revision for intellectual content and critical feedback on manuscript drafts.

Paper 2 (Chapter 3): Jones, A., Bruce, E., Davies, K. P., Cato, D. H. (2022). Enhancing UAV images to improve the observation of submerged whales using a water column correction method. *Marine Mammal Science*. https://doi.org/10.1111/mms.12994

This chapter provides complete Introduction, Methods, Results, Discussion unlike the publication which is a Note. The published Note is provided in Appendix A.

I co-designed this study in collaboration with my co-authors. I collected and analysed the data and wrote the manuscript. All co-authors revision for intellectual content and critical provided feedback on manuscript drafts.

Paper 3 (Chapter 4) of this thesis is being prepared for submission for publication. I co-designed this study with EB, KD, DC. I collected and analysed the data and wrote the manuscript. All co-authors provided revision for intellectual content and critical feedback on manuscript drafts.

Paper 4 (Chapter 5): Jones, A., Bruce, E., Cato, D. H., Hu, T., Davies, K. P., Wong, K., Sheehan, S., Bishop, M., Optimising the use of thermal infrared imaging for mitigating impacts of cetacean and human interactions: a review and case study, *in review, Ecosphere*.

I co-designed this study in collaboration with EB, DC, TH, KW. Technical support was provided by KD, SS, and MB. I collected data with TH, and SS. All co-authors provided revision for intellectual content and critical feedback on manuscript drafts.

In addition to the statements above, in cases where I am not the corresponding author of a published item, permission to include the published material has been granted by the corresponding author.

Alexandra Jones,

13 March 2023

As supervisor for the candidature upon which this thesis is based, I can confirm that the authorship attribution statements above are correct.

Eleanor Bruce,

13 March 2023

TABLE OF CONTENTS

ABBREVIATIONS

AI	Artificial Intelligence
EAC	East Australian Current
EPBC	Environment Protection and Biodiversity Conservation Act 1999
FLIR	Forward Looking Infrared
IMUs	Inertial Measurement Units
IUCN	International Union for Conservation of Nature
IWC	International Whaling Commission
LWIR	Longwave infrared (8 – 12 μm)
M2EA	DJI Mavic 2 Enterprise Advanced
M2ED	DJI Mavic 2 Enterprise Dual
M600 Pro	DJI Matrice 600 Pro
MC	Mother and calf humpback whale group
MCE	Mother, calf, and escort humpback whale group
MSL	Mean sea level
MWIR	Mid-wave infrared (3 – 5 μm)
NIR	Near-infrared
NUC	Non-uniformity correction
RGB	Red-green-blue sensors (visual)
ROI	Region of interest
SST	Sea surface temperature
TIR	Thermal infrared
UAV	Unoccupied aerial vehicle
VADAR	Visual Detection and Ranging at sea
VHR	Very high resolution

1 THESIS INTRODUCTION

1.1 HUMPBACK WHALE MIGRATION PATTERNS

The humpback whale (*Megaptera novaeangliae*) is a cosmopolitan species, found in all oceans of the world. These whales undertake one of the most extensive mammalian annual migrations between high-latitude summer feeding areas and low-latitude winter breeding and calving areas (Dawbin, 1966; Rasmussen et al., 2007; Stevick et al., 2011). The International Whaling Commission (IWC) currently recognises seven breeding stocks (IWC, 1998) (A – G ; Figure 1). They are classified according to their distributions in winter breeding areas: (A) east coast of South America; (B) west coast of Africa; (C) east coast of South Africa, Africa and western Indian ocean; (D) west coast of Australia; (E) east coast of Australia and western Pacific Ocean; (F) south central Pacific Ocean; and (G) west coast of South America. All seven breeding stocks, excluding the isolated Arabian Sea Population (known as 'Group X'; Mikhalev, 1997; Pomilla et al., 2014), with each stock undertaking well-documented seasonal migrations (Dawbin, 1966). The Northern and Southern Hemisphere populations remain mostly distinct, although some gene flow between populations has been identified (Baker et al., 1994; Schmitt et al., 2014).

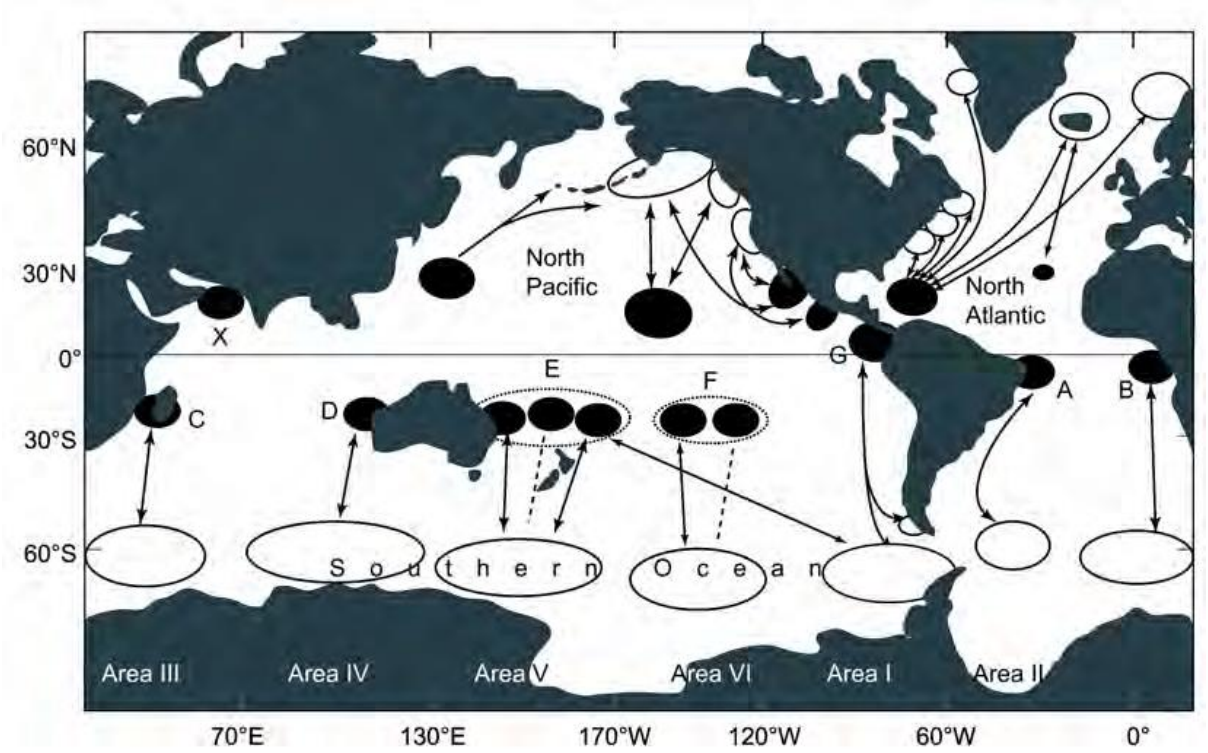

Figure 1. Geographic distribution of humpback whale populations globally illustrating IWC stock structure. Migration from high latitude feeding grounds (empty ellipses) to low latitude breeding grounds (filled ellipses) and known (solid line) and assumed (broken line) migration paths are shown. Area's I – VI denote Antarctic feeding areas (Donovan, 1991). Figure taken from Olavarría (2008).

The timing of both the northbound and southbound migrations are temporally staggered by age, sex, and reproductive status. The first whales to migrate from the feeding to the breeding grounds are yearlings and lactating females, followed by immature whales, mature males and resting females (Chittleborough, 1965; Dawbin, 1966). This pattern is mirrored for the southern migration. Non-lactating females are the first to leave the breeding grounds, followed by immature males and females, mature males, and finally lactating females with their newly born calves (Dawbin, 1966; Craig et al., 2003; Franklin, 2012).

During the migration, there is distinct temporal and geographic separation of breeding, feeding, and resting activities. From late autumn the humpback whales migrate to low latitudes where they predominantly engage in breeding and calving during the winter and early spring months before migrating south to the feeding grounds (Chittleborough,

1965). The extensive migration is likely driven by the warmer waters of the breeding grounds, providing calves an environment in which to conserve energy and prioritise growth and development (Clapham, 2001; Rasmussen et al., 2007). Feeding is largely absent during the migration and time spent on the breeding grounds, with whales relying on stored energy reserves acquired on the seasonal feeding grounds. However, supplemental feeding has been observed off south-east Australia (Owen et al., 2015; Pirotta et al., 2021), South Africa (Barendse et al., 2010; Findlay et al., 2017), and South America (Pinto de sa Alves et al., 2009).

During the southbound migration, lactating females and nursing calves have shown a preference for resting in calm, sheltered waters (Franklin et al., 2011; Bejder et al., 2019). This behaviour is considered beneficial for mothers who can reduce their energy consumption during lactation, by avoiding the open oceanographic conditions, and consequently provide greater maternal energetic investment (milk transfer) to their nursing calf (Bejder et al., 2019). Christiansen et al. (2016) used UAV-captured aerial images to determine lactating mothers in better body condition (greater width and girth) produced calves in better body condition. They proposed that during gestation and lactation, females in poor condition will prioritise their own body condition over that of their calf. Increased energetic investment results in larger calves that will be stronger, faster, and more resilient to environmental variations, such as reduced food supply (Christiansen et al., 2016; Christiansen et al., 2018). This has direct implications for a successful migration returning to nutrient rich colder polar feeding grounds.

In Australian waters, resting behaviour has been observed on the migratory corridor (Noad & Cato, 2007), but previous research has focused more on large open embayments south of the breeding grounds. Two well researched sites are Hervey Bay on the east coast (Corkeron et al., 1994; Chaloupka et al., 1999; Franklin et al., 2011; Stack et al., 2019), and Exmouth Gulf on the west coast (Bejder et al., 2019; Ejrnæs & Sprogis, 2021; Sprogis & Waddell, 2022). High proportions of mother-calf groups have also been observed in Jervis Bay, towards the southern end of east coast of Australia (Bruce et al., 2014) which differs from these other sites as it is a semi-enclosed embayment.

Humpback whales are the most extensively studied whale species, particularly in relation to population structure, distribution, and migratory movements. In the Northern Hemisphere, research has been concentrated on their breeding grounds where water is typically calm and relatively shallow, such as off Hawaii (Herman et al., 2011; Cartwright et al., 2012; Craig et al., 2014). This is likely because most humpback whales in the Northern Hemisphere migrate across deep open oceans that are difficult to access, limiting research on these animals. In the Southern Hemisphere, a significant proportion of the migrations occur in predominantly coastal waters before the oceanic section south of the continents. Substock populations D and E1 migrate along the continental shelf along west and east coast of Australia, respectively (Figure 1). This provides an opportunity to research these population mid-migration, and obtain a sound understanding of their distributions, migratory corridors and timings, and apparent rates of population growth (Paterson et al., 1994; Corkeron & Brown, 1995; Jenner et al., 2001; Salgado Kent et al., 2012; Noad et al., 2019).

1.2 CONSERVATION STATUS OF HUMPBACK WHALES IN AUSTRALIAN WATERS

Modern whaling began in Australian waters in 1912 (Chittleborough, 1965). This and substantial unreported Soviet whaling in the Southern Ocean substantial reduced population numbers. When whaling ceased in 1963, populations were thought to be as low as 3.5-5% of pre-whaling numbers (Bannister & Hedley, 2001). Numbers on the east coast may have been as few as 100 (Paterson et al., 1994) and less than 300 on the west coast (Bannister & Hedley, 2001). Despite this, populations on both coasts have made remarkable recovery, increasing at rates of about 11.0% (95% confidence interval (CI) 10.6–11.3%) from 1984 – 2015 for the east coast, with no evidence this rate is slowing down (Salgado Kent et al., 2012; Noad et al., 2019). The most recent population estimate of the east coast population by Noad et al. (2019), who conducted land surveys in 2007, 2010 and 2015, predicted the absolute abundance and rate of recovery of this population to be 24,545 (95% CI 21,631 – 27,851). The west coast, population estimates ranged from 26,100 (95% CI 20,152 – 33,272) from Salgado Kent et al. (2012) who used aerial surveys to 34,290 (95% CI 27,350 - 53,50) Hedley et al. (2020), who used aerial and land surveys. Both studies acknowledged potential data limitations, including a limited number of

samples, not accounting for perception bias, and restricted view from land surveys.

In Australia, the Environmental Protection and Biodiversity Conservation (EPBC) Act 1999 is the primary legislation protecting humpback whales. The EPBC Act protects all cetaceans within the Australian Whale Sanctuary that encompasses all Commonwealth waters, from the state limit (three nautical miles) to the Australian Exclusive Economic Zone boundary (200 nautical miles). In February 2022, the Threatened Species Scientific Committee removed humpback whales as a vulnerable species from Australia's EPBC Act list of threatened species, resulting from strong population recovery and no current threats to prevent population growth. They are still protected under the EPBC Acts as a listed Migratory Species and under EPBC Act Division 3, where it is an offence to interfere with a cetacean. In New South Wales, humpback whales are protected by the Biodiversity Conservation Regulation 2017 (Division 2.1). Any activity within Australian waters that is likely to have an impact on a humpback whale requires government approval and permits. In 2018, humpback whale populations globally, except for the endangered Arabian Sea population, had their status changed from 'vulnerable' to least 'least concern' on the International Union for Conservation of Nature (IUCN) Red List.

1.3 STUDY AREA

Fieldwork for this thesis was undertaken in Jervis Bay (35° 07' S, 150° 42' E), a semi-enclosed embayment situated along the New South Wales (NSW) coastline (Figure 2). Jervis Bay is roughly 3,500 km north of Antarctic feeding grounds and 1,500 km south of the breeding and calving grounds for the E1 population, in the waters of the Great Barrier Reef (Smith et al., 2012). In addition to a migratory humpback whale population, a population of resident Indo-Pacific bottlenose dolphins (*Tursiops aduncus*) inhabit Jervis Bay (Möller et al., 2002).

Humpback whales were abundant in Jervis Bay during the migration season prior to industrial whaling and whaling operations commenced in the Bay during 1912 - 1913 (Dakin, 1938). Over the last two decades, citizen science data and opportunistic sightings have highlighted increased sighting of mother-calf groups in Jervis Bay, highlighting the area as potential resting ground (Sheehan & Blewitt, 2013; Bruce et al., 2014). Jervis Bay

encompasses the multiple-use Jervis Bay Marine Park, waters of the Booderee National Park and part of the East Australian Defence Exercise Area, an important naval training site. Within the Bay, there is significant naval activity, commercial whale watching, recreational boating and fishing. Since 2019 two commercial dive operators have acquired permits to operate swim-with-activities. The strong recovery of the E1 population, has increased the potential for spatio-temporal overlap with anthropogenic activities.

Compared to other identified resting areas, Jervis Bay is geomorphologically distinct. The relatively narrow entrance to the Bay (3.7 km) runs northeast-southwest, parallel to the migration, compared to that of the entrances of Hervey Bay (70 km) and Exmouth Gulf (50 km) that run west-east, facing the migration. The southbound migration closely follows the Australian coastline (Paterson & Paterson, 1989; Gales et al., 2010), requiring whales to change their direction of travel to enter Jervis Bay. Furthermore, the elevation of the Point Perpendicular headland (75 m), at the northern end of Jervis Bay provides an optimal vantage point to track whales entering the Bay, their movements in the Bay and allows for a comparison with whales migrating south offshore (within 10km).

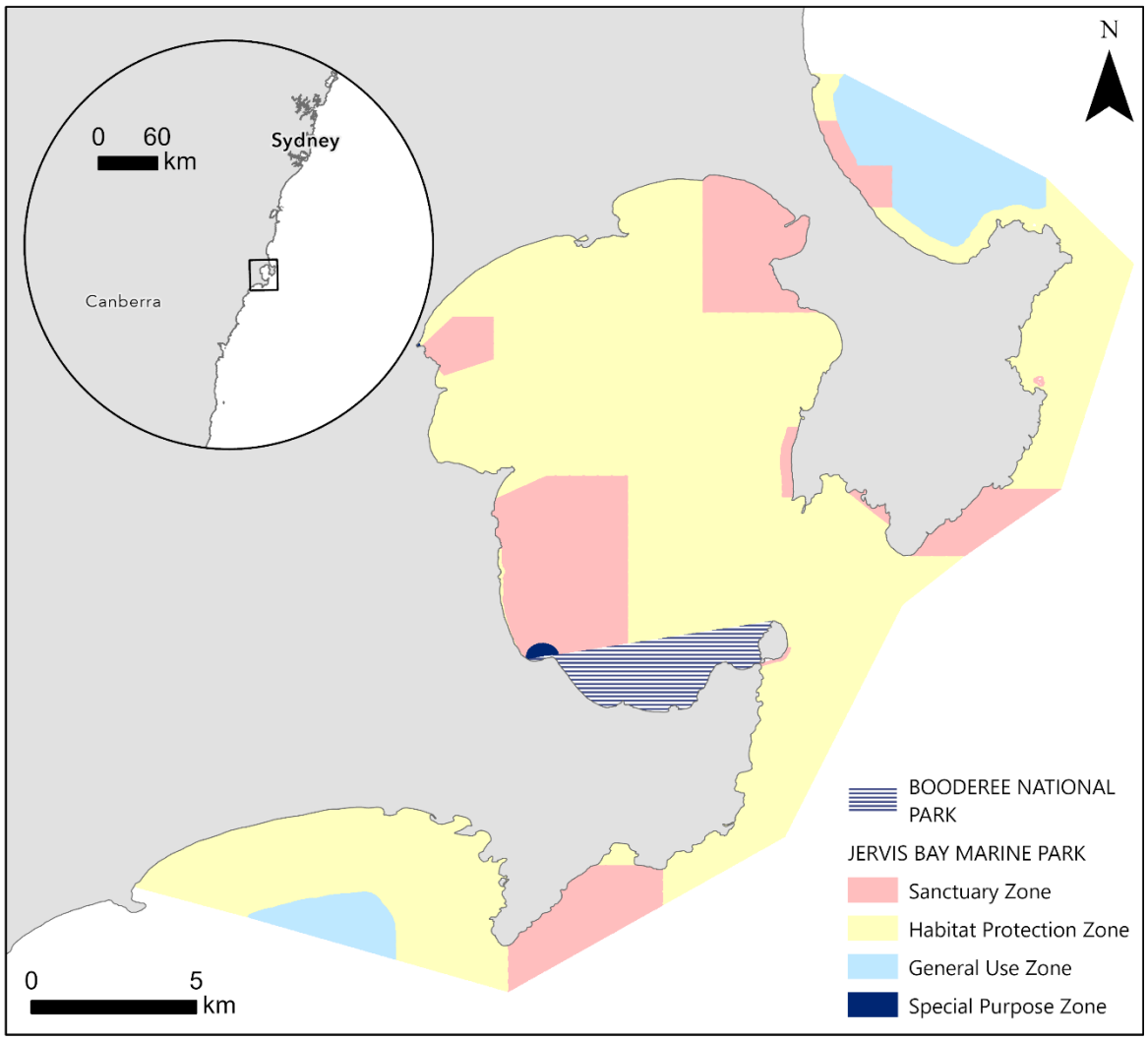

Figure 2. Jervis Bay study site illustrating the zoning of the Jervis Bay Marine Park and Booderee National Park

1.4 NOVEL METHODS FOR MONITORING WHALE MOVEMENTS

Highly mobile cetacean species are notoriously difficult to study as they spend large periods of time underwater, surface for short periods, have unpredictable movement patterns, and are often found in remote habitats that extend over large areas. Cetacean survey methods traditionally involve obtaining counts of whales from land-based vantage points, piloted aerial surveys or boat surveys (Eberhardt et al., 1979). These methods can be very labour intensive, involving long hours of recording, and as whales' range over large geographic areas, these survey methods can be costly and inefficient. These methods are also subject to visibility biases, which includes both availability bias, when an animal is present in the study area but not available to the observer (e.g., submerged), and perception bias, where an animal is available for detection but missed by observers

or an automated detection algorithm (Marsh & Sinclair, 1989; Brack et al., 2018).

The past decade has seen an emergence of new and innovative methods for surveying cetacean species, particularly remote aerial methods providing large spatial coverage without the risks associated with piloted surveys. The use of sub-metre very high resolution (VHR) satellites for whale detection have been proposed and demonstrated as a relatively cost-effective method, for one-off abundance counts in surveying relatively large areas (Fretwell et al., 2014; Cubaynes et al., 2018; Guirado et al., 2019). However, these methods are only useful if the timing of data collection is not critical. Additionally, satellites cannot provide imagery at the temporal and spatial scales required to explore whale movements or behaviour, and many satellite systems are subject to atmospheric and weather effects (e.g., cloud contamination, Johnston, 2019). Importantly, species can still be difficult to detect, and detection probabilities remain unknown (Fretwell et al., 2014; Cubaynes et al., 2018).

Unoccupied aerial vehicles (UAVs), commonly referred to as drones, provide a cost-effective, unobtrusive solution with flexibility unlike other survey approaches, including land- or boat-based methods or other aerial surveys. Larger, fixed-wing models have been used for transect surveys (Hodgson et al., 2013) and demonstrated to have detection probabilities for humpback whales within the range of piloted aerial surveys (Hodgson et al., 2017). Smaller UAV models, such as quadcopters, are particularly beneficial as they can be flown opportunistically (Horton et al., 2019), launched from small boats (Christiansen et al., 2016), and hover over target animal(s). This is particularly advantageous for marine research when surveying vagile and often elusive animals.

In the last decade there has been an increase in marine studies utilizing UAVs (Schofield et al., 2019), which allows for novel insights on the abundance (Hodgson et al., 2017), behaviour (Torres et al., 2018; Fiori et al., 2019), and body condition (Christiansen et al., 2016; Hodgson et al., 2020) of marine wildlife. The potential of UAVs for behavioural studies has been recognised (Nowacek et al., 2016), although research to date has been somewhat limited (Schofield et al., 2019). Continuous, unbiased observations are required to study animal behaviour and boat-based surveys are restricted to horizontally

observing a snapshot of the animals' behaviour at the surface. Torres et al. (2018) demonstrated that UAVs provided three times more observational capacity than boat-based observations when surveying gray whales (*Eschrichtius robustus*), finding UAVs provided longer observation of all primary behaviour states (travelling, foraging, socializing, and rest) and documented fine-scale foraging and social behaviour. Similarly, Fiori et al. (2019) found socializing and nurturing behaviours of humpback whales on a calving ground in Tonga were significantly underrepresented in boat-based observations compared to UAV-based data. Currently the main limitation is the restricted flight time of small UAV models (e.g., 30 minutes for the Phantom 4). However, rapid advancements in UAV platform technology resulting in increased flight times will likely improve their flexibility for marine surveys in the near future (Nowacek et al., 2016).

1.4.1 Sensors

While UAV surveys to date have primarily focused on the visual red-green-blue (RGB) spectrum for detection of marine wildlife, advances in the miniaturisation of payloads provide flexibility for mounting alternative sensors, including thermal infrared (TIR), multispectral (four or more bands), and hyperspectral (30 to hundreds of narrow bands), onto many UAV models. These sensors have the potential to overcome limitations encountered with traditional RGB imagery where animal detection is subject to light levels and requires clear contrast between an animal and their surrounds (Hinke et al., 2022). The effectiveness of thermal sensors for discriminating animals in low-light conditions has been well established in terrestrial environments, for example, the night-time detection of arboreal mammals (Kays et al., 2018; Witt et al., 2020; McCarthy et al., 2022). Thermal sensors for detecting cetaceans are limited to detecting animals on the surface, as infrared waves are rapidly attenuated in water. Previous research from UAV-mounted thermal sensors has focused on detection of cetacean footprints, where sub-surface fluke strokes result in a cold anomaly on the surface (Churnside et al., 2009; Florko et al., 2021; Lonati et al., 2022), and whale health through biometric measurements (Horton et al., 2019). From near-horizontal platforms (e.g., off a vessel) thermal infrared imaging has been used to detect the warm exhalations of cetacean in the distance (Zitterbart et al., 2013; Smith et al., 2020; Zitterbart et al., 2020).

Multispectral and hyperspectral sensors have the potential to be particularly beneficial

in marine environments as wavelengths can be selected to improve detection of submerged objects. Colefax et al. (2021) used a UAV fitted with a hyperspectral sensor (400 – 1000nm) to identify the optimal wavelengths for detecting submerged marine fauna, finding the key wavelengths to be 474 – 594 nm provided the greatest contrast. Similarly, Fretwell et al. (2014) identified wavelengths of 400-450 nm (coastal band) from a VHR multispectral satellite image to be optimal for detecting southern right whales (*Eubalaena australis*), due to increased water penetration. Detection of submerged objects using optical remote sensing from satellites and UAVs is also subject to sun glint contamination which is present in an image when the solar irradiance is reflected directly toward the sensor (specular reflectance) due to the relative orientation of the water surface. Sun glint causes high brightness in images, reduces the signal-to-noise ratio, and reduces the accuracy of remotely sensed observation data (Muslim et al., 2019). Sun glint is influenced by sun position, viewing angle and sea surface state (Kay et al., 2009). The effects of sun glint can be avoided by selectively choosing to survey in the early morning or later afternoon. Whilst this can be effective for static objects, including the mapping of nearshore benthos, this is not always feasible for moving and wide-ranging marine vertebrates. In the absence of flexibility in survey timing, there are robust methods to remove sun glint contamination from multispectral images (Hedley et al., 2005; Martin et al., 2016). Whilst these techniques are effective for multi-spectral images containing a NIR band, they are not suitable for images containing only red, green and blue bands. This limits the use of sun glint removal techniques for most off-the-shelf UAVs, fitted with RGB cameras, commonly used in wildlife studies (Anderson & Gaston, 2013).

1.5 THESIS AIMS AND OVERVIEW

The broader objective of this research is to evaluate multiple methods for optimising the detection of whales and to characterise the movement patterns of humpback whales during the southern migration (Figure 3).

Chapter 2 provides the first comprehensive analysis of the behaviour and movement parameters of mother-calf humpback whale groups in Jervis Bay. These movement patterns, including speed and linearity, are compared with whales travelling south on the

main migratory pathway. This is achieved using predominantly traditional survey techniques, including land-based theodolite surveys and boat-based photo-identification methods. Additionally, UAV surveys are employed to provide insight on fine-scale behaviour in Jervis Bay, particularly resting and nurturing behaviour.

Chapters 3 and 4 investigate different methods to overcome limitations commonly encountered in aerial surveys, particularly perception bias. Chapter 3 presents a modified water column correction for enhancing UAV-acquired visual image data to improve the contrast of whales on the water surface and submerged near the surface. A modified version of Chapter 3 is published in *Marine Mammal Science* (Jones et al., 2022). Chapter 4 evaluates the effectiveness of thermal sensors for detecting direct and indirect whale cues on the surface through comparison of simultaneous acquired UAV thermal and visual image data. This chapter also considers trade-offs between different UAV-borne thermal sensors for optimising whale detections taken at oblique or nadir angles, including sensor resolution, radiometric capability, and model size.

Chapter 5 evaluates how thermal infrared sensor configuration will influence cetacean detection rates from near-horizontal ship and shore platforms for cetacean mitigation from human activities. In this chapter the capabilities of three thermal that differ in sensitivity, resolution, spectral range, and detector temperature, for discriminating bottlenose dolphin from surrounding waters are assessed. The current state of knowledge on the use of thermal imaging for the long-range detection of cetaceans from ship and shore systems is reviewed to provide a detailed understanding of how the characteristics of cetacean cues and environmental conditions will influence automated detection methods.

Chapter 6 provides a general discussion and synthesis of the key research findings. Future research priorities and conservation implications of this research are presented.

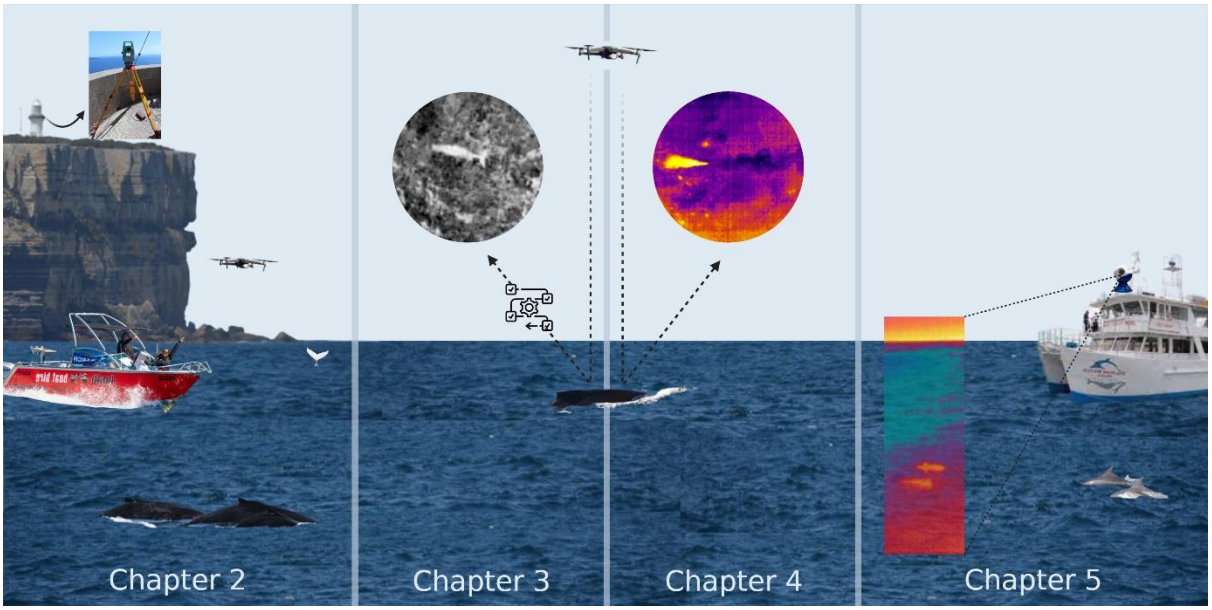

Figure 3. Overview of methods used in each data chapter. All images were taken during fieldwork in Jervis Bay. Created with BioRender.com.

1.6 REFERENCES

Anderson, K., & Gaston, K. J. (2013). Lightweight unmanned aerial vehicles will revolutionize spatial ecology. *Frontiers in Ecology and the Environment, 11*(3), 138-146. doi:10.1890/120150

Baker, C., Slade, R., Bannister, J., Abernethy, R., Weinrich, M., Lien, J., . . . Vasquez, O. (1994). Hierarchical structure of mitochondrial DNA gene flow among humpback whales Megaptera novaeangliae, world-wide. *Molecular Ecology, 3*(4), 313-327.

Bannister, J., & Hedley, S. (2001). Southern Hemisphere group IV humpback whales: their status from recent aerial survey. *Memoirs-Queensland Museum, 47*(2), 587-598.

Barendse, J., Best, P. B., Thornton, M., Pomilla, C., Carvalho, I., & Rosenbaum, H. C. (2010). Migration redefined? Seasonality, movements and group composition of humpback whales *Megaptera novaeangliae* off the west coast of South Africa. *African Journal of Marine Science, 32*(1), 1-22. doi:10.2989/18142321003714203

Bejder, L., Videsen, S., Hermannsen, L., Simon, M., Hanf, D., & Madsen, P. T. (2019). Low energy expenditure and resting behaviour of humpback whale mother-calf pairs highlights conservation importance of sheltered breeding areas. *Scientific Reports, 9*(1), 771. doi:10.1038/s41598-018-36870-7

Brack, I. V., Kindel, A., Oliveira, L. F. B., & Scales, K. (2018). Detection errors in wildlife abundance estimates from Unmanned Aerial Systems (UAS) surveys: Synthesis, solutions, and challenges. *Methods in Ecology and Evolution, 9*(8), 1864-1873. doi:10.1111/2041-210x.13026

Bruce, E., Albright, L., Sheehan, S., & Blewitt, M. (2014). Distribution patterns of migrating humpback whales (*Megaptera novaeangliae*) in Jervis Bay, Australia: A spatial analysis using geographical citizen science data. *Applied Geography, 54*, 83-95. doi:10.1016/j.apgeog.2014.06.014

Cartwright, R., Gillespie, B., Labonte, K., Mangold, T., Venema, A., Eden, K., & Sullivan, M. (2012). Between a rock and a hard place: habitat selection in female-calf humpback whale (*Megaptera novaeangliae*) Pairs on the Hawaiian breeding grounds. *PLoS One, 7*(5), e38004. doi:10.1371/journal.pone.0038004

Chaloupka, M., Osmond, M., & Kaufman, G. (1999). Estimating seasonal abundance trends and survival probabilities of humpback whales in Hervey Bay (east coast Australia). *Marine Ecology Progress Series, 184*, 291-301.

Chittleborough, R. (1965). Dynamics of two populations of the humpback whale, *Megaptera novaeangliae* (Borowski). *Marine and Freshwater Research, 16*(1), 33-128.

Christiansen, F., Dujon, A. M., Sprogis, K. R., Arnould, J. P., & Bejder, L. (2016). Noninvasive unmanned aerial vehicle provides estimates of the energetic cost of reproduction in humpback whales. *Ecosphere, 7*(10), e01468.

Christiansen, F., Vivier, F., Charlton, C., Ward, R., Amerson, A., Burnell, S., & Bejder, L. (2018). Maternal body size and condition determine calf growth rates in southern right whales. *Marine Ecology Progress Series, 592*, 267-281.

Churnside, J., Ostrovsky, L., & Veenstra, T. (2009). Thermal Footprints of Whales. *Oceanography, 22*(1), 206-209. doi:10.5670/oceanog.2009.20

Clapham, P. (2001). Why do baleen whales migrate? A response to Corkeron and Connor. *Marine Mammal Science, 17*(2), 432-436.

Colefax, A. P., Kelaher, B. P., Walsh, A. J., Purcell, C. R., Pagendam, D. E., Cagnazzi, D., & Butcher, P. A. (2021). Identifying optimal wavelengths to maximise the detection rates of marine fauna from aerial surveys. *Biological Conservation, 257*, 109102.

Corkeron, P., & Brown, M. (1995). Pod characteristics of migrating humpback whales (Megaptera novaeangliae) off the east Australian coast. *Behaviour, 132*(3-4), 163-179.

Corkeron, P. J., Brown, M., Slade, R. W., & Bryden, M. M. (1994). Humpback whales, *Megaptera novaeangliae* (Cetaceaa: Balaenopteridae), in Hervey Bay, Queensland. *Wildlife Research, 21*(3), 293-205.

Craig, A., Gabriele, C., Herman, L., & Pack, A. (2003). Migratory timing of humpback whales (*Megaptera novaeangliae*) in the central North Pacific varies with age, sex and reproductive status. *Behaviour, 140*(8-9), 981-1001.

Craig, A. S., Herman, L. M., Pack, A. A., & Waterman, J. O. (2014). Habitat segregation by female humpback whales in Hawaiian waters: avoidance of males? *Behaviour, 151*(5), 613-631.

Cubaynes, H. C., Fretwell, P. T., Bamford, C., Gerrish, L., & Jackson, J. A. (2018). Whales from space: Four mysticete species described using new VHR satellite imagery. *Marine Mammal Science, 35*(2), 466-491. doi:10.1111/mms.12544

Dakin, W. J. (1938). *Whalemen Adventurers: The Story of Whaling in Australian Waters and*

Other Southern Seas Related Thereto, from the Days of Sails to Modern Times: Angus & Robertson.

Dawbin, W. (1966). The seasonal migratory cycle of humpback whales. In: *Whales, dolphins and porpoises*. University of California Press, Berkeley. 145 – 170.

Donovan, G. (1991). A review of IWC stock boundaries. *Report of the International Whaling Commission. Special Issue 13.* , 39-68.

Eberhardt, L. L., Chapman, D. G., & Gilbert, J. R. (1979). A review of marine mammal census methods. *Wildlife Monographs*(63), 3-46.

Ejrnæs, D. D., & Sprogis, K. R. (2021). Ontogenetic changes in energy expenditure and resting behaviour of humpback whale mother–calf pairs examined using unmanned aerial vehicles. *Wildlife Research, 49*(1), 34-45.

Findlay, K. P., Seakamela, S. M., Meyer, M. A., Kirkman, S. P., Barendse, J., Cade, D. E., . . . Wilke, C. G. (2017). Humpback whale "super-groups" - A novel low-latitude feeding behaviour of Southern Hemisphere humpback whales (*Megaptera novaeangliae*) in the Benguela Upwelling System. *PLoS One, 12*(3), e0172002. doi:10.1371/journal.pone.0172002

Fiori, L., Martinez, E., Bader, M. K. F., Orams, M. B., & Bollard, B. (2019). Insights into the use of an unmanned aerial vehicle (UAV) to investigate the behavior of humpback whales (*Megaptera novaeangliae*) in Vava'u, Kingdom of Tonga. *Marine Mammal Science, 36*(1), 209-223. doi:10.1111/mms.12637

Florko, K. R. N., Carlyle, C. G., Young, B. G., Yurkowski, D. J., Michel, C., & Ferguson, S. H. (2021). Narwhal (*Monodon monoceros*) detection by infrared flukeprints from aerial survey imagery. *Ecosphere, 12*(8). doi:10.1002/ecs2.3698

Franklin, T. (2012). The social and ecological significance of Hervey Bay Queensland for eastern Australian humpback whales (*Megaptera novaeangliae*). *Southern Cross University, Lismore, Australia*.

Franklin, T., Franklin, W., Brooks, L., Harrison, P., Baverstock, P., & Clapham, P. (2011). Seasonal changes in pod characteristics of eastern Australian humpback whales (*Megaptera novaeangliae*), Hervey Bay 1992-2005. *Marine Mammal Science, 27*(3), E134-E152. doi:10.1111/j.1748-7692.2010.00430.x

Fretwell, P. T., Staniland, I. J., & Forcada, J. (2014). Whales from space: counting southern right whales by satellite. *PLoS One, 9*(2), e88655.

doi:10.1371/journal.pone.0088655

Gales, N., Double, M. C., Robinson, S., Jenner, C., Jenner, M., King, E., . . . Paton, D. (2010). Satellite tracking of Australian humpback (*Megaptera novaeangliae*) and pygmy blue whales (*Balaenoptera musculus brevicauda*). *White paper presented to the Scientific Committee of the International Whaling Commission*.

Guirado, E., Tabik, S., Rivas, M. L., Alcaraz-Segura, D., & Herrera, F. (2019). Whale counting in satellite and aerial images with deep learning. *Scientific Reports, 9*(1), 14259.

Hedley, J. D., Harborne, A. R., & Mumby, P. J. (2005). Technical note: Simple and robust removal of sun glint for mapping shallow-water benthos. *International Journal of Remote Sensing, 26*(10), 2107-2112. doi:10.1080/01431160500034086

Hedley, S. L., Bannister, J. L., & Dunlop, R. A. (2020). Abundance estimates of Southern Hemisphere Breeding Stock 'D' humpback whales from aerial and land-based surveys off Shark Bay, Western Australia, 2008. *Journal of Cetacean Research and Management*, 209-221.

Herman, L. M., Pack, A. A., Rose, K., Craig, A., Herman, E. Y. K., Hakala, S., & Milette, A. (2011). Resightings of humpback whales in Hawaiian waters over spans of 10-32 years: Site fidelity, sex ratios, calving rates, female demographics, and the dynamics of social and behavioral roles of individuals. *Marine Mammal Science, 27*(4), 736-768. doi:10.1111/j.1748-7692.2010.00441.x

Hinke, J. T., Giuseffi, L. M., Hermanson, V. R., Woodman, S. M., & Krause, D. J. (2022). Evaluating Thermal and Color Sensors for Automating Detection of Penguins and Pinnipeds in Images Collected with an Unoccupied Aerial System. *Drones, 6*(9), 255.

Hodgson, A., Kelly, N., & Peel, D. (2013). Unmanned aerial vehicles (UAVs) for surveying marine fauna: a dugong case study. *PLoS One, 8*(11), e79556. doi:10.1371/journal.pone.0079556

Hodgson, A., Peel, D., & Kelly, N. (2017). Unmanned aerial vehicles for surveying marine fauna: assessing detection probability. *Ecological Applications, 27*(4), 1253-1267.

Hodgson, J. C., Holman, D., Terauds, A., Koh, L. P., & Goldsworthy, S. D. (2020). Rapid condition monitoring of an endangered marine vertebrate using precise, non-invasive morphometrics. *Biological Conservation, 242*, 108402. doi:https://doi.org/10.1016/j.biocon.2019.108402

Horton, T. W., Hauser, N., Cassel, S., Klaus, K. F., Fettermann, T., & Key, N. (2019). Doctor Drone: Non-invasive Measurement of Humpback Whale Vital Signs Using Unoccupied Aerial System Infrared Thermography. *Frontiers in Marine Science, 6*. doi:10.3389/fmars.2019.00466

IWC. (1998). Report of the Sub-Committee on comprehensive assessment of Southern Hemisphere humpback whales. Report of the Scientific Committee. Annex G. Report of the International Whaling Commission. (48), 170 - 182.

Jenner, K. C., Jenner, M. M., & McCabe, K. A. (2001). Geographical and temporal movements of humpback whales in Western Australian waters. *The APPEA Journal, 41*(1), 749-765.

Johnston, D. W. (2019). Unoccupied Aircraft Systems in Marine Science and Conservation. *Annual Review of Marine Science, 11*, 439-463. doi:10.1146/annurev-marine-010318-095323

Jones, A., Bruce, E., Davies, K. P., & Cato, D. H. (2022). Enhancing UAV images to improve the observation of submerged whales using a water column correction method. *Marine Mammal Science*.

Kays, R., Sheppard, J., McLean, K., Welch, C., Paunescu, C., Wang, V., . . . Crofoot, M. (2018). Hot monkey, cold reality: surveying rainforest canopy mammals using drone-mounted thermal infrared sensors. *International Journal of Remote Sensing, 40*(2), 407-419. doi:10.1080/01431161.2018.1523580

Lonati, G. L., Zitterbart, D. P., Miller, C. A., Corkeron, P., Murphy, C. T., & Moore, M. J. (2022). Investigating the thermal physiology of Critically Endangered North Atlantic right whales *Eubalaena glacialis* via aerial infrared thermography. *Endangered Species Research, 48*, 139-154. doi:10.3354/esr01193

Marsh, H., & Sinclair, D. F. (1989). Correcting for visibility bias in strip transect aerial surveys of aquatic fauna. *The Journal of wildlife management*, 1017-1024.

Martin, J., Eugenio, F., Marcello, J., & Medina, A. (2016). Automatic Sun Glint Removal of Multispectral High-Resolution Worldview-2 Imagery for Retrieving Coastal Shallow Water Parameters. *Remote Sensing, 8*(1). doi:10.3390/rs8010037

McCarthy, E. D., Martin, J. M., Boer, M. M., & Welbergen, J. A. (2022). Ground-based counting methods underestimate true numbers of a threatened colonial mammal: an evaluation using drone-based thermal surveys as a reference. *Wildlife Research*.

Mikhalev, Y. A. (1997). Humpback whales *Megaptera novaeangliae* in the Arabian Sea. *Marine Ecology Progress Series, 149*, 13-21.

Möller, L. M., S. J. Allen, & R. G. Harcourt. (2002). "Group characteristics, site fidelity and seasonal abundance of bottlenosed dolphins (Tursiops aduncus) in Jervis Bay and Port Stephens, South-Eastern Australia." *Australian Mammalogy* 24.1, 11-22.

Muslim, A. M., Chong, W. S., Safuan, C. D. M., Khalil, I., & Hossain, M. S. (2019). Coral Reef Mapping of UAV: A Comparison of Sun Glint Correction Methods. *Remote Sensing, 11*(20), 2422.

Noad, M. J., & Cato, D. H. (2007). Swimming Speeds of Singing and Non-Singing Humpback Whales during Migration. *Marine Mammal Science, 23*(3), 481-495. doi:10.1111/j.1748-7692.2007.02414.x

Noad, M. J., Kniest, E., & Dunlop, R. A. (2019). Boom to bust? Implications for the continued rapid growth of the eastern Australian humpback whale population despite recovery. *Population Ecology, 61*(2), 198-209. doi:10.1002/1438-390x.1014

Nowacek, D. P., Christiansen, F., Bejder, L., Goldbogen, J. A., & Friedlaender, A. S. (2016). Studying cetacean behaviour: new technological approaches and conservation applications. *Animal Behaviour, 120*, 235-244. doi:10.1016/j.anbehav.2016.07.019

Olavarría, C. (2008). *Population structure of Southern Hemisphere humpback whales.* Doctoral Dissertation ResearchSpace@ Auckland,

Owen, K., Warren, J. D., Noad, M. J., Donnelly, D., Goldizen, A. W., & Dunlop, R. A. (2015). Effect of prey type on the fine-scale feeding behaviour of migrating east Australian humpback whales. *Marine Ecology Progress Series, 541*, 231-244. doi:10.3354/meps11551

Paterson, R., & Paterson, P. (1989). The status of the recovering stock of humpback whales *Megaptera novaeangliae* in east Australian waters. *Biological Conservation, 47*(1), 33-48.

Paterson, R., Paterson, P., & Cato, D. H. (1994). The status of humpback whales *Megaptera novaeangliae* in east Australia thirty years after whaling. *Biological Conservation, 70*(2), 135-142.

Pinto de sa Alves, L. C., Andriolo, A., Zerbini, A., Altmayer Pizzorno, J. L., & Clapham, P. (2009). Record of feeding by humpback whales (*Megaptera novaeangliae*) in

tropical waters off Brazil. *Publications, Agencies and Staff of the US Department of Commerce*, 45.

Pirotta, V., Owen, K., Donnelly, D., Brasier, M. J., & Harcourt, R. (2021). First evidence of bubble-net feeding and the formation of 'super-groups' by the east Australian population of humpback whales during their southward migration. *Aquatic Conservation: Marine and Freshwater Ecosystems, 31*(9), 2412-2419.

Pomilla, C., Amaral, A. R., Collins, T., Minton, G., Findlay, K., Leslie, M. S., . . . Rosenbaum, H. (2014). The world's most isolated and distinct whale population? Humpback whales of the Arabian Sea. *PLoS One, 9*(12), e114162. doi:10.1371/journal.pone.0114162

Rasmussen, K., Palacios, D. M., Calambokidis, J., Saborio, M. T., Dalla Rosa, L., Secchi, E. R., . . . Stone, G. S. (2007). Southern Hemisphere humpback whales wintering off Central America: insights from water temperature into the longest mammalian migration. *Biol Lett, 3*(3), 302-305. doi:10.1098/rsbl.2007.0067

Salgado Kent, C., Jenner, C., Jenner, M., Bouchet, P., & Rexstad, E. (2012). Southern hemisphere breeding stock D humpback whale population estimates from North West Cape, Western Australia. *J. Cetacean Res. Manage., 12*(1), 29-38.

Schmitt, N. T., Double, M. C., Jarman, S. N., Gales, N., Marthick, J. R., Polanowski, A. M., . . . Jenner, M. N. (2014). Low levels of genetic differentiation characterize Australian humpback whale (*Megaptera novaeangliae*) populations. *Marine Mammal Science, 30*(1), 221-241.

Schofield, G., Esteban, N., Katselidis, K. A., & Hays, G. C. (2019). Drones for research on sea turtles and other marine vertebrates – A review. *Biological Conservation, 238*. doi:10.1016/j.biocon.2019.108214

Sheehan, S., & Blewitt, M. (2013). *Jervis Bay: an Area of Significance for Southward Migrating Humpback Whale Cow/Calf Pairs?* Paper presented at the Australian Marine Science Association (AMSA), Gold Coast, Queensland, Australia.

Smith, H. R., Zitterbart, D. P., Norris, T. F., Flau, M., Ferguson, E. L., Jones, C. G., . . . Moulton, V. D. (2020). A field comparison of marine mammal detections via visual, acoustic, and infrared (IR) imaging methods offshore Atlantic Canada. *Marine Pollution Bulletin, 154*, 111026. doi:10.1016/j.marpolbul.2020.111026

Smith, J. N., Grantham, H. S., Gales, N., Double, M. C., Noad, M. J., & Paton, D. (2012).

Identification of humpback whale breeding and calving habitat in the Great Barrier Reef. *Marine Ecology Progress Series, 447*, 259-272. doi:10.3354/meps09462

Sprogis, K. R., & Waddell, T. L. (2022). Marine mammal distribution on the western coast of Exmouth Gulf, Western Australia. *Report to the Australian Marine Conservation Society.(Aarhus University and Carijoa Marine Environmental Consulting: Rivervale, WA, Australia) p, 17*.

Stack, S. H., Currie, J. J., McCordic, J. A., Machernis, A. F., & Olson, G. L. (2019). Distribution patterns of east Australian humpback whales (*Megaptera novaeangliae*) in Hervey Bay, Queensland: a historical perspective. *Australian Mammalogy*. doi:10.1071/am18029

Stevick, P. T., Neves, M. C., Johansen, F., Engel, M. H., Allen, J., Marcondes, M. C., & Carlson, C. (2011). A quarter of a world away: female humpback whale moves 10,000 km between breeding areas. *Biology Letters, 7*(2), 299-302. doi:10.1098/rsbl.2010.0717

Torres, L. G., Nieukirk, S. L., Lemos, L., & Chandler, T. E. (2018). Drone Up! Quantifying Whale Behavior From a New Perspective Improves Observational Capacity. *Frontiers in Marine Science, 5*. doi:10.3389/fmars.2018.00319

Witt, R. R., Beranek, C. T., Howell, L. G., Ryan, S. A., Clulow, J., Jordan, N. R., . . . Roff, A. (2020). Real-time drone derived thermal imagery outperforms traditional survey methods for an arboreal forest mammal. *PLoS One, 15*(11), e0242204. doi:10.1371/journal.pone.0242204

Zitterbart, D. P., Kindermann, L., Burkhardt, E., & Boebel, O. (2013). Automatic round-the-clock detection of whales for mitigation from underwater noise impacts. *PLoS One, 8*(8), e71217. doi:10.1371/journal.pone.0071217

Zitterbart, D. P., Smith, H. R., Flau, M., Richter, S., Burkhardt, E., Beland, J., . . . Boebel, O. (2020). Scaling the Laws of Thermal Imaging–Based Whale Detection. *Journal of Atmospheric and Oceanic Technology, 37*(5), 807-824. doi:10.1175/jtech-d-19-0054.1

2 CHARACTERISING RESTING PATTERNS OF MOTHER-CALF HUMPBACK WHALE GROUPS IN A SEMI-ENCLOSED EMBAYMENT ALONG THE AUSTRALIAN EAST COAST MIGRATION PATHWAY

Jones, A., Bruce, E., Cato, D. H. (2023). Characterising resting patterns of mother-calf humpback whale groups in a semi-enclosed embayment along the Australian east coast migration pathway, *Scientific Reports, 13,* 14702.
https://doi.org/10.1038/s41598-023-41856-1

scientific reports

Check for updates

OPEN

Characterising resting patterns of mother-calf humpback whale groups in a semi-enclosed embayment along the Australian east coast migration pathway

Alexandra Jones[1,2]✉, Eleanor Bruce[1,2] & Douglas H. Cato[1,2]

On migration from low latitude breeding grounds to high latitude feeding grounds, humpback whale mothers and calves spend time resting in coastal embayments. Unlike other areas where resting has been documented, Jervis Bay, on Australia's east coast, is remote from both breeding and feeding grounds, and provides a unique opportunity to compare resting behaviour observed within a semi-enclosed embayment to observations offshore. Land-based, and UAV surveys were conducted in Jervis Bay in 2018, 2019, and 2021. We show that (i) a disproportionately high percentage of groups with a calf enter Jervis Bay during the southbound migration, (ii) travelling speeds are significantly slower in the Bay compared to offshore, indicating resting behaviour, and (iii) aerial observations highlight resting and nurturing behaviour. Subsequently, we conclude that Jervis Bay is an important area for resting mother-calf humpback whale groups. Comparison with reports of resting behaviour during migration in areas nearer the breeding grounds shows commonalities that characterise resting behaviour in mothers and calves. This characterisation will allow improved monitoring and management of humpback whales in nearshore embayments during a critical stage of calf development, particularly those with increased anthropogenic activities.

Humpback whales (*Megaptera novaeangliae*) undertake one of the most extensive mammalian annual migrations between high-latitude summer feeding areas and low-latitude winter breeding and calving areas [1–3]. This migration may be driven by the energetic benefits provided by the warm waters of breeding grounds that allow calves to conserve energy, leading to increased growth, development, and potentially future reproductive success [2,4]. Travelling to warmer waters for whales to molt their skin has also been proposed as a factor potentially driving the migration[5]. During the migration, distinct temporal, and geographic separation of activities, namely breeding/calving, resting, and feeding, is linked to functional adaptations in resource availability [6,7]. Humpback whales migrate along both the east and west coasts of Australia, to and from breeding grounds in the warm sheltered waters within the Great Barrier Reef on the east coast (International Whaling Commission (IWC) designated substock E1) [6] and on the North West Shelf on the west coast (substock D) [8]. Whales are present inside the Great Barrier Reef from June to September [6]. From here, the population migrates, ~5000 km south along a narrow migratory pathway [9] along the east Australian coastline to the nutrient rich Antarctic summer feeding grounds (IWC Antarctic Management Areas IV, V and VI). During the southbound migration females and their calves have been observed to rest in large open bays near the breeding grounds. Hervey Bay on the east coast [10–12] and Exmouth Gulf on the west coast [13,14]. Resting has also been observed in open oceanic waters off Peregian Beach [15] on the east coast, however it is generally considered that mothers and calves prefer to rest in relatively shallow, calm waters or protected embayments [16]. It has been proposed that these sheltered waters provide protection from rough seas, predators and conspecifics [17] and the calm surface conditions reduce energy consumption of lactating mothers and nursing calves [18].

The E1 subpopulation size was substantially reduced by commercial whaling, both from stations on the east Australian coast[19] and from Soviet Union whaling ships in the Southern Ocean[20]. Whaling of this subpopulation ceased off the east coast in 1962 and in the Southern Ocean in 1968, but by then the population had been reduced

[1]School of Geosciences, University of Sydney, Sydney, NSW 2006, Australia. [2]Marine Studies Institute, University of Sydney, Sydney, NSW 2006, Australia. ✉email: alexandra.jones1@sydney.edu.au

to possibly as low as 100 individuals[19]. Since then there has been a substantial recovery of this subpopulation. Population size was estimated to be about 25,500 in 2015, increasing at about 11% per annum [21]. The strong recovery of substock E1, has seen increased observations of humpback whales in coastal embayments along the southern migration pathway, including Hervey Bay, Queensland (QLD) [10–12] and Jervis Bay, New South Wales (NSW) [22].

Jervis Bay is a semi-enclosed embayment encompassing the multiple-use Jervis Bay Marine Park, waters of the Booderee National Park and part of the East Australian Defence Exercise Area, an important naval training site. In 1998, the area was declared a marine park by the NSW government based on its unique geology and oceanography, diverse habitats and ecosystems, and abundant flora and fauna. Humpback whales were abundant in Jervis Bay during the migration season prior to industrial whaling [23]. Citizen science data collected from a commercial whale watching platform between 2007 and 2010 demonstrated the prevalence of mother-calf groups within the Bay from September to November corresponding to the southern migration [22]. Whales, predominantly groups with calves, come into the Bay on the southbound migration thus geographically separating groups in the Bay from those migrating south, allowing for direct comparison of behaviour. Unlike other areas where resting has been documented previously, Jervis Bay is further from the recognised breeding grounds (~ 1500 km) almost one third of the way to the Antarctic feeding grounds which are ~ 3500 km further south. Although opportunistic feeding by sub-adult humpback whales has been observed at Eden, NSW [24], ~ 230 km south of Jervis Bay, this is linked to variable nutrient-rich upwelling events associated with the East Australian Current (EAC) and is unlikely to provide a consistent feeding area for energy intake by lactating mothers.

Previous studies have examined humpback whale movement trends and aggregations in breeding/resting grounds [13] and potential resting areas within migratory corridors [10,11,25], but there has been no systematic surveys of humpback whale usage patterns in semi-enclosed coastal embayments located at remote distances from breeding and feeding grounds. Off Australia, humpback whales follow the coastline during the migration [26,27]. Due to the geomorphic configuration of Jervis Bay, access requires humpback whales to divert from the migration direction. Whales will enter Exmouth Gulf and Hervey Bay without needing to change their course of direction. However, whales will travel south past Jervis Bay in a southwest direction and to enter the Bay need to travel in a northwest direction. Jervis Bay has a much narrower entrance (3.7 km) which runs almost parallel to the migration compared with entrances of 70 km for Hervey Bay and 50 km for Exmouth Gulf, both of which run east to west and face the oncoming migration.

Resting opportunities involving low energetic expenditure are likely critical for minimising the rate of decline in body condition of lactating females [13] and optimising calf growth during key development stages which may have implications for individual reproductive success in adulthood [2]. Additionally, in baleen whales calf growth is directly related to maternal energetic investment (milk transfer). Females with better body condition will produce larger calves who are stronger, faster and more resilient to environmental fluctuations (e.g., food shortages) [28,29]. This has direct implications for surviving the migration back to colder polar feeding grounds.

Sheltered waters along the migration pathway, as in Jervis Bay, may facilitate nursing and energy conservation allowing calves to allocate energy to growth rather than movement [30]. The fine-scale neonate humpback whale suckling behaviour of eight calves were quantified in Exmouth Gulf, Western Australia, and showed calves suckling 20.7 ± 7% of the total tagging time during which mothers were resting on the surface or submerged [13,30]. Furthermore, these studies demonstrated that lactating mothers and their calves spent considerable time resting (~ 35%).

Jervis Bay is an area of significant naval, commercial, and recreational activity. Two commercial whale watching companies operate in the Bay and since 2019, permits have been approved for two commercial dive operators to offer swim-with-whale activities. Thus, with increasing numbers of resting whales, there is increasing potential for spatio-temporal overlap with anthropogenic activities which may impact on the energy conservation of lactating mothers and their calves.

Understanding how humpback whales use Jervis Bay is critical for guiding policy and management decisions regarding commercial, military, and recreational use of this area. This paper presents a characterisation of the behaviour of mother-calf groups resting in a semi-enclosed embayment, remote from the breeding grounds, where there is clear separation from the whales travelling past the bay on the migration. We compare results with observations in other areas in which humpback whales have been observed resting along the migration pathway to identify the characteristics of resting behaviour. The specific objectives were to: (i) determine the composition of humpback whale groups entering Jervis Bay during the southern migration using systematic surveys; (ii) compare the movement patterns of mother-calf groups, including speed and linearity, in Jervis Bay with whales travelling south on the main migratory pathway; (iii) quantify the behavioural states most frequently observed in the Bay; (iv) compare the results with those from other areas to determine general characteristics of resting behaviour. Land-based theodolite surveys and unoccupied aerial vehicles (UAVs) were employed during 2018, 2019 and 2021 to meet these objectives.

Results

Land-based theodolite surveys were conducted on 23 (72%) of the scheduled survey days between 24 September and 25 October 2018, on 34 (89%) of the scheduled survey days between 30 September and 6 November 2019, and 14 (64%) of the scheduled surveys days between 6 and 27 October 2021.

Group size and composition. A total of 609 humpback whales in 326 groups were observed entering/leaving, or within, Jervis Bay and 1955 humpback whales in 1181 groups, were observed travelling southwest past Point Perpendicular without entering the Bay. Humpback whale groups observed entering/leaving or within Jervis Bay, ranged in size from one to four whales (mean ± SD = 1.9 ± 0.7). Mother-calf pairs were the

most frequently observed group composition (72%) followed by non-calf groups (15%), and mother-calf-escort groups (13%). Overall, 84% of groups that entered the Bay contained at least one calf. A total of 1181 groups were observed bypassing Jervis Bay, 22% of these groups contained a calf. A total of 507 groups containing a calf were observed, 247 of these (49%) entered/left Jervis Bay.

Three or more reliable fixes were obtained for 477 humpback whale groups. Of these, 158 groups were tracked entering/leaving, or within, Jervis Bay. Of these, 31 remained in the inshore area during observations (category 1), 57 groups entered/left the inshore area from offshore or the mouth of the Bay (category 2), and 70 groups entered/left the Bay but did not enter the inshore area (category 3). 319 groups were tracked offshore but did not enter the Bay. Groups were tracked on average for 44.3 min ± 45.9 (SD), the shortest track lasting for 10 min and the longest 247 min.

Speed and linearity of movement. Mother-calf pairs tracked in the inshore area only (category 1), had significantly slower average track speeds (Mann–Whitney U = 247, $Z = -5.015$, $p < 0.001$, 2-tailed), average net speeds (Mann–Whitney U = 95, $Z = -6.309$, $p < 0.001$, 2-tailed), and lower linearity measurements (Mann–Whitney U = 86, $Z = -6.386$, $p < 0.001$, 2-tailed) compared to mother-calf pairs migrating south offshore (category 4). The comparison of movement parameters for the four track categories are summarised in Table 1.

Assessment of the proportion of mother-calf pairs travelling in almost straight lines, displaying "strong" linearity > 0.95[31], showed that 39% of groups entering/leaving, or within, the Bay displayed strong linearity compared to 68.2% of groups travelling offshore. For groups that entered Jervis Bay, 30.1% had a linearity score below 0.5, suggesting meandering behaviour, compared to 3.5% of groups that did not enter the Bay. Of the groups that were tracked only in the inshore area (category 1), one (< 5%) had a linearity > 0.95 while 52% were < 0.5.

Mother-calf pair groups spent considerably more time travelling at speeds < 1 km/h, indicating resting or drifting behaviour [15], within Jervis Bay compared to groups offshore (Fig. 1). Categories 1 and 3 demonstrated a clear preference (> 30% of the time) for travelling at speeds < 1 km/h. Whales in category 2 spent 48.7% of the time travelling at speeds 2–4 km/h. Offshore (category 4), whales showed a peak distribution of travelling at speeds 3.01–4 km/h (24.6% of the time). Offshore calf groups spent 3.2% of the time travelling at speeds < 1 km/h.

	Track category			
	1	2	3	4
Sample size	25	38	51	76
Average track speed ± SD (km/h)	2.4 ± 1.3	3.5 ± 1.3	3.3 ± 1.3	4.6 ± 1.8
Average net speed ± SD (km/ h)	1.1 ± 0.9	2.7 ± 1.6	2.9 ± 1.4	4.3 ± 1.7
Average linearity ± SD	0.5 ± 0.3	0.6 ± 0.3	0.8 ± 0.3	0.9 ± 0.2

Table 1. Summary of movement paraments of mother-calf humpback whale pairs with averages ± standard deviation (SD) using data pooled from land surveys conducted from the Point Perpendicular Lighthouse in 2018, 2019, and 2021. Track categories represented groups that were tracked; (1) entirely within the inshore area, (2) from offshore/mouth of Jervis Bay into the inshore area, (3) entering/leaving the entrance of the Bay, (4) offshore. "Track speed" is the sum of the distances between consecutive fixes for a track divided by the sum of times between fixes. "Net speed" is the linear distance between the first and last fixes of a track divided by the total time. "Linearity" is track distance divided by net distance.

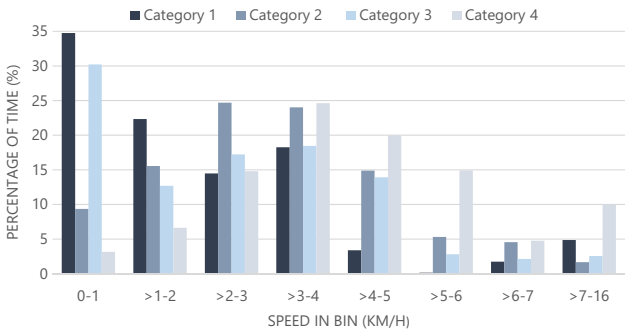

Figure 1. Frequency distributions of the percentage of time spent in speed classes grouped in bins of 1 km/h for mother-calf groups. Data taken from individual leg speeds (n = 1364). Bins from > 7 to 16 km /h were grouped given the low proportion of time spent at these speeds. Track categories represented groups that were tracked; (1) entirely within the inshore area, (2) from offshore/mouth of Jervis Bay into the inshore area, (3) entering/leaving the entrance of the Bay, (4) offshore.

UAV behaviour observations. UAV flights were conducted over four days during 2019 and 2021 (summarised in Table 2). The behaviour of six mother-calf groups were observed from UAV surveys (five mother-calf pair groups and one mother-calf-escort group) (Fig. 2).

Resting was the most observed behavioural state over the four days of flights (29% for both mother and calf resting, 9% when mother was resting and calf was active). This was followed by nurturing behaviour (29%), travelling (19%), socialising (10%), and surface-active behaviour (5%). 55% of the time spent 'travelling' were whales observed leaving the Bay. During 39% of observations, whales were completely submerged. All UAV flights were conducted in the inshore area.

Discussion

This study used two complementary survey methods to provide detailed observations of humpback whales (E1 east coast population) in Jervis Bay, a site remote from the breeding grounds, during the southern migration during 2018, 2019, and 2021. The combination of (i) a high proportion of groups entering/leaving Jervis Bay containing a calf, (ii) a high proportion of time observed resting and (iii) aerial observations of resting and nurturing behaviour indicate that the area is a resting ground for mother-calf groups.

Over the observation period, 84% of humpback whale groups within Jervis Bay contained a calf. Of all groups that entered or left the inshore area (track categories 1 and 2), 92% contained a calf. Such a high proportion of groups with calves has not been observed elsewhere. Observing a high proportion of mother-calf groups towards the end of the southern migration is not unexpected. The migratory timing of humpback whales leaving the breeding and calving grounds is temporally staggered. Non-lactating females are the first to leave the breeding grounds, followed by immature males and females, mature males, and finally lactating females with their newly born calves [1,11,32]. However, the proportion of groups within Jervis Bay containing a calf is considerably higher than other Australian areas where resting has been observed at equivalent seasonal timing. In Hervey Bay, Queensland, a peak occurrence of 40% of groups containing a calf was recorded from early August to mid-October [10]. Similarly, the Exmouth Gulf, Western Australia, had an average of 41% for humpback whale groups containing a calf, peaking at 61% in mid-October [33]. Off Peregian Beach, Queensland, the proportion of calf

Year	Dates	Flights flown between	Flight time (to nearest min)	Duration of recorded behaviours (min)	Platform
2019	31 Oct	0805–0829	24	3	DJI Mavic 2 enterprise dual
	3 Nov	0715–1111	23	A: 10	
				B: 5	
2021	23 Oct	08011–0917	43	A: 37	DJI Mavic 2 enterprise advanced
				B: 6	
	28 Oct	1004–1316	33	33	

Table 2. Summary of UAV flights conducted in 2019 and 2021. Dates where two groups were recorded denote an A and B group.

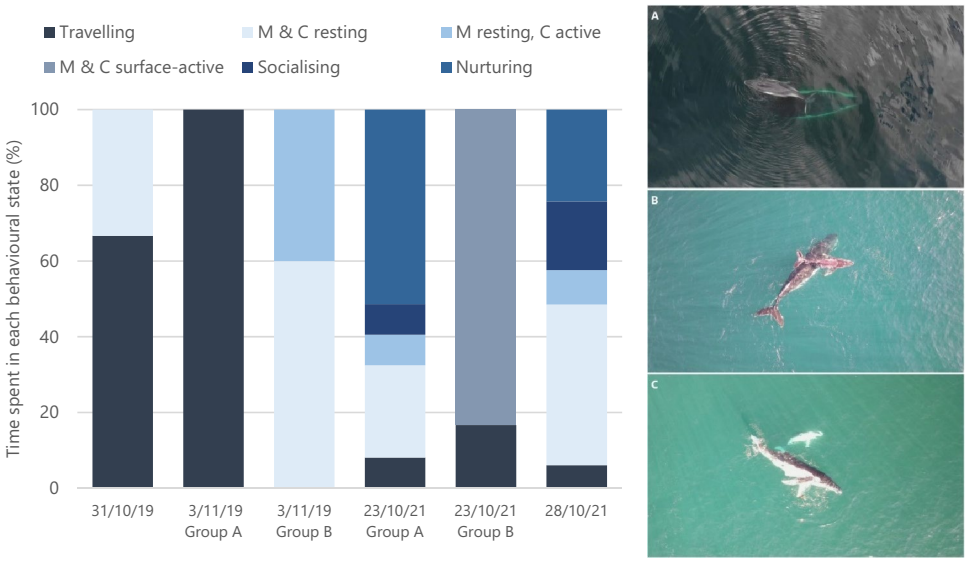

Figure 2. The proportion of time spent in behavioural states for six mother-calf humpback whale groups in Jervis Bay based on UAV aerial observations (left). M and C denote mother and calf, respectively. Humpback whales captured within Jervis Bay displaying: (**A**) resting, (**B**) nurturing, and (**C**) socialising behaviours (right).

groups was 24% of all migrating groups over a similar time period [15]. These calculations were taken of whales on the migratory corridor, indicating this is typical for whales offshore. Thus, the observations in Exmouth Gulf and Hervey Bay have a higher concentration than expected for the migration as a whole. Calf groups were about 22% of all groups passing Jervis Bay, similar to the proportion observed off Peregian Beach.

Mother-calf pairs inshore Jervis Bay (category 1) spent ~ 35% of the time resting at speeds < 1 km/h, consistent with 38% resting observed during UAV surveys (29% for mother and calf resting, 9% when mother was resting and calf was active). This is comparable with the 35% of time resting in Exmouth Gulf which was determined based on acceleration data from DTAGs [13], recognising that the different methods limit the accuracy of comparison. Aerial surveys over the Hawaiian breeding grounds observed that 26% of mother-calf pairs were resting [34]. During the predominantly southbound migration off Peregian Beach, calf groups were observed to be drifting at < 1 km/h, apparently resting 16% of the time whereas non-calf groups drifted for 5.5% of the time [15]. Results off Peregian Beach highlight resting behaviour in exposed oceanic waters, however, high proportions of mother-calf groups in embayments suggests these waters are preferred. Resting in exposed oceanic waters is likely during migrations when whales are moving from breeding areas (e.g., Hawaii or the South Pacific Islands) to feeding grounds in open waters rather than along coastlines.

The semi-enclosed embayment of Jervis Bay, with an irregular ellipsoidal shape, provides a distinct geomorphic setting along the eastern Australian coastline. A continuous stretch of ocean cliffs that form the coastal pathway between Beecroft Head and Cape St George is breached by the relatively narrow entrance of the bay (3.7 km). This discontinuity in the coastline is parallel to the south westerly direction of the migration and requires whales to detour from the main migratory pathway to move into the Bay. Although wind waves are generated across the surface of the bay, ocean swell (from the Tasman Sea and Southern Pacific Ocean) that pass through the entrance are increasingly refracted by a gently shelving bathymetry [35]. The entrances to Hervey Bay and the Exmouth Gulf are oriented east–west facing towards the migrating whales and span close to 70 km and 50 km, respectively, each with a total area of ~ 4000 km^2, so that whales of all group compositions are likely to move into these bays as they move south. This is consistent with the lower proportion of calf group observations in these locations than in Jervis Bay. The importance of Jervis Bay as an area for resting is further highlighted when considering the vast distances between both breeding (~ 1500 km) and feeding grounds (~ 3500 km).

Humpback whale mother-calf pairs in Jervis Bay travel at slower speeds, with less directed movements compared to groups travelling offshore on the southern migration. Travel speed and directional, linear movements offshore were as expected and consistent with other research along the Australian coast [15,27]. Slow, non-linear movements, as observed by lactating females and their calves in Jervis Bay, suggest low energy expenditure and resting by these groups.

Resting implies saving of energy. For marine mammals, the rate of energy expended by travelling to overcome the drag resistance of water theoretically increases as the 3rd power of their speed[36]. Total energy expenditure also includes the basal metabolic rate and factors involved in thermal regulation. Measurements of energy expenditure rate as a function of speed for a range of small marine mammal species generally show a gradual increase above the basal metabolic rate at the lowest speeds [36,37,39]. With increasing speed, the energy expenditure increases at a progressively faster rate as the effect of travelling becomes more dominant. Hind and Gurney [36] provide a comprehensive model of the metabolic cost of swimming in marine homeotherms in which the basal metabolic rate dominates at very low speeds and the energy to overcome drag resistance dominates at high speeds, consistent with measurements. In this model, part of the basal metabolic rate at rest includes the generation of heat required to maintain thermal equilibrium of the body core if heat is lost to the surrounding colder water. Heat generated by travelling can to some extent compensate for this heat loss thus reducing the net additional energy expenditure during travel at low speeds. The result is that the increase in energy with speed from rest is more gradual than without this compensation, up to a speed where the heat from travelling exceeds that needed to compensate for heat loss to the water.

However, this effect may not be significant for large whales in warm waters, such as those in [40] and outside Jervis Bay where temperatures are typically 18–19 °C during the southbound migration. Modelling of thermal processes in marine mammals [40–42] has shown that large whales may need to dissipate excess heat in warm waters, especially when travelling, and that blood circulation through flippers, fins and flukes is important in dissipation. Energy saving through reduced speed may therefore be more for humpback whales in warm water than expected from the measurements for small marine mammals because there is not the need to generate heat at low speeds to compensate for heat loss to the water, as in the model of Hind and Gurney. With their rapid growth, calves have higher metabolic rates per kilogram of body mass than conspecific adults and higher than for adults of similar size from other smaller species[40] so measurements of smaller marine mammal adults are not applicable, even if of similar size. There appear to be no measurements of the dependence of energy expenditure on speed for large whales in warm waters, or the data required to evaluate the model of Hind and Gurney to clarify this. However, it seems likely that there is considerable saving of energy by the significant reduction in speed and the high proportion of time spent with little movement by humpback whale mothers and calves in Jervis Bay compared to similar groups travelling offshore.

Respiration rate has been also be used to estimate energy expenditure in large whales [14,43]. However, this assumes that expiration and inspiration gas exchange (tidal volume) is constant irrespective of speed or the rate of energy consumption. This is not supported by gas flow measurements at low speeds which found significant variation in tidal volume as flow rate of the blow as well as the duration varied and blows were observed to be weaker and more difficult to observe as the whales rested[44]. Hence respiration rates are likely to overestimate energy expenditure at low speeds and resting, leading to an underestimate of the dependence of energy expenditure on speed. In Jervis Bay, we found that blows from whales were often too weak to be reliably counted from the observation site, especially for calves and for longer distances, thus respiration rates were not measured. In

studies off Peregian Beach, theodolite observations were found to underestimate respiration rates of migrating humpback whales compared with boat observation, especially the smaller blows from calves [45].

Bejder et al. [13] found that respiration rates of humpback whale mothers and calves in Exmouth Gulf were significantly less than for foraging whales off Greenland, based on aural detection of blows recorded on tags affixed to whales by suction cups. If respiration rate tends to overestimate energy expenditure at low speeds, the difference in energy expenditure between resting and foraging would be even more pronounced.

UAV surveys were conducted to observe fine-scale behaviour of humpback whales in Jervis Bay and complement movement parameters calculated using land-based theodolite data. Clear resting and nurturing behaviour was evident. In addition to the energetic advantages afforded by resting behaviour, as discussed above, maternal behaviour, including nursing and back riding, is linked to calf survival [46]. Back-riding is particularly beneficial for younger calves by helping calves to stay afloat right after birth and facilitating protection from predators during developmental stages [29,47]. Close proximity between mother and calf provides several advantages, including close access to milk, saving on energetic costs of travelling, reducing the need for loud acoustic communication which may attract predators [30,47]. Few observations of surface-active behaviours in the UAV surveys further support minimisation of energy expenditure by mother-calf groups during their time in Jervis Bay.

UAVs provide a superior platform to visualise more subtle social and nurturing behaviours, as well as behaviours immediately below the surface, when compared to oblique methods from land or on a vessel which underestimate these activities [48]. In our UAV surveys, whales were submerged for 39% of observations. Compared to boat-based observations, UAVs provide three times more observational capacity for the same time period [49]. Additionally, UAV observation methods improve reliability of assigned behavioural states as video footage can be examined multiple times, by multiple researchers post-flight [48]. The authors recognise the limitations associated with the restricted data available from four flights coordinated during periods of COVID related travel and fieldwork restrictions. However, these flights provided insights on nurturing and resting behaviour of submerged whales, that would not have been distinguishable from land or boat surveys.

This study confirms the role of Jervis Bay as a resting ground for mother-calf pairs from the east Australian humpback whale population as suggested by Bruce et al. [22]. It also provides information that, when combined with other studies in the literature, allows a characterisation of resting behaviour that could be applied generally. Unlike other seasonally significant habitats for humpback whales, such as breeding and feeding grounds, requirements for an area to be considered a resting ground is less established in the literature. Jervis Bay meets the requirements of a resting ground as defined in other research studies in that it is an enclosed coastal area which provides shelter from open oceanographic conditions [54] where whales are not actively travelling and making up distance on their migration [8]. We argue that these definitions are inadequate and not inclusive of all conditions and behaviours in which resting has been observed. Within the literature, it is accepted that resting behaviour involves whales near or on the surface displaying little activity other than breathing, also known as logging behaviour, but may also include calf back riding [48,55,56]. Humpback whale mother-calf groups have been observed resting in exposed oceanic waters on the migration path [15], so resting is not confined to sheltered waters. An approach for improving the definition and characterisation of an area as a resting ground would be to conduct systematic surveys to quantify movements and observe behaviours over a significant proportion of the migration for more than one migration season. These could be directed towards open ocean areas to improve our knowledge of resting in non-enclosed and unsheltered waters. In this study we have demonstrated the benefits of using multiple survey methods to establish resting behaviour. This allowed validation across different data sets and showed the degree of complementarity between trends in the travel speed, linearity of movement and aerial UAV observations.

Resting mother-calf groups in Jervis Bay, and other sheltered waters, are especially vulnerable to human disturbances as they move at slow speeds and spend high proportions of time resting stationary at or near the surface [13]. Despite being protected within the Jervis Bay Marine Park and Booderee National Park, mother-calf groups are temporally and geographically coincident with naval, recreational, and commercial activities during October, the peak time for their presence in Jervis Bay. Commercial whale watching and recently introduced swim-with-whale activities are also focused on observing these animals at close distances. This highlights the need to monitor and manage potential impacts of these activities during an important stage for calves undertaking their first southern migration.

Materials and methods

Field surveys. Fieldwork was undertaken in Jervis Bay (35°07′S, 150°42′E; Figs. 3 and 4), a semi-closed embayment on the NSW coastline, 115 km^2 in area with an average depth of 15–20 m (maximum depth 40 m). Fieldwork was completed over three annual seasons; 24 September to 5 October, 2018; 30 September to 6 November, 2019; 4 October to 31 October, 2021. Restrictions resulting from the COVID-19 pandemic prohibited fieldwork in 2020. Survey timing and duration was based on the peak southern migration of humpback whales in the Jervis Bay area [22]. Two survey methods were employed; daily land surveys and UAV surveys (summarised in Table 3). During all survey methods no signs of disturbance, as outlined in the scientific permits, were observed.

Theodolite tracking. Point Perpendicular headland (75 m elevation), at the entrance of Jervis Bay, provided an optimal vantage point to observe whales entering or bypassing the Bay (Fig. 4). Operating from the Point Perpendicular Lighthouse upper balcony (~93 m above sea level), trained observers worked in teams of 3–4 on 2.5 h shift rotation with 1–2 dedicated spotters, 1 theodolite operator and 1 data entry operator, during daylight survey hours (Table 2). Spotters scanned the ocean and the Bay using the naked eye and 7 × 50 magnitude binoculars. Sighted whales were tracked using a theodolite (TC1105) connected directly to a laptop with custom software, VADAR© Version 2.0[57], which determined the whale position using the horizontal angle

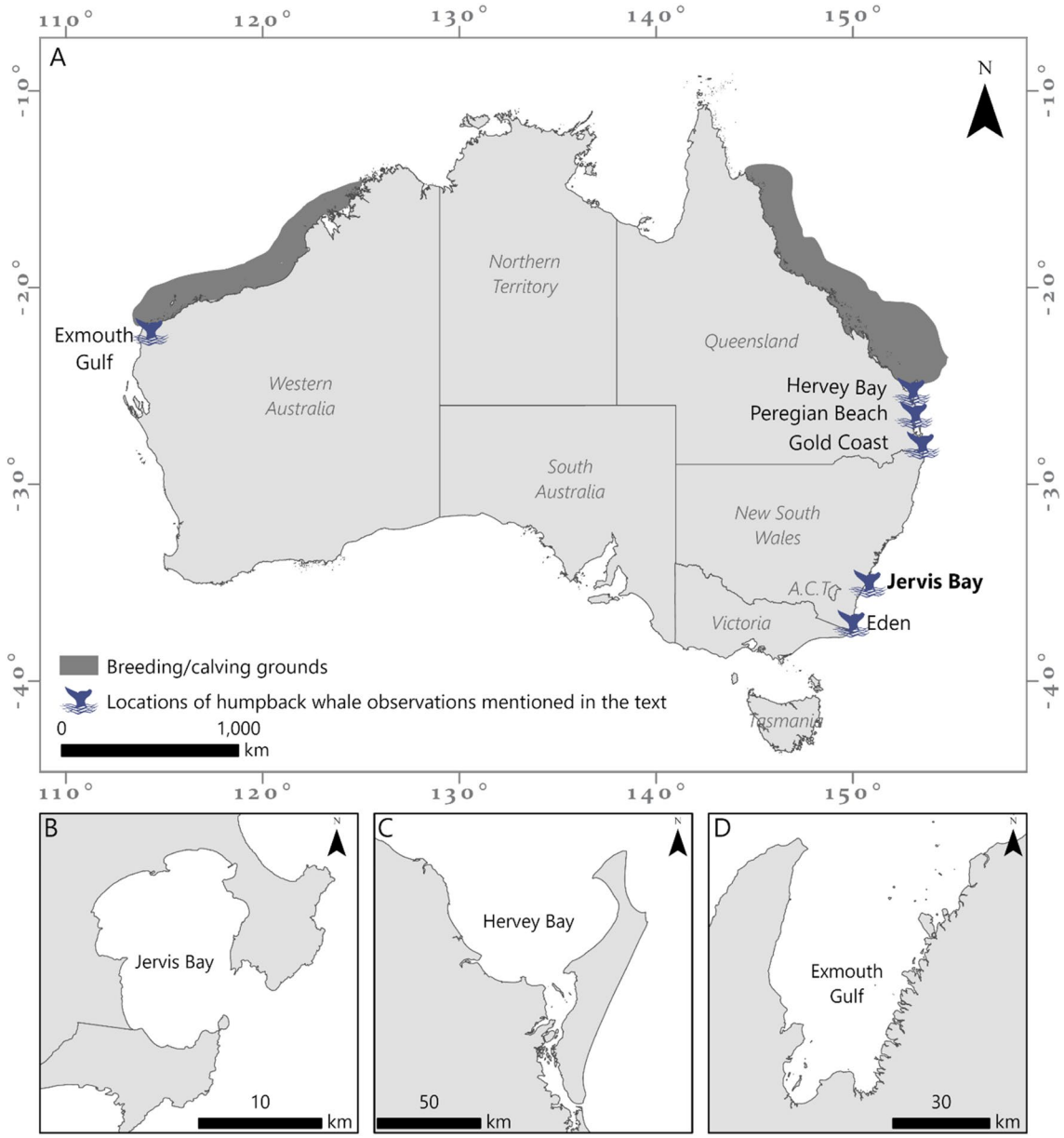

Figure 3. (**A**) Locations of documented aggregations for humpback whales migrating along the east and west coasts of Australia. A comparison of three areas where humpback whale resting has been observed off Australia is illustrated in (**B–D**). Figure created using ArcGIS Pro (v 2.9).

(bearing) and the vertical angle to the whale to calculate the distance, as in previous experiments off Peregian Beach [15,58]. If ≤ 5 whale groups were in the study area, all groups were tracked. For > 5 groups, groups within, entering, or leaving the Bay were prioritised. Consequently, to the best of our knowledge, most of the groups west of the entrance line (Fig. 4) were tracked. For groups offshore, we acknowledge some groups would have been missed.

Theodolite tracking was limited to whale groups within 10 km, the distance of sufficient visibility under good survey conditions (clear and calm). For a small area of the Bay (~ 2.8 km^2), directly under the Point Perpendicular cliffs and behind (north of) Honeymoon Bay, observations were obscured by land (Fig. 4).

A whale group was defined as either a lone whale or multiple individuals (usually two or three) within 100 m of each other and surfacing at similar times. Following sighting, the group position was tracked at every surfacing event until they left the study area, travelled south offshore past Bowen Island, or were no longer detected. The group composition (e.g. lone adult; mother and calf (MC); mother, calf and escort (MCE)) was recorded for all sighted groups. A calf was defined as a whale of less than 70% the length of the accompanying whale, presumably its mother, with whom it maintained a close and constant association [59]. Groups that merged or split were not included in the analysis.

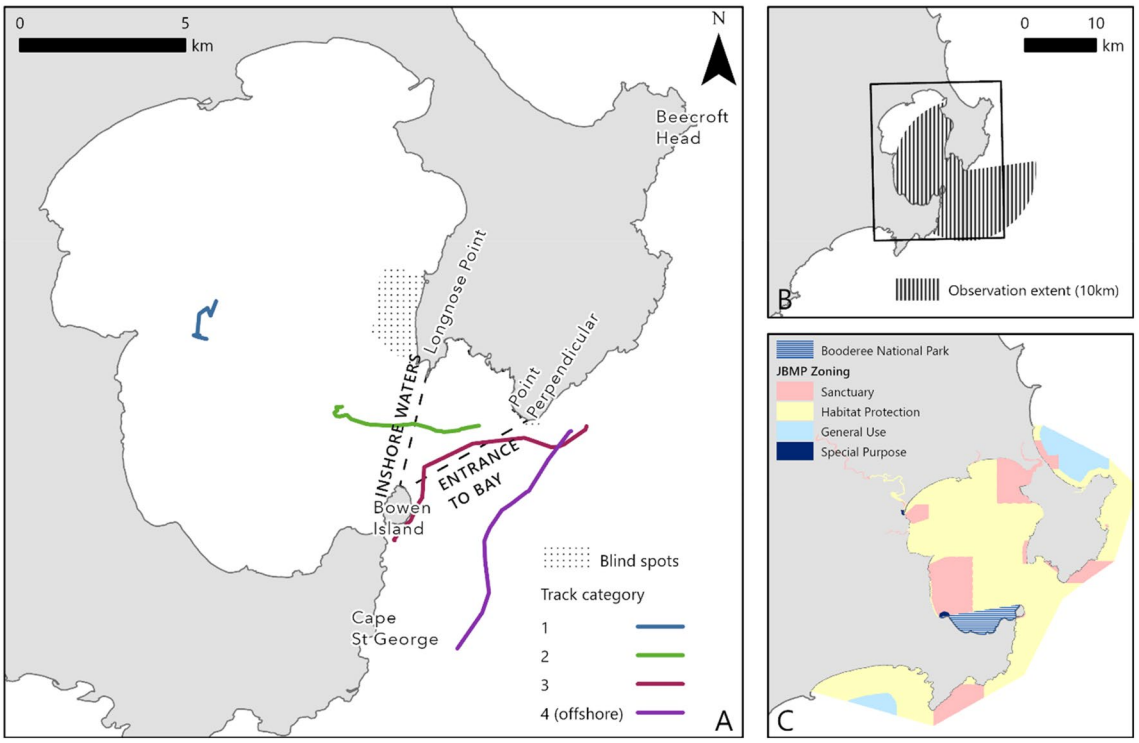

Figure 4. (**A**) Jervis Bay study site illustrating observation areas and example tracks to demonstrate movement from each category. (**B**) The 10 km observation extent from the Point Perpendicular Lighthouse. (**C**) The zoning and extent of the Jervis Bay Marine Park (JBMP) and the extent of the waters of the Booderee National Park. Figure created using ArcGIS Pro (v 2.9).

		2018	2019	2021
Land surveys	Survey hours	0800–1700	0800–1700	0900–1500
	Dates	28 Sept–5 Oct	30 Sept–6 Nov	4–31 Oct
UAV surveys	Dates	N/A	31 Oct, 3 Nov	23, 28 Oct

Table 3. Summary of field methods conducted during the 2018, 2019, 2021 southern migration seasons.

Sectioning of observation area, group composition and movement analysis. The observation area was divided into three sections (Fig. 4): (a) inshore Jervis Bay: the area west of the line from Bowen Island to Longnose Point, (b) the entrance of Jervis Bay: the area between the entrance line (west of the line from Bowen Island to Point Perpendicular) and area (a), and (c) offshore: all areas seaward of the line from Bowen Island to Point Perpendicular. The boundary of area (a) was derived using seabed exposure models [60] as a proxy for protection from ocean swell.

For the movement analysis, whale groups were assigned to four categories based on their tracked movements during the period of observation: category (1) groups whose tracks remained entirely within the inshore area, category (2) groups that were tracked from offshore or the mouth into the inshore area (including both tracks entering or leaving the inshore area), category (3) groups that entered or left the entrance without entering the inshore area, and category (4) groups that were tracked entirely offshore. The proportion of groups within the Bay were recorded and categorised by their composition.

Comparative analysis of whale movement patterns for the four categories was performed on time-enabled data points in ArcGIS Pro (version 2.9). Only tracks containing > 3 reliable theodolite position fixes and tracked for a total of duration > 10 min were included in the data sample. Track distance (m), duration (s), and speed (km/h) were calculated using ArcGIS Pro Motion Statistics.

The distance between any two consecutive fix positions is referred to as a leg. For each track the following parameters were calculated:

(a) Leg speed: the speed of each individual leg.
(b) Track speed: the swimming speed along a track calculated by summing the leg distances for entire track and dividing by the sum of the leg durations.

Both mother and calf resting	Mother and calf are motionless and horizontal at, or just below, the water's surface, surfacing only to breathe
Mother resting, calf active	Mother is motionless and horizontal at, or just below, the water's surface, surfacing only to breathe. The calf is displaying surface-active behaviours, including rolling, breaching, spy hopping, pectoral fin or head slapping
Travelling	Mother and calf are travelling from location to location with persistent, directional movement, covering noticeable distances
Surface-Active	Mother and calf are causing displacement of water at the surface by rolling, breaching, spy hopping, pectoral fin or head slapping. Behaviours in quick succession (< 1 min) but not necessarily simultaneous
Socialising	A whale mother or her calf are actively chasing or circling around the other whale
Nurturing	A whale mother and her calf are rubbing or touching; this includes mother lifting the calf with its rostrum. Suckling may be observed

Table 4. Definitions of behavioural states of humpback whale groups modified from Fiori et al.[67].

(c) Net speed: the straight line speed calculated by dividing the linear distance between the first and last position fixes in a track by the travel time between them (i.e. total duration of track);
(d) Linearity: a form of migration index, calculated by dividing the net distance covered over a track (i.e. the linear distance between the first and last fixes) by its cumulative distance (the sum of all leg distances). Linearity values range between 0 and 1, with values close to 1 representing a straight track-line, and values close to 0 indicating no constant direction.

Mann–Whitney-U tests were performed to compare the three movement parameters between mother-calf pairs in the inshore waters of Jervis Bay (category 1) and mother-calf pairs travelling south offshore (category 4). Mother-calf escort groups were excluded from these comparisons because the sample size in the bay/inshore was too small. Movement parameters from these two geographical areas could be assumed to be statistically independent which may not be the case for groups in categories 2 or 3. Non-parametric statistics do not assume normal data distribution and are less sensitive to unequal sample sizes [61].

UAV surveys. UAV surveys were conducted using a DJI Mavic 2 Enterprise Dual (M2ED) in 2019, and a DJI Mavic 2 Enterprise Advanced (M2EA) in 2021. At the time of survey these were the most suitable lightweight UAV models available for launch and recovery on a small research boat. Following a confirmed whale sighting, whale's behaviour and travel direction were observed for five minutes from a distance > 300 m at idle speed before the whales were approached whilst maintaining > 100 m distance. During flights the boat remained at this distance to provide a clear line of sight to the UAV and facilitate vertical positioning over the whales. The UAV was operated by the University of Sydney Chief UAV Pilot in accordance with Australian Civil Aviation Safety Authority regulations. A field researcher deployed and recovered the UAV by hand, assisted by a customised platform at the rear of the boat. An initial launch altitude of 55 m provided sensor field of view for whale detection within the video frame. The UAV pilot monitored the live video feed and once the whales were visible lowered to ≥ 25 m altitude. Video footage was captured at continuous 2–3 min intervals until the whales were no longer visible or travelling to a new location with direct movements or until 20% of the battery remained.

Jervis Bay is a restricted airspace and UAV flights are only approved during non-military use this confined the survey window to weekends and specified < 2 h time blocks on weekdays approved at short notice.

UAV data analysis. Post-capture UAV video analysis of behavioural states followed methods outlined by Fiori et al. [48,67]. Six mutually exclusive and cumulatively inclusive behavioural states were defined to describe whale group behaviour during each encounter: both mother and calf resting, mother resting whilst calf is active, travelling, surface-active, socialising, and nurturing (Table 4). Only behaviours observed were included in the analysis.

Behavioural states were recorded at one-minute sampling intervals and assumed to remain constant between observations [56]. If whales were last observed diving, travelling was the behavioural state allocated until the whales were resighted [67]. The proportion of time that whales were fully submerged in the footage was also calculated.

Ethics and permit statement. Fieldwork activities were compliant with guidelines and regulatory requirements under permits authorization by the University of Sydney Animal Ethic Committee (permit 2019/1592), the Department of Primary Industries Marine Parks (permit MEAA19/179) and the Department of Planning, Industry and Environment, New South Wales (SL102287). Compliant with the Australian Civil Aviation Authority (CASA) all UAV flights were within visual line of sight. UAV flight approval within the Restricted Airspaces (R421A Nowra and R452 Beecroft Head) overlapping the Jervis Bay study site was obtained from the Australian Department of Defence.

Data availability

All datasets collected and analysed during the current study are available from the corresponding author on reasonable request.

Received: 12 March 2023; Accepted: 1 September 2023
Published online: 07 September 2023

References

1. Dawbin, W. The seasonal migratory cycle of humpback whales. in *Whales, Dolphins and Porpoises* (University of California Press, Berkeley, 1966).
2. Rasmussen, K. *et al.* Southern Hemisphere humpback whales wintering off Central America: Insights from water temperature into the longest mammalian migration. *Biol. Lett.* **3**, 302–305. https://doi.org/10.1098/rsbl.2007.0067 (2007).
3. Stevick, P. T. *et al.* A quarter of a world away: Female humpback whale moves 10,000 km between breeding areas. *Biol. Lett.* **7**, 299–302. https://doi.org/10.1098/rsbl.2010.0717 (2011).
4. Clapham, P. Why do baleen whales migrate? A response to Corkeron and Connor. *Mar. Mamm. Sci.* **17**, 432–436 (2001).
5. Pitman, R. L. *et al.* Skin in the game: Epidermal molt as a driver of long-distance migration in whales. *Mar. Mamm. Sci.* **36**, 565–594 (2020).
6. Smith, J. N. *et al.* Identification of humpback whale breeding and calving habitat in the Great Barrier Reef. *Mar. Ecol. Prog. Ser.* **447**, 259–272. https://doi.org/10.3354/meps09462 (2012).
7. Owen, K. *et al.* Effect of prey type on the fine-scale feeding behaviour of migrating east Australian humpback whales. *Mar. Ecol. Prog. Ser.* **541**, 231–244. https://doi.org/10.3354/meps11551 (2015).
8. Jenner, K. C., Jenner, M. M. & McCabe, K. A. Geographical and temporal movements of humpback whales in Western Australian waters. *APPEA J.* **41**, 749–765 (2001).
9. Burns, D. *et al.* Migratory movements of individual humpback whales photographed off the eastern coast of Australia. *Mar. Mamm. Sci.* **30**, 562–578. https://doi.org/10.1111/mms.12057 (2014).
10. Franklin, T. *et al.* Seasonal changes in pod characteristics of eastern Australian humpback whales (*Megaptera novaeangliae*), Hervey Bay 1992–2005. *Mar. Mamm. Sci.* **27**, E134–E152. https://doi.org/10.1111/j.1748-7692.2010.00430.x (2011).
11. Franklin, T., Franklin, W., Brooks, L. & Harrison, P. Site-specific female-biased sex ratio of humpback whales (*Megaptera novaeangliae*) during a stopover early in the southern migration. *Can. J. Zool.* **96**, 533–544 (2018).
12. Franklin, T. *et al.* Social behaviour of humpback whales (*Megaptera novaeangliae*) in Hervey Bay, Eastern Australia, a preferential female stopover during the southern migration. *Front. Mar. Sci.* **8**, 1761 (2021).
13. Bejder, L. *et al.* Low energy expenditure and resting behaviour of humpback whale mother-calf pairs highlights conservation importance of sheltered breeding areas. *Sci. Rep.* **9**, 771. https://doi.org/10.1038/s41598-018-36870-7 (2019).
14. Ejrnæs, D. D. & Sprogis, K. R. Ontogenetic changes in energy expenditure and resting behaviour of humpback whale mother–calf pairs examined using unmanned aerial vehicles. *Wildl. Res.* **49**, 34–45 (2021).
15. Noad, M. J. & Cato, D. H. Swimming speeds of singing and non-singing humpback whales during migration. *Mar. Mamm. Sci.* **23**, 481–495. https://doi.org/10.1111/j.1748-7692.2007.02414.x (2007).
16. Ersts, P. J. & Rosenbaum, H. C. Habitat preference reflects social organization of humpback whales (*Megaptera novaeangliae*) on a wintering ground. *J. Zool.* **260**, 337–345. https://doi.org/10.1017/s0952836903003807 (2003).
17. Smultea, M. A. Segregation by humpback whale (*Megaptera novaeangliae*) cows with a calf in coastal habitat near the island of Hawaii. *Can. J. Zool.* **72**, 805–811 (1994).
18. Cartwright, R. *et al.* Between a rock and a hard place: habitat selection in female-calf humpback whale (*Megaptera novaeangliae*) Pairs on the Hawaiian breeding grounds. *PLoS ONE* **7**, e38004. https://doi.org/10.1371/journal.pone.0038004 (2012).
19. Paterson, R., Paterson, P. & Cato, D. H. The status of humpback whales *Megaptera novaeangliae* in east Australia thirty years after whaling. *Biol. Conserv.* **70**, 135–142 (1994).
20. Clapham, P. *et al.* Catches of humpback whales, *Megaptera novaeangliae*, by the Soviet Union and other nations in the Southern Ocean, 1947–1973 (2009).
21. Noad, M. J., Kniest, E. & Dunlop, R. A. Boom to bust? Implications for the continued rapid growth of the eastern Australian humpback whale population despite recovery. *Popul. Ecol.* **61**, 198–209. https://doi.org/10.1002/1438-390x.1014 (2019).
22. Bruce, E., Albright, L., Sheehan, S. & Blewitt, M. Distribution patterns of migrating humpback whales (*Megaptera novaeangliae*) in Jervis Bay, Australia: A spatial analysis using geographical citizen science data. *Appl Geogr* **54**, 83–95. https://doi.org/10.1016/j.apgeog.2014.06.014 (2014).
23. Dakin, W. J. *Whalemen Adventurers: The Story of Whaling in Australian Waters and Other Southern Seas Related Thereto, from the Days of Sails to Modern Times* (Angus & Robertson, 1938).
24. Silva, I. *et al.* Mid-migration humpback whale feeding behavior off Eden, NSW, Australia. Report-International Whaling Commission (Report Number SC/63/SH12, 2013).
25. McCulloch, S., Meynecke, J. O., Franklin, T., Franklin, W. & Chauvenet, A. L. M. Humpback whale (*Megaptera novaeangliae*) behaviour determines habitat use in two Australian bays. *Mar. Freshw. Res.* https://doi.org/10.1071/mf21065 (2021).
26. Paterson, R. & Paterson, P. The status of the recovering stock of humpback whales *Megaptera novaeangliae* in east Australian waters. *Biol. Conserv.* **47**, 33–48 (1989).
27. Gales, N. *et al.* Satellite tracking of Australian humpback (*Megaptera novaeangliae*) and pygmy blue whales (*Balaenoptera musculus brevicauda*). (2010).
28. Christiansen, F., Dujon, A. M., Sprogis, K. R., Arnould, J. P. & Bejder, L. Noninvasive unmanned aerial vehicle provides estimates of the energetic cost of reproduction in humpback whales. *Ecosphere* **7**, e01468. https://doi.org/10.1002/ecs2.1468 (2016).
29. Christiansen, F. *et al.* Maternal body size and condition determine calf growth rates in southern right whales. *Mar. Ecol. Prog. Ser.* **592**, 267–281 (2018).
30. Videsen, S. K. A., Bejder, L., Johnson, M., Madsen, P. T. & Goldbogen, J. High suckling rates and acoustic crypsis of humpback whale neonates maximise potential for mother-calf energy transfer. *Funct. Ecol.* **31**, 1561–1573. https://doi.org/10.1111/1365-2435.12871 (2017).
31. Barendse, J. & Best, P. B. Shore-based observations of seasonality, movements, and group behavior of southern right whales in a nonnursery area on the South African west coast. *Mar. Mamm. Sci.* **30**, 1358–1382 (2014).
32. Franklin, T. *The social and ecological significance of Hervey Bay Queensland for eastern Australian humpback whales (Megaptera novaeangliae)*, (2012).
33. Irvine, L. & Salgado Kent, C. The distribution and relative abundance of marine mega-fauna, with a focus on humpback whales (2019).
34. Herman, L. M. & Antinoja, R. C. Humpback whales in the Hawaiin breeding waters: Population and pod characteristics. *Sci. Rep. Whales Res. Inst.* **29**, 59–85 (1977).
35. Walker, G. T. *The Coastal Geomorphology of the Jervis Bay Area* (The Australian National University (Australia), 1967).
36. Hind, A. & Gurney, W. The metabolic cost of swimming in marine homeotherms. *J. Exp. Biol.* **200**, 531–542 (1997).
37. Yazdi, P., Kilian, A. & Culik, B. Energy expenditure of swimming bottlenose dolphins (*Tursiops truncatus*). *Mar. Biol.* **134**, 601–607 (1999).
38. Worthy, G. A., Worthy, T. A., Yochem, P. K. & Dold, C. Basal metabolism of an adult male killer whale (*Orcinus orca*). *Mar. Mamm. Sci.* **30**, 1229–1237 (2013).
39. SchytteBlix, A. & Folkow, L. P. Daily energy expenditure in free living minke whales. *Acta Physiol. Scand.* **153**, 61–66 (1995).

40. Lavigne, D., Innes, S., Worthy, G. & Edwards, E. F. Lower critical temperatures of blue whales, *Balaenoptera musculus*. *J. Theor. Biol.* **144**, 249–257 (1990).
41. Ryg, M. *et al.* Scaling of insulation in seals and whales. *J. Zool.* **230**, 193–206 (1993).
42. Hokkanen, J. Temperature regulation of marine mammals. *J. Theor. Biol.* **145**, 465–485 (1990).
43. Christiansen, F., Rasmussen, M. H. & Lusseau, D. Inferring energy expenditure from respiration rates in minke whales to measure the effects of whale watching boat interactions. *J. Exp. Mar. Biol. Ecol.* **459**, 96–104. https://doi.org/10.1016/j.jembe.2014.05.014 (2014).
44. Sumich, J. & May, M. Scaling and remote monitoring of tidal lung volumes of young gray whales, *Eschrichtius robustus*. *Mar. Mamm. Sci.* **25**, 221–228 (2009).
45. Dunlop, R. A. *et al.* The behavioural response of humpback whales (*Megaptera novaeangliae*) to a 20 cubic inch air gun. *Aquat. Mamm.* **41**, 412–433. https://doi.org/10.1578/am.41.4.2015.412 (2015).
46. Smultea, M. *et al.* in *Animal Behavior and Cognition* Vol. 4 1–23 (2017).
47. Nielsen, M. L., Sprogis, K. R., Bejder, L., Madsen, P. T. & Christiansen, F. Behavioural development in southern right whale calves. *Mar. Ecol. Prog. Ser.* **629**, 219–234 (2019).
48. Fiori, L., Martinez, E., Bader, M. K. F., Orams, M. B. & Bollard, B. Insights into the use of an unmanned aerial vehicle (UAV) to investigate the behavior of humpback whales (*Megaptera novaeangliae*) in Vava'u, Kingdom of Tonga. *Mar. Mamm. Sci.* https://doi.org/10.1111/mms.12637 (2019).
49. Torres, L. G., Nieukirk, S. L., Lemos, L. & Chandler, T. E. Drone up! Quantifying whale behavior from a new perspective improves observational capacity. *Front. Mar. Sci.* https://doi.org/10.3389/fmars.2018.00319 (2018).
50. Barendse, J., Best, P. B., Carvalho, I. & Pomilla, C. Mother knows best: occurrence and associations of resighted humpback whales suggest maternally derived fidelity to a Southern Hemisphere coastal feeding ground. *PLoS ONE* **8**, e81238. https://doi.org/10.1371/journal.pone.0081238 (2013).
51. Sheehan, S. & Blewitt, M. in *Australian Marine Science Association (AMSA)* (Gold Coast, Queensland, Australia, 2013).
52. Clapham, P. J. & Mayo, C. A. Reproduction and recruitment of individually identified humpback whales, *Megaptera novaeangliae*, observed in Massachusetts Bay, 1979–1985. *Can. J. Zool.* **65**, 2853–2863 (1987).
53. Clapham, P. J. *et al.* Seasonal occurrence and annual return of humpback whales, *Megaptera novaeangliae*, in the southern Gulf of Maine. *Can. J. Zool.* **71**, 440–443 (1993).
54. Braithwaite, J. E., Meeuwig, J. J. & Jenner, K. C. Estimating cetacean carrying capacity based on spacing behaviour. *PLoS ONE* **7**, e51347. https://doi.org/10.1371/journal.pone.0051347 (2012).
55. Sprogis, K. R., Bejder, L. & Christiansen, F. Swim-with-whale tourism trial in the Ningaloo Marine Park, Western Australia (2017).
56. Lundquist, D. *et al.* Response of southern right whales to simulated swim-with-whale tourism at Península Valdés, Argentina. *Mar. Mamm. Sci.* **29**, E24–E45 (2013).
57. Visual and Acoustic Detection and Ranging at Sea (VADAR) v. 2.0 (University of Newcastle).
58. Cato, D. H. *et al.* A study of the behavioural response of whales to the noise of seismic air guns: Design, methods and progress. *Acoust. Aust.* **41**, 88–97 (2013).
59. Sprogis, K. R., Bejder, L., Hanf, D. & Christiansen, F. Behavioural responses of migrating humpback whales to swim-with-whale activities in the Ningaloo Marine Park, Western Australia. *J. Exp. Mar. Biol. Ecol.* https://doi.org/10.1016/j.jembe.2019.151254 (2020).
60. Geoscience, A. (data.gov.au, 2017).
61. MacFarland, T. W. & Yates, J. M. *Introduction to Nonparametric Statistics for the Biological Sciences Using R* (Springer, 2016).
62. Katona, S. *et al.* Identification of humpback whales by fluke photographs In *Behavior of Marine Animals* 33–44 (Springer, 1979).
63. Craig, A., Herman, L. & Pack, A. Estimating residence times of humpback whales in Hawaii (2001).
64. Calambokidis, J. *et al.* Movements and population structure of humpback whales in the North Pacific. *Mar. Mamm. Sci.* **17**, 769–794 (2001).
65. Constantine, R. *et al.* Abundance of humpback whales in Oceania using photo-identification and microsatellite genotyping. *Mar. Ecol. Prog. Ser.* **453**, 249–261. https://doi.org/10.3354/meps09613 (2012).
66. Friday, N., Smith, T. D., Stevick, P. T. & Allen, J. Measurement of photographic quality and individual distinctiveness for the photographic identification of humpback whales, *Megaptera novaeangliae*. *Mar. Mamm. Sci.* **16**, 355–374 (2000).
67. Fiori, L., Martinez, E., Orams, M. B. & Bollard, B. Using Unmanned Aerial Vehicles (UAVs) to assess humpback whale behavioral responses to swim-with interactions in Vava'u, Kingdom of Tonga. *J. Sustain. Tour.* **28**, 1743–1761 (2020).

Acknowledgements

Thank you to Scott Sheehan and Jeremy Randle for assistance in conducting the UAV surveys. VADAR software was designed by Eric Kniest who customized it for this research. Thank you to Alessandra Cani, Andrea Mendez-Bye, David Lorieux, Duncan Morton, Euan Smith, Evie Hyland, Gaby Genty, Kelly Coffin, Kennadie Haigh, Lisa McComb, Matthew Clements, Natasha Garner, Nathan Angelakis, Nicola Kennedy for support in the field.

Author contributions

The submitted work is original research carried out by the authors and all authors agree to the submission. Author contributions to the manuscript are as follows: A.J., E.B., and D.C. conceived the study. A.J. collected the data. A.J., E.B., and D.C. wrote the manuscript. A.J., and D.C carried out the analysis.

Funding

This research was funded by the Defence Science and Technology Group (Maritime Division) through the ARC Training Centre for Cubesats, UAVs and Their Applications (CUAVA) ICI70100023.

Competing interests

The authors declare no competing interests.

Additional information

Correspondence and requests for materials should be addressed to A.J.

3 ENHANCING UAV IMAGES TO IMPROVE THE OBSERVATION OF SUBMERGED WHALES USING A WATER COLUMN CORRECTION METHOD

3.1 INTRODUCTION

Ultra-high spatial resolution sensors made available by advancements in the miniaturization of instruments deployable on unoccupied aerial vehicle (UAVs)[2], present new and innovative opportunities for remote detection of marine wildlife. The spatio-temporal resolution and survey responsiveness afforded by these low-cost platforms enables the collection of data that can provide insights on the spatio-temporal dynamics of individual marine animals at close range (Anderson & Gaston, 2013). In the last decade there has been an increase in marine studies utilizing UAVs (Schofield et al., 2019), which allows for novel insights on the abundance (Hodgson et al., 2017), behaviour (Torres et al., 2018; Fiori et al., 2019), and body condition (Christiansen et al., 2016; Hodgson et al., 2020) of marine wildlife. Importantly, UAV-based image capture has the potential to increase the duration of visible observation through detection of animals below the water surface (Torres et al., 2018). This has significant ramifications for the study of mother-calf humpback whale groups that rest in shallow protected embayments (Bruce et al., 2014; McCulloch et al., 2021), spending high proportions of time resting at depths of less than 5 m (Bejder et al., 2019; Iwata et al., 2021). However, the use of remotely sensed data in coastal environments is challenged by the optical complexity of the water column (Figure 1).

Environmental conditions (e.g. sun glint, water turbidity and sea state) associated with UAV-captured images are well recognized as limiting factors impacting detection rates (Aniceto et al., 2018; Colefax et al., 2018). Processing techniques are commonly used in remote sensing research to enhance or enable the detection of underwater features, including benthic habitat (Mumby et al., 1998; Zoffoli et al., 2014; Hedley et al., 2016). Similar techniques, including water column correction, can be applied to UAV-captured

[2] Also commonly referred to as drones, unmanned, uncrewed aerial vehicles, or remotely piloted aircraft system.

images to enhance visibility of animals below the water surface, which may be missed in manual counts or automated deep-learning based classifications (Gray et al., 2019). This chapter presents remote sensing-based methods for enhancing UAV-acquired visual image data to improve the contrast of whales on the water surface and submerged near the surface. Application of these methods has the potential to compensate for perception bias (when an animal is present but missed by the observer) which is influenced by environmental conditions (e.g., contrast between an animal and their environment) (Brack et al., 2018). By removing complexities in the water column, through a water column correction technique, there is potential to improve rates of detection. Image correction is demonstrated using UAV data captured over the Jervis Bay Marine Park, a case study site on the eastern Australian coastline that is frequented by humpback whale (*Megaptera novaeangliae*) mother-calf groups during the southern migration from the breeding grounds (Bruce et al., 2014; Jones, 2019).

3.1.1 Background: Water Column Correction

Remote sensing measurements of submerged features are impacted by variations below the water surface including depth, water quality and variations in bottom substrate (Figure 1, Holden & LeDrew, 2002). The overlying water column significantly affects the remotely sensed signal of an object or substrate due to the optical attenuation (scattering and absorption) of light as it passes through water. Differential attenuation of light in the water column results in a decreased ability to discriminate between underwater objects (Hamylton, 2011). Water column correction techniques remove much of the depth-induced variation in spectral data and may improve discrimination of submerged objects. Importantly, the decay of the radiance within the water column caused by absorption and scattering is wavelength dependent and the spectral bands (radiometric channels) of the sensor will influence the effectiveness of correction methods for improving discrimination of submerged objects. The most widely used water column correction is that proposed by Lyzenga (1978, 1981), based on the assumptions that: 1) depth plays a significant role in changing the reflected radiance of an object, and 2) that water quality is constant over the image (Manessa et al., 2016). This method, suitable for high clarity water, produces a depth-invariant bottom index by ratioing the radiance values of each pair of spectral (wavelength) bands. Visual (RGB) sensors with an RGB array filter, most commonly found on UAVs, are limited to three possible band pairs (i.e. red/green,

red/blue, green/blue) which are limited in providing optimal band ratios for detailed outputs (Hamylton, 2011). However, due to higher cost and payload requirements of multispectral sensors, to date many UAV-based marine wildlife surveys have used RGB sensors integrated on standard small payload rotary UAVs (e.g. DJI Phantom models; Torres et al., 2018; Fiori et al., 2020) or fixed wing platforms (e.g. ScanEagle; Hodgson et al., 2017).

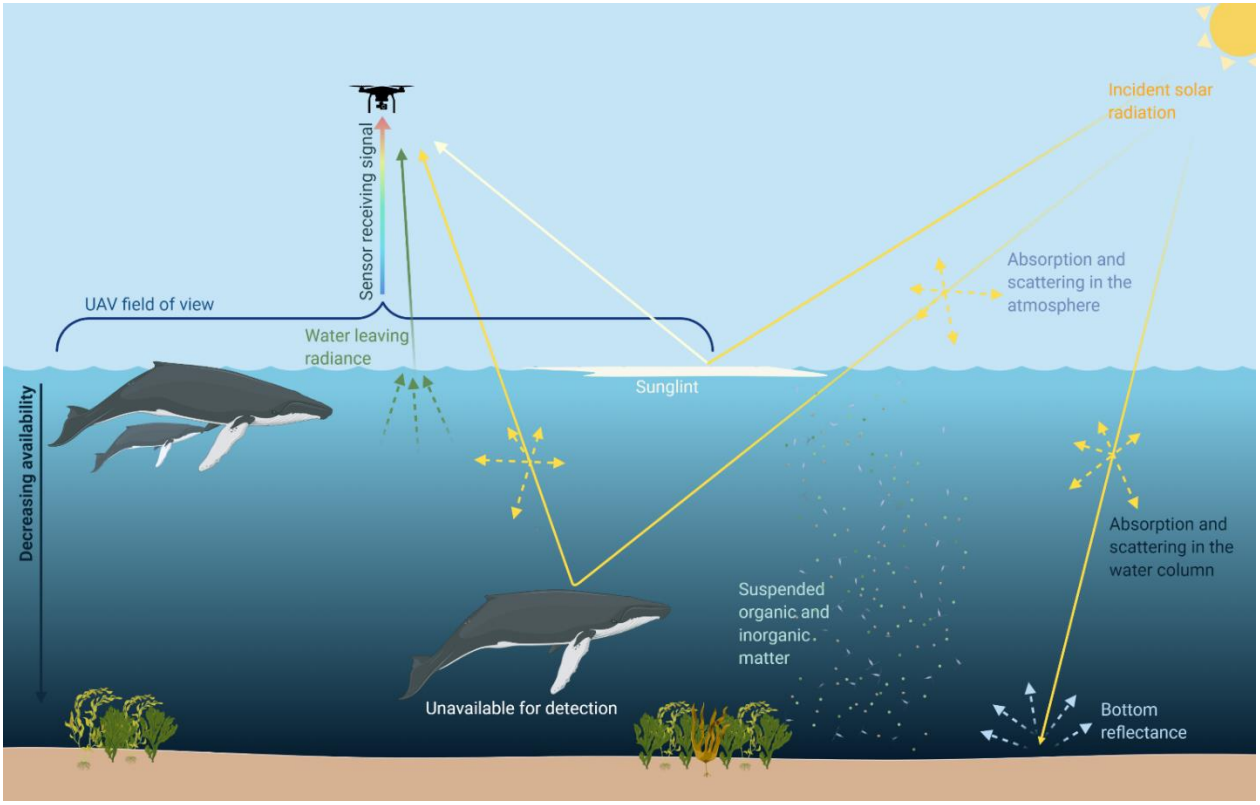

Figure 2. Diagram illustrating the various processes contributing to complexities in surveying large marine species from a UAV platform. Created with BioRender (https://biorender.com/).

3.2 METHODS

3.2.1 UAV data capture

All fieldwork was conducted in Jervis Bay (see Section 4.3 for detailed site description). Jervis Bay is a restricted airspace and UAV flights are only approved during times the

airspace was not in military use. This restricted the window of survey opportunity to weekends and specified one-two hour time blocks during weekdays often approved at short notice. Surveys were conducted when there was no rain, visibility was >5 km with clear skies, and sea state at or below Beaufort force 2.

The visible RGB imaging capabilities of sensors for detecting whales were evaluated using a DJI Mavic 2 Enterprise Dual (M2ED). This was the most suitable light-weight UAV option available for launch and recovery on a small research vessel. The Bay was visually scanned by researchers on the vessel. Following a confirmed whale sighting, the whale's behaviour and direction of travel were observed for five minutes from the vessel at a distance >300 m before an approach was made to a distance >100 m from the whale.

The UAV was launched and landed using a portable wooden platform at the stern of the boat. The initial launch altitude was 55 m to provide sufficient sensor field of view for identifying the whale. The UAV pilot viewed the live feed (visible mode) throughout the flight and lowered the altitude to ≥ 25 m once the whales were visible on the controller screen. As soon as whales were no longer visible in the live feed, the UAV was raised to an altitude >50 m. The vessel remained at a distance >100 m from the whales during the flights to provide a clear line of sight to the UAV and facilitate positioning over the whales. Still images and videos were captured throughout the flight and GPS timestamped.

3.2.2 Water column correction

The spectral signal of the whale in contrast to the surrounding waters was enhanced by using Lyzenga's water column correction model for clear water environments (Lyzenga, 1981), as modified by Mumby et al. (1998) and Hamylton (2011). Three images taken from the M2ED, containing two different mother-calf groups at different depths were used to assess the water column correction. This included both still images and images extracted from video footage. All processing steps were performed in ENVI™ 5.5.3.

To remove light scattering and absorption effects within the atmosphere and water column, the following algorithm was used to calculate a depth-invariant index:

$$X_i = ln\,(L_i) \quad (1)$$

where L_i is the radiance in band i and

$$\frac{k_i}{k_j} = a + \sqrt{a^2 + 1}, \quad a = \frac{\sigma_{ii} + \sigma_{jj}}{2\sigma_{ij}} \tag{2}$$

where k_i is the irradiance attenuation coefficient of the water in band i, σ_{ii} is the variance of X_i in band i and σ_{ij} is the covariance between bands i and j. The depth invariant bands between bands i and j are then calculated as:

$$depth\ invariant\ band_{ij} = ln(L_i) - \left[\left(\frac{k_i}{k_j}\right) ln(L_j)\right] \tag{3}$$

The model generates a single depth invariant band from each pair of spectral bands within the image. This image-based correction method assumes the reflectance of an object is a function of water depth and that water quality is constant across the area of interest. In this study, it could be assumed that there was no variability in the water optical properties across the small area of interest confined to the region immediately adjacent to the whale. In this correction, depth in each pixel is constant for all bands and thus attempts to linearise the relation between two bands *i* and *j* and water depth.

The following steps outline the process for a single image (illustrated in Figure 2). First a natural logarithm was applied to the raw RGB image. The next correction step was to select the pixel samples across the whale. The focus here was to reduce the effects of depth between the whale and ocean surface. Thus, radiance values were taken from the whale's body surface along transects. Subsequently, a polyline region of interest (ROI) was traced along the centerline of the whale's body, down the center of each tail fluke, and across the widest part of the body between the dorsal and pectoral fins. This ROI was used to calculate radiance values and thus ensured inclusion of body surface pixels at different depths accounting for the characteristic fusiform shape of the whale's body. The covariance values across the ROI for each RGB band were determined and depth invariant indices were calculated for all three band pairs (i.e. red/green, red/blue, green/blue) using equation 3 above. Subsequently, the three processed images were converted back to base values using an exponential function.

To compare the pixel values between the original image and processed images, all pixels were converted into Z-scores (equation 4) enabling detection of anomalies, for all four images used (RGB image and three band pairs).

$$Z = \frac{[pixel\ value - mean]}{standard\ deviation} \quad (4)$$

The performance of the applied image processing methods was assessed visually, and quantitively by evaluating the mean Z-score values extracted across the whale's surface, for the original RGB images and the three resulting band pairs. Additionally, a horizontal profile was taken across the original RGB images and the three band pairs.

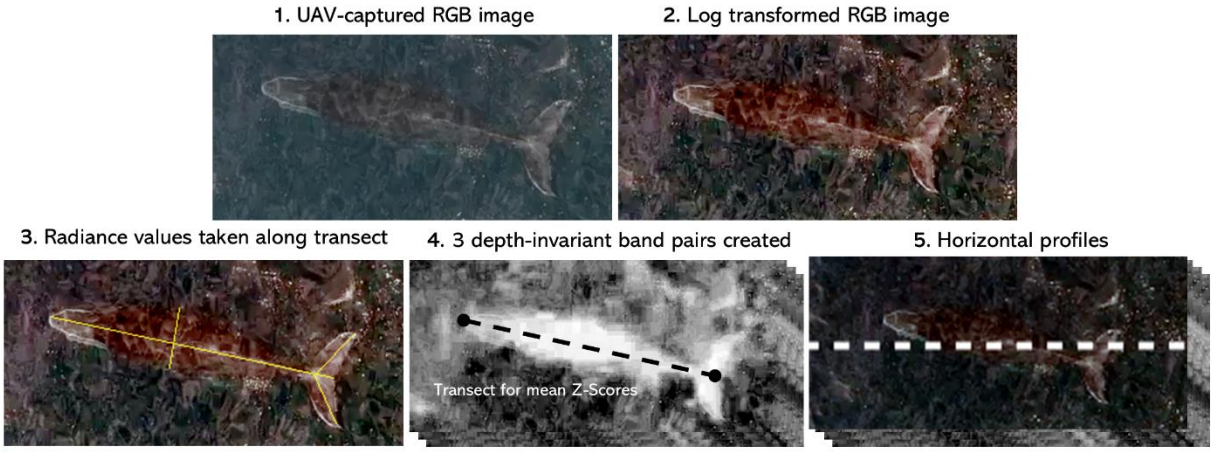

Figure 3. Overview of processing steps applied in the depth invariant analysis. In Step 3, the yellow transect outlines where the radiance values were extracted for inclusion in the correction. The correction process resulted in three depth-invariant band pairs. These images were then converted into Z-scores. Transects (black dotted line, Step 4) were extracted along the length of the whale to determine average values for each image and horizontal profiles were taken along the whales in the image (Step 5).

3.3 RESULTS

In Figure 3, the calf's body is predominantly on the surface, whilst the mother's body is predominantly submerged, with the mother's rostrum at the deepest point. The red/green band pair provided the highest Z-scores both across the whale (Table 1) and the highest peak when comparing the whale to surrounding water, as demonstrated in the horizontal profiles (Figure 3G). This improved contrast is evident in the visual results (Figure 3B). These results were followed closely by the improved contrast provided by the red/blue band pair (Table 1, Figure 3C, H). Across the whale, the green band provided the least deviation from the mean (mean Z=-0.28).

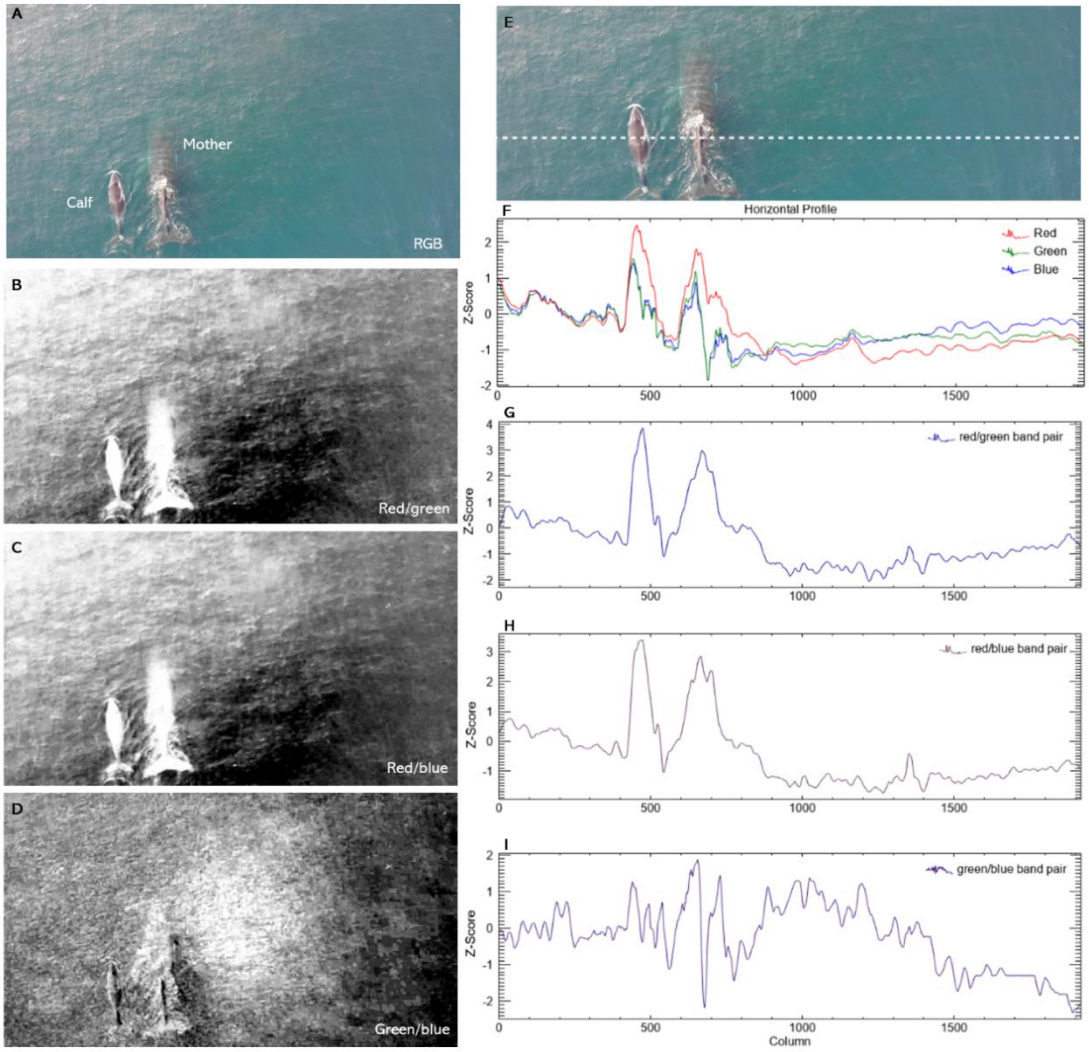

Figure 4. A) RGB image, B-D) visual results of depth invariant images derived from band pairs red/green (B), red/blue (C), green/blue (D), E) RGB image demonstrating where the horizontal transects were taken, F-I) horizontal profiles of the individual bands within the RGB image (F) and processed band pairs red/green (G), red/blue (H), green/blue (I)

The image in Figure 4 was captured five seconds after the image in Figure 5 and shows both the mother and calf submerged. The mother is noticeably deeper in the water column compared with the image in Figure 3, and the green/blue band pair demonstrated the best overall contrast between the mother whale and her surrounds (mean Z-score across whale = 1.64). This is supported by the visual result illustrating the clear outline of the whales submerged below the water surface (Figure 4D). In contrast, the horizontal profiles demonstrate the red/green and red/blue band pairs provide the greatest contrast with surrounding waters (Figure 4G-H). The green/blue band pair (Figure 4I)

still provides a greater contrast compared to the RGB image (Figure 4F). The influence of sun glint is evident in this image, particularly in the top left corner.

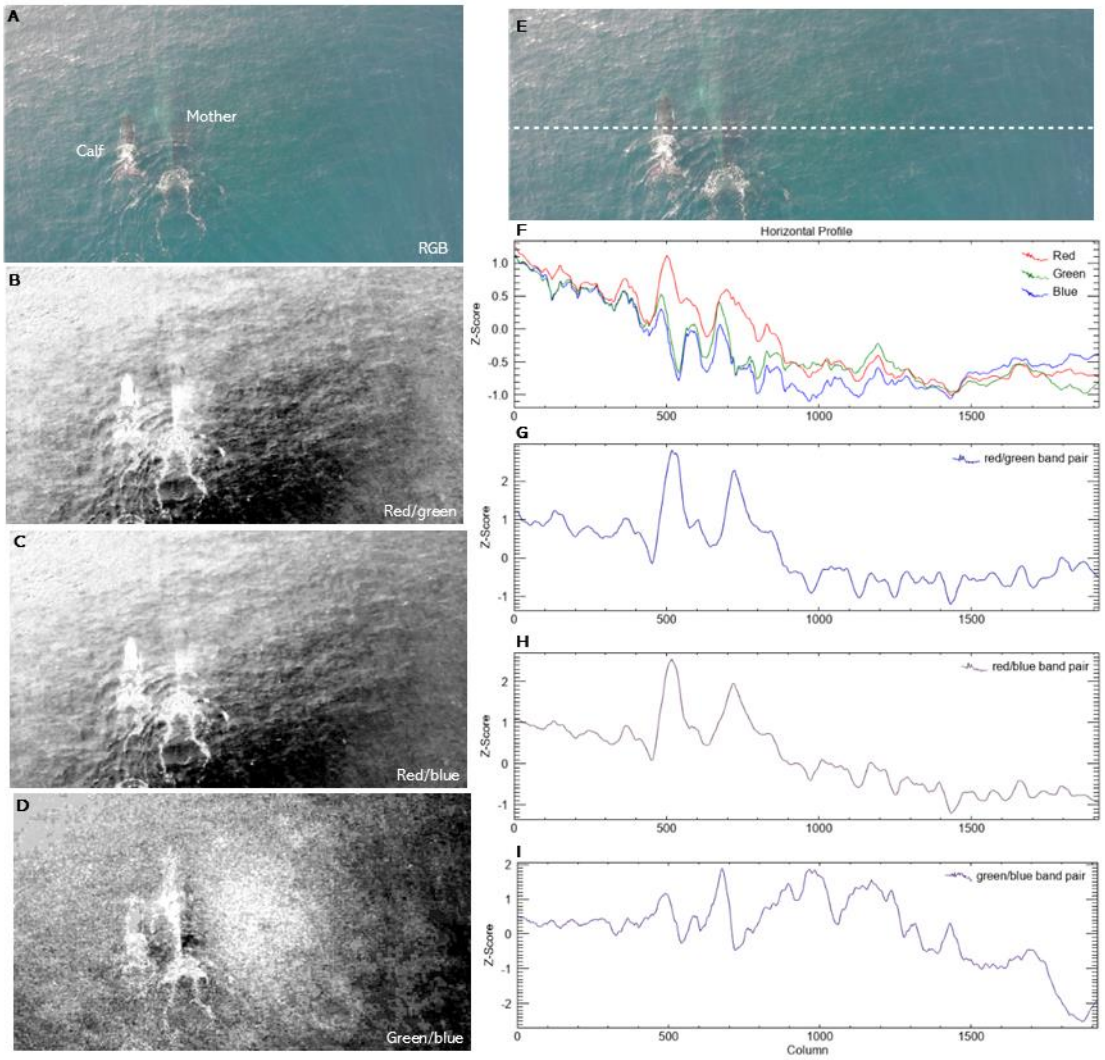

Figure 5. A) RGB image, B-D) visual results of depth invariant images derived from band pairs red/green (B), red/blue (C), green/blue (D), E) RGB image demonstrating where the horizontal transects were taken, F-I) horizontal profiles of the individual bands within the RGB image (F) and processed band pairs red/green (G), red/blue (H), green/blue (I)

Figure 5 also shows a fully submerged whale. The visual results in Figure 6 highlight that band pairs red/green and red/blue most successfully enhanced the shape (edge definition) of the submerged whale. This is quantitively supported by the mean Z-scores across the whale for red/green and red/blue band pairs of 1.85 and 1.88, respectively. The green/blue band pair had a mean Z-score of 1.25 across the whale. The red, green,

and blue bands of the RGB image had notably lower mean Z-scores of 0.40, 0.07, and -0.08, respectively. In the horizontal profiles (Figure 5F-I) there are no obvious peaks that correspond to the whale in the water. In these profiles the whitewash has been observed as a more dominant visual feature than the whale object.

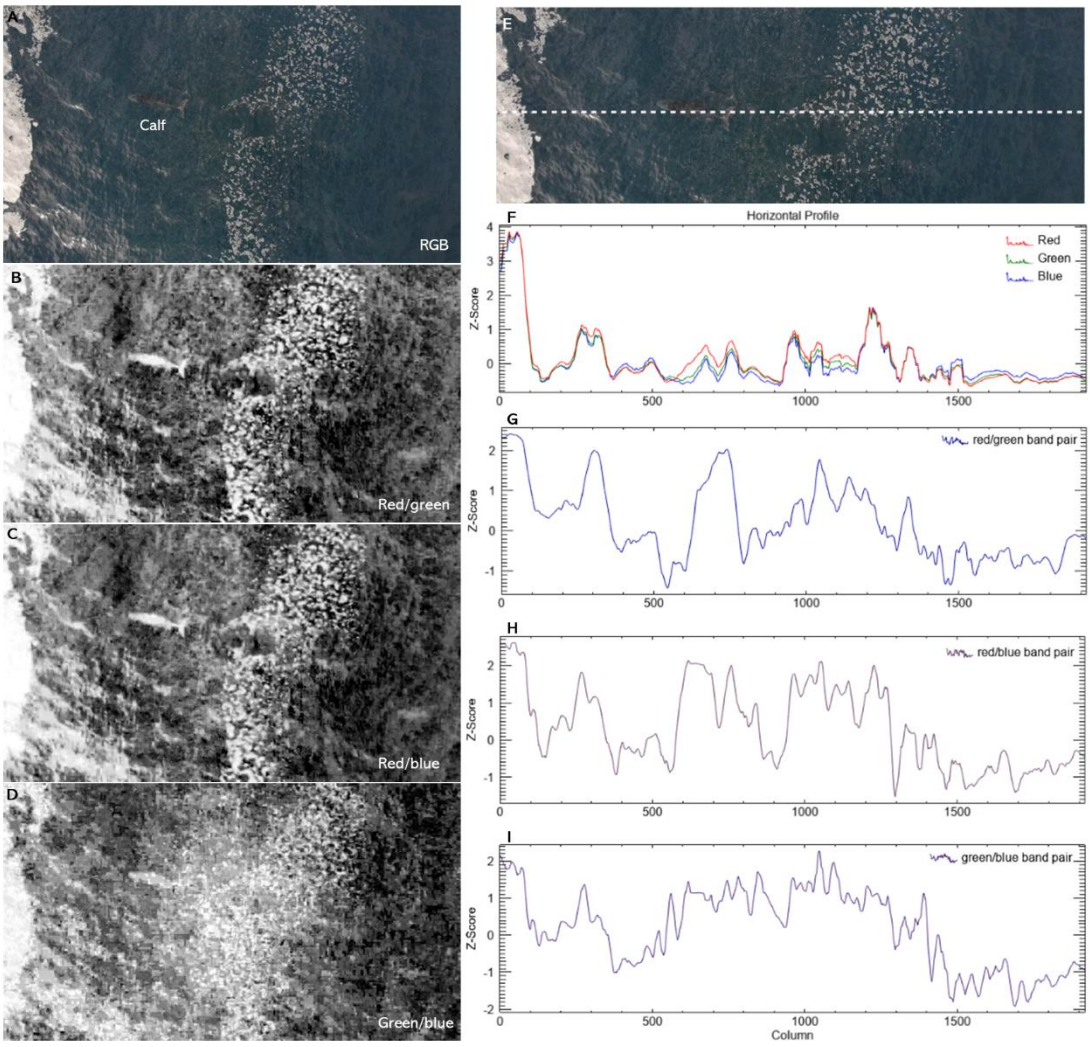

Figure 6. A) RGB image, B-D) visual results of depth invariant images derived from band pairs red/green (B), red/blue (C), green/blue (D), E) RGB image demonstrating where the horizontal transects were taken, F-I) horizontal profiles of the individual bands within the RGB image (F) and processed band pairs red/green (G), red/blue (H), green/blue (I).

Table 1. Mean Z-scores extracted along pixel profile lines across the whales in the three images shown in Figures 3-5, presenting results from the RGB image and three depth invariant images derived from band pair combinations. The results from the RGB image are presented as individual red, green, and blue bands. The highest value for each image is shown in bold.

	Mean Z-scores		
	Figure 3	**Figure 4**	**Figure 5**
Red	1.00	0.85	0.40
Green	-0.28	0.90	0.07
Blue	-0.45	0.54	-0.08
Red/green	**2.21**	0.67	1.85
Red/blue	2.11	1.05	**1.88**
Green/blue	0.32	**1.64**	1.25

3.4 DISCUSSION

The accurate detection of marine vertebrates in aerial images is made complex by environmental factors, including light attenuation in the water column, white caps and specular reflection, particularly sun glint (Hodgson et al., 2013). This study demonstrated a modified version of Lyzenga's water column correction method has the potential to improve the detection of humpback whales in UAV-captured RGB imagery. Overall, the red/green and red/blue band pair ratios were the most effective band pair combination for enhancing contrast between the whale and surrounding waters in the visual qualitative results and horizontal profiles. This is consistent with Niroumand-Jadidi et al. (2018) who applied Lyzenga's water column correction using an 8-band WorldView-2 satellite image and identified the red/green band pair to be optimal for mapping a shallow (<1 metre deep) river environment. In the current study, the red/blue band pair provided comparable results, highlighting the effectiveness of the red band in shallow and clear waters, for discriminating submerged objects, before it is fully attenuated at greater depth. The effectiveness of the red band for animals on or near the surface is consistent with findings from Colefax et al. (2021), who demonstrated the red band produced the greatest spectral contrast for detecting dolphins, sharks, and other marine

fauna from a UAV.

At increasing depths, attenuation of light within the red region increases limiting the value of this waveband. This is demonstrated in this study which showed that images in which the whale or parts of the whale body were at greater depth (Figure 4) have a stronger visual green/blue band pair result and the highest Z-score across the whale. However, the red/green and red/blue band pairs still provided the best detection peaks in the horizontal profiles. This is likely due to the sun glint noise present in the green/blue band pair ratio. The depth of the target animal/s will influence the optimal band pairing and subsequent object enhancement within the image. The red band (610-700 nm), and other bands with wavelengths approaching the red end of the spectrum, will become fully attenuated around 2-3 metres depth (Mishra et al., 2005; Hamylton, 2011). Thus, the effectiveness of band pairs using the red band will substantially reduce at this depth. However, in turbid waters, where sightability below the surface is limited, longer wavelength bands may be optimal for increasing the contrast of animals just below the surface (Colefax et al., 2021). Image enhancement methods for improving whale detection rates even in optically shallow waters (<3 metres) has important implications for studies reliant on accurate detection such as abundance surveys (e.g., Hodgson et al., 2017). Compensating for water attenuation is also important for research conducted on breeding/resting grounds, with lactating females and their calves spending over 50% of time within 3 metres of the surface (Bejder et al., 2019).

3.4.1 Conservation Implications

The methods presented here have the potential to increase the confidence of machine learning and automated detection models. Machine learning techniques for automated detection of whales are increasingly being applied to UAV-collected data sets providing an efficient way to process large amounts of data. Between 2004 and 2018, 15% of ecological studies involving UAVs used machine learning (Dujon & Schofield, 2019). However, data driven machine learning models require a large-scale archive of 'ground-truthed' images for model training and validation to optimize model accuracy gain. Studies using machine learning to detect individual animals or plants rely on the detection of target objects against mostly homogenous backgrounds which provide a clear contrast to reliably discriminate animals from their environment (Laliberte &

Ripple, 2003). The use of machine learning for detecting marine vertebrates is further complicated by colouration similarities between some species and the surrounding water (e.g. blue whales; Gray et al., 2019) and non-uniform backgrounds that are subject to varying environmental conditions. In ecological studies, object-based image analysis (OBIA) is a commonly used image segmentation method (Dujon & Schofield, 2019). It provides versatility for detecting objects in varied backgrounds with confounding features, objects that vary in size and shape, and may be sparsely distributed in the image dataset (Chabot et al., 2018), making it ideal for abundance and distribution studies. Importantly, even with increased flexibility over other methods such as machine learning, OBIA is still reliant on the object/s of interest in the image being localized from surrounding pixels through a local brightness contrast, either as a relatively brighter or relatively darker group of image pixels (Groom et al., 2013). For whale detection, increasing the anomaly (Z-score) of the whale object, as demonstrated here, could potentially improve OBIA segmentation and classification results and increase detection availability.

In all RGB images the contrast between humpback whales, on or near the surface, and their surroundings can be increased, or at least maintained, using a modified water column correction. There is a clear value of these methods in improving the detection, and reducing the perception bias associated with aerial surveys, of resting mother and calf whale groups who spend significant proportions of time resting less than 5 metres from the surface (Bejder et al., 2019; Iwata et al., 2021).

Depth is a key limiting factor in the detection of submerged marine animals. Butcher et al. (2019) found that an increase in depth by 1 metre reduced the odds of detection by 58% when reviewing UAV footage of shark analogues post-capture. At depths greater than 3.5 metres, the probability of detection was less than 50%. Similarly, Dujon et al. (2021) used machine learning to detect loggerhead sea turtles (*Caretta caretta*) in UAV-captured imagery, finding detection decreased significantly with each metre in depth and was close to zero at 5 metres. In clear water, their machine learning model detected less than 40% of turtles at 2 metres depth (Dujon et al., 2021). The correction methods presented here clearly enhanced the whales' fluke shape and outline, demonstrated in

the visual results. The distinctive shape of the fluke could provide an opportunity to train more sophisticated machine learning models to detect whales using this feature. The effectiveness of these results will depend on several factors, including the depth of the whales, their orientation in the water column (i.e., horizontal or vertical), water turbidity and specular reflection including sun glint. Although resting mother and calf humpback whale groups were the focus of this study, the methods presented here are applicable to other marine vertebrate species that are often found in clear, shallow waters, such as dugongs (*Dugong dugon*), sea turtles and stingrays.

3.4.2 Limitations of RGB sensors

This study demonstrated that water column correction techniques can enhance the visual outline and anomaly signal over the body of whales on the surface and submerged at shallow depths. However, constraints associated with the limited spectral resolution provided when working with three bands (i.e., red, green, and blue) within the visible range (wavelength 400-700 nm) are recognised. The higher number of wavelength bands available in multispectral sensors and hyperspectral sensors provide a greater selection of band pairs for depth-invariant processing and are demonstrated to improve the detectability of submerged objects (Colefax et al., 2018). Employing multispectral or hyperspectral sensors and customising or selecting bands configured to focus on wavelength bands optimal for the spectral characteristics of the water body, such as the coastal band (Fretwell et al., 2014), and target species may further reduce perception bias and subsequently improve animal availability at depth compared to standard RGB sensors (Colefax et al., 2018). For example, the MicaSense RedEdge-MX Dual Camera Imaging System has 10 bands, including a coastal blue band for monitoring shallow water environments (Román et al., 2021) and a near infrared band (NIR) allowing for sun glint correction.

Specular reflectance including sun glint was evident in all water column correction results presented here. The specular reflection apparent in the visual RGB images shows as noise in the corrected images and where present there is a noticeable reduction in contrast between the whale/s and surrounding water (e.g., adjacent to the mother whale in Figure 4). In coastal UAV surveys, the effects of sun glint can be avoided, or reduced, by scheduling data capture in the early morning or later afternoon which is a viable option

for static objects, such as nearshore benthos. However, for moving and wide-ranging marine vertebrates this is not always feasible. Whilst studies have reported that sun glint had no significant impact on sighting rates (Hodgson et al., 2013; Butcher et al., 2019), removing the effects of sun glint may further improve the image enhancement methods demonstrated here and should be considered when designing UAV based marine surveys. NIR bands are present in most multispectral sensors and can be used to remove sun glint contamination through post-processing techniques (Hedley et al., 2005; Martin et al., 2016). However, the need for a NIR band limits the use of sun glint removal techniques for most off-the-shelf UAVs, fitted with an RGB sensor, commonly used in wildlife studies. Furthermore, there is a trade-off between spectral resolution and UAV cost. For example, the DJI Phantom 4 (RGB; 1/2.3" CMOS; 12.4 MP) currently retails for one sixth of the price of the DJI Phantom 4 multispectral with 5 bands: RGB, Red Edge, and NIR (1/2.9" CMOS; 2.12 MP) with a lower sensor resolution.

3.4.3 Future Directions

Obtaining a larger image data set is critical for understanding the effectiveness of depth invariant indices derived from possible band pairs, and whether these differ with the whale depth and environmental factors (e.g., turbidity). The irradiance attenuation coefficients $\left(\frac{k_i}{k_j}\right)$ calculated in this study did not vary by more than 0.44 within each band pair, suggesting little variation in a range of conditions. Calculating an optimal index value for each band pair, with little variation in results, has important ramifications for automated detection methods by removing the necessity to first identify if a whale is present in the image. This would involve acquiring images with whales at known depths achieved through DTAGS (Bejder et al., 2019) for accurate depth measurements. However, the need to tag individual animals may limit sample size. The use of analogues, similar to those used in Butcher et al. (2019), would overcome this issue and allow for controlled depths in range of environmental conditions and flights at range of altitudes. This would also require an understanding of the similarity between the reflective signatures of whales and the analogue surface.

Marine wildlife surveys to date have predominantly employed visual (RGB) sensors which highlights the importance of correction methods suitable for visible images,

particularly for time series studies using historical data. However, there is a need to evaluate the role of multispectral sensors, particularly the use of the NIR band, for water column correction methods focused on the detection of marine wildlife. Methods for detecting and removing the sun glint from images using data in the NIR waveband (700-1,500 nm) are well established (Kay et al., 2009). Finally, increasing the number of potential band pair combinations will provide a greater range of results which may offer superior enhancement of submerged objects in UAV imagery.

3.5 CONCLUSIONS

An understanding of the role of water column attenuation correction is critical for accurate detection of whales and is particularly relevant with the increasing use of low-cost UAV platforms and machine learning techniques for achieving estimates of population abundance and monitoring movement patterns of marine wildlife in shallow coastal habitats. Water column correction techniques can enhance the visual outline and anomaly signal over the body of whales on the surface and submerged at shallow depths. Finally, the optimal band pair combination will depend on whale depth and therefore it is not possible to recommend a single band combination for achieving improved overall detection.

3.6 REFERENCES

Anderson, K., & Gaston, K. J. (2013). Lightweight unmanned aerial vehicles will revolutionize spatial ecology. *Frontiers in Ecology and the Environment, 11*(3), 138-146. doi:https://doi.org/10.1890/120150

Aniceto, A. S., Biuw, M., Lindstrøm, U., Solbø, S. A., Broms, F., & Carroll, J. (2018). Monitoring marine mammals using unmanned aerial vehicles: quantifying detection certainty. *Ecosphere, 9*(3), e02122.

Bejder, L., Videsen, S., Hermannsen, L., Simon, M., Hanf, D., & Madsen, P. T. (2019). Low energy expenditure and resting behaviour of humpback whale mother-calf pairs highlights conservation importance of sheltered breeding areas. *Scientific Reports, 9*(1), 771. doi: https://doi.org/10.1038/s41598-018-36870-7

Brack, I. V., Kindel, A., Oliveira, L. F. B., & Scales, K. (2018). Detection errors in wildlife abundance estimates from Unmanned Aerial Systems (UAS) surveys: Synthesis, solutions, and challenges. *Methods in Ecology and Evolution, 9*(8), 1864-1873. doi:10.1111/2041-210x.13026

Bruce, E., Albright, L., Sheehan, S., & Blewitt, M. (2014). Distribution patterns of migrating humpback whales (*Megaptera novaeangliae*) in Jervis Bay, Australia: A spatial analysis using geographical citizen science data. *Applied Geography, 54*, 83-95. doi:https://doi.org/10.1016/j.apgeog.2014.06.014

Butcher, P. A., Piddocke, T. P., Colefax, A. P., Hoade, B., Peddemors, V. M., Borg, L., & Cullis, B. R. (2019). Beach safety: can drones provide a platform for sighting sharks? *Wildlife Research, 46*(8). doi:10.1071/wr18119

Chabot, D., Dillon, C., & Francis, C. M. (2018). An approach for using off-the-shelf object-based image analysis software to detect and count birds in large volumes of aerial imagery. *Avian Conservation and Ecology, 13*(1). doi:10.5751/ace-01205-130115

Christiansen, F., Dujon, A. M., Sprogis, K. R., Arnould, J. P., & Bejder, L. (2016). Noninvasive unmanned aerial vehicle provides estimates of the energetic cost of reproduction in humpback whales. *Ecosphere, 7*(10), e01468. doi: https://doi.org/10.1002/ecs2.1468

Colefax, A. P., Butcher, P. A., Kelaher, B. P., & Browman, H. (2018). The potential for unmanned aerial vehicles (UAVs) to conduct marine fauna surveys in place of manned aircraft. *ICES Journal of Marine Science, 75*(1), 1-8.

doi:https://doi.org/10.1093/icesjms/fsx100

Colefax, A. P., Kelaher, B. P., Walsh, A. J., Purcell, C. R., Pagendam, D. E., Cagnazzi, D., & Butcher, P. A. (2021). Identifying optimal wavelengths to maximise the detection rates of marine fauna from aerial surveys. *Biological Conservation, 257*, 109102. doi:https://doi.org/10.1016/j.biocon.2021.109102

Dujon, A. M., Ierodiaconou, D., Geeson, J. J., Arnould, J. P. Y., Allan, B. M., Katselidis, K. A., . . . Bouchet, P. (2021). Machine learning to detect marine animals in UAV imagery: effect of morphology, spacing, behaviour and habitat. *Remote Sensing in Ecology and Conservation*. doi:10.1002/rse2.205

Dujon, A. M., & Schofield, G. (2019). Importance of machine learning for enhancing ecological studies using information-rich imagery. *Endangered Species Research, 39*, 91-104. doi:https://doi.org/10.3354/esr00958

Fiori, L., Martinez, E., Bader, M. K. F., Orams, M. B., & Bollard, B. (2019). Insights into the use of an unmanned aerial vehicle (UAV) to investigate the behavior of humpback whales (*Megaptera novaeangliae*) in Vava'u, Kingdom of Tonga. *Marine Mammal Science*, 1-15. doi:10.1111/mms.12637

Fiori, L., Martinez, E., Orams, M. B., & Bollard, B. (2020). Using Unmanned Aerial Vehicles (UAVs) to assess humpback whale behavioral responses to swim-with interactions in Vava'u, Kingdom of Tonga. *Journal of Sustainable Tourism, 28*(11), 1743-1761.

Fretwell, P. T., Staniland, I. J., & Forcada, J. (2014). Whales from space: counting southern right whales by satellite. *PLoS One, 9*(2), e88655. doi:https://doi.org/10.1371/journal.pone.0088655

Gray, P. C., Bierlich, K. C., Mantell, S. A., Friedlaender, A. S., Goldbogen, J. A., Johnston, D. W., & Ye, H. (2019b). Drones and convolutional neural networks facilitate automated and accurate cetacean species identification and photogrammetry. *Methods in Ecology and Evolution, 10*(9), 1490-1500. doi:https://doi.org/10.1111/2041-210X.13246

Groom, G., Stjernholm, M., Nielsen, R. D., Fleetwood, A., & Petersen, I. K. (2013). Remote sensing image data and automated analysis to describe marine bird distributions and abundances. *Ecological Informatics, 14*, 2-8. doi:https://doi.org/10.1016/j.ecoinf.2012.12.001

Hamylton, S. (2011). An evaluation of waveband pairs for water column correction using band ratio methods for seabed mapping in the Seychelles. *International Journal of Remote Sensing, 32*(24), 9185-9195. doi:https://doi.org/10.1080/01431161.2010.550648

Hedley, J. D., Harborne, A. R., & Mumby, P. J. (2005). Technical note: Simple and robust removal of sun glint for mapping shallow-water benthos. *International Journal of Remote Sensing, 26*(10), 2107-2112. doi:10.1080/01431160500034086

Hedley, J. D., Roelfsema, C. M., Chollett, I., Harborne, A. R., Heron, S. F., Weeks, S., . . . Christensen, T. R. (2016). Remote sensing of coral reefs for monitoring and management: a review. *Remote Sensing, 8*(2), 118. doi:https://doi.org/10.3390/rs8020118

Hodgson, A., Kelly, N., & Peel, D. (2013). Unmanned aerial vehicles (UAVs) for surveying marine fauna: a dugong case study. *PLoS One, 8*(11), e79556. doi:10.1371/journal.pone.0079556

Hodgson, A., Peel, D., & Kelly, N. (2017). Unmanned aerial vehicles for surveying marine fauna: assessing detection probability. *Ecological Applications, 27*(4), 1253-1267. doi:https://doi.org/10.1002/eap.1519

Hodgson, J. C., Holman, D., Terauds, A., Koh, L. P., & Goldsworthy, S. D. (2020). Rapid condition monitoring of an endangered marine vertebrate using precise, non-invasive morphometrics. *Biological Conservation, 242*, 108402. doi:https://doi.org/10.1016/j.biocon.2019.108402

Holden, H., & LeDrew, E. (2002). Measuring and modeling water column effects on hyperspectral reflectance in a coral reef environment. *Remote Sensing of Environment, 81*(2-3), 300-308.

Iwata, T., Biuw, M., Aoki, K., Miller, P. J. O. M., & Sato, K. J. B. p. (2021). Using an omnidirectional video logger to observe the underwater life of marine animals: Humpback whale resting behaviour. *186*, 104369.

Jones, A., Bruce, E., Cato, D., Davies, K. (2019). *Tracking of humpback whales by theodolite from Point Perpendicular, Jervis Bay: Fieldwork Report 2018*. unpublished report University of Sydney. *unpublished report*.

Kay, S., Hedley, J., & Lavender, S. (2009). Sun Glint Correction of High and Low Spatial Resolution Images of Aquatic Scenes: a Review of Methods for Visible and Near-

Infrared Wavelengths. *Remote Sensing, 1*(4), 697-730. doi:10.3390/rs1040697

Kniest, E. Visual and Acoustic Detection and Ranging at Sea (VADAR) (Version 2.0). University of Newcastle.

Laliberte, A. S., & Ripple, W. J. J. W. S. B. (2003). Automated wildlife counts from remotely sensed imagery. *Wildlife Society Bulletin,* 362-371.

Lyzenga, D. R. (1978). Passive remote sensing techniques for mapping water depth and bottom features. *Applied Optics, 17*(3), 379-383.

Lyzenga, D. R. (1981). Remote sensing of bottom reflectance and water attenuation parameters in shallow water using aircraft and Landsat data. *International Journal of Remote Sensing, 2*(1), 71-82.

Manessa, M. D. M., Haidar, M., Budhiman, S., Winarso, G., Kanno, A., Sagawa, T., & Sekine, M. (2016). Evaluating the performance of Lyzenga's water column correction in case-1 coral reef water using a simulated Wolrdview-2 imagery. *IOP Conference Series: Earth and Environmental Science, 47*. doi:10.1088/1755-1315/47/1/012018

Martin, J., Eugenio, F., Marcello, J., & Medina, A. (2016). Automatic Sun Glint Removal of Multispectral High-Resolution Worldview-2 Imagery for Retrieving Coastal Shallow Water Parameters. *Remote Sensing, 8*(1). doi:10.3390/rs8010037

McCulloch, S., Meynecke, J.-O., Franklin, T., Franklin, W., Chauvenet, A. J. M., & Research, F. (2021). Humpback whale (*Megaptera novaeangliae*) behaviour determines habitat use in two Australian bays.

Mishra, D. R., Narumalani, S., Rundquist, D., & Lawson, M. (2005). Characterizing the vertical diffuse attenuation coefficient for downwelling irradiance in coastal waters: Implications for water penetration by high resolution satellite data. *ISPRS Journal of photogrammetry and remote sensing, 60*(1), 48-64. doi:https://doi.org/10.1016/j.isprsjprs.2005.09.003

Mumby, P., Clark, C., Green, E., & Edwards, A. (1998). Benefits of water column correction and contextual editing for mapping coral reefs. *International Journal of Remote Sensing, 19*(1), 203-210. doi:https://doi.org/10.1080/014311698216521

Niroumand-Jadidi, M., Vitti, A., & Lyzenga, D. R. (2018). Multiple Optimal Depth Predictors Analysis (MODPA) for river bathymetry: Findings from spectroradiometry, simulations, and satellite imagery. *Remote Sensing of Environment, 218*, 132-147.

Román, A., Tovar-Sánchez, A., Olivé, I., & Navarro, G. (2021). Using a UAV-Mounted Multispectral Camera for the Monitoring of Marine Macrophytes. *Frontiers in Marine Science*, 1225.

Schofield, G., Esteban, N., Katselidis, K. A., & Hays, G. C. (2019). Drones for research on sea turtles and other marine vertebrates – A review. *Biological Conservation, 238*. doi:https://doi.org/10.1016/j.biocon.2019.108214

Torres, L. G., Nieukirk, S. L., Lemos, L., & Chandler, T. E. (2018). Drone Up! Quantifying Whale Behavior From a New Perspective Improves Observational Capacity. *Frontiers in Marine Science, 5*. doi:https://doi.org/10.3389/fmars.2018.00319

Zoffoli, M. L., Frouin, R., & Kampel, M. (2014). Water column correction for coral reef studies by remote sensing. *Sensors, 14*(9), 16881-16931. doi:https://doi.org/10.3390/s140916881

4 ASSESSING THE EFFECTIVENESS OF UAV-BORNE THERMAL IMAGERY FOR WHALE DETECTION

4.1 ABSTRACT

Unoccupied aerial vehicles (UAVs) [3] provide flexibility when surveying vagile, highly mobile species, such as whales. However, UAV research to date has predominantly focused on detection with visual (RGB) sensors which are limited by light levels and require a clear contrast between an animal and its surrounds. Thermal infrared imaging enables the detection of animals in low light conditions and high water turbidity. Here we tested the whale detection capabilities of three sensors that allowed for synchronous visual (RGB) and thermal capture in a sheltered coastal embayment in NSW, Australia. The results highlight the importance of thermal sensor resolution for improving aerial detection. The highest resolution sensor (Zenmuse XT2) detected whales on the surface at distances over 500 m. The lowest resolution sensor (M2ED thermal camera) was unable to detect whales on the surface, however, could detect the thermal gradient of a whale's surface footprints, extending the available time for observation. Thermal images were often contaminated by sun glint, water surface roughness and angular effects on emissivity which can impact the discrimination of whale cues. UAV-borne thermal sensors can be used to complement data captured from visual sensors to enhance whale detection rates, but preliminary results indicate these sensors are not a viable option to replace visual sensors for daytime detection in marine environments.

4.2 INTRODUCTION

Growth in humpback whale (*Megaptera novaeangliae*) populations, particularly in the Southern Hemisphere (Wedekin et al., 2017; Noad et al., 2019), is likely to result in greater potential of whale exposure to vessel disturbances and acoustic energy, especially from naval and seismic vessels, which may impact on whale health and behaviour long-term (Dunlop et al., 2017). Areas of particular concern are humpback whale resting areas

[3] Also commonly referred to as drones, unmanned, uncrewed aerial vehicles, or remotely piloted aircraft system.

where mothers and calves rest in shallow protected embayments (Bruce et al., 2014; Bejder et al., 2019). These groups are especially vulnerable to disturbances due to their slower movements and high proportions of time spent resting in depths of less than 5 metres (Bejder et al., 2019; Iwata et al., 2021). However, whales are intrinsically difficult to observe and monitor, spending a significant proportion of time submerged, only surfacing for short periods (Nowacek et al., 2016), and exhibiting wide-ranging and unpredictable movement patterns (Schofield et al., 2019). These challenges highlight the need to evaluate the effectiveness of alternative UAV-borne methods for detection of whales in coastal waters.

Remote sensing methods enable synoptic coverage and high temporal resolution which are particularly beneficial in ecological surveys. Advancements in micro-UAV platforms (<5kg) and payloads including Inertial Measurement Units (IMUs), GPS receivers and image sensors has increased the commercialisation of these platforms (Turner et al., 2014; Nex et al., 2022). This has enabled the accessibility of ultra-high resolution remote sensing image data for marine wildlife surveys using methods that are both less obtrusive and repeatable over time and space (Anderson & Gaston, 2013; Christie et al., 2016). The flexibility afforded by UAV surveys is unparalleled by other survey approaches, including piloted aerial surveys, boat, or land surveys. Whilst larger, fixed-wing models can be used for transect surveys (Hodgson et al., 2013), smaller models, such as quadcopters, can be flown opportunistically (Horton et al., 2019) and launched from small boats (Christiansen et al., 2016). This is particularly advantageous for marine research when surveying vagile and often elusive animals. UAVs have enabled detection probabilities within the range of piloted aerial surveys for humpback whales (Hodgson et al., 2017). However, research until now has focused primarily on image detection based on the visual spectrum (RGB) with limited evaluation of thermal sensors for improving detection rates.

Traditional visual (RGB) imagery is subject to animal detection dependent on light levels, contrast of the target animal with their background habitat, and shadows that may mask targets (Hinke et al., 2022). One useful progression in UAV surveys is the improved payload capability for multiple passive sensors (e.g. optical RGB and thermal infrared) to be deployed simultaneously allowing synchronous image capture. Dual visible-thermal

camera methods have been demonstrated in wetland environments (McKellar et al., 2021).

Thermal infrared sensors generally provide a lower spatial resolution than many RGB or RGB-NIR sensors, but provide an alternative to detect animals, in low light conditions or turbid waters where the animal's surface temperature is warmer than the surrounding environment (Hughey et al., 2018; Verfuss et al., 2018; Burke et al., 2019). These sensors operate in two wavelength bands in the infrared portion of the infrared spectrum: 3–5 μm or mid-wave infrared (MWIR), and 8 - 12 μm or longwave infrared (LWIR). UAV-deployed thermal imaging systems have been demonstrated to outperform traditional, ground-based survey methods for the detection of arboreal mammals (Kays et al., 2018; Witt et al., 2020; McCarthy et al., 2022). Thermal sensing methods have also been effective for aerial surveys of marine mammal species that come ashore (pinnipeds and fissipeds) in open habitats, such as rocky substrates (Seymour et al., 2017; Gooday et al., 2018; Young et al., 2019; Christman et al., 2022) and snow (Smith et al., 2020). However, detecting temperature differentials using thermal methods is considerably less effective in the marine environment where infrared waves are rapidly attenuated by the water column. Cetacean species present further challenges: the insulative properties of their specialised blubber layer (Favilla et al., 2022) reduces the thermal contrast between the animal and surrounds, and the thin layer of water that covers the body when surfacing can partially or completely mask skin temperature. However, in cetacean surveys, additional cues are advantageous to thermal infrared detection, including: warm exhalations or blows (Horton et al., 2019), and the cold thermal signature of a cetaceans footprint where animal movement has disturbed the water column resulting in localised upwelling of colder water referred to as a thermal footprint (Churnside et al., 2009; Florko et al., 2021). Churnside et al. (2009) used a simple hydrodynamic model of the jet, generated by the upward movement of a humpback whale fluke, as it hits the water surface and disperses. They modelled the rate of turbulent mixing of the cooler water with the warmer surface water to estimate the magnitude of temperature change and rate of signature decay to explain the persistence of this thermal cue. Florko et al. (2021) found that infrared video complemented visible camera data in the detection of narwhals (*Monodon monoceros)* in high latitude waters with the footprint providing an indirect

indicator of animal presence. Although these methods are still in their infancy, the thermal detection of thermo-stratified water mixing associated with cetacean fluke movements has the potential to increase the duration of an animal's detectability.

This paper aims to: (1) analyse surface water thermal gradients associated with the presence of humpback whale(s) in temperate coastal waters; (2) review the trade-offs between three UAV-integrated thermal sensors to assess sensor resolution, radiometric capability, and the impact of payload size on launch and recovery options.

4.3 METHODS

4.3.1 Study Site

Jervis Bay is a semi-closed embayment situated along the New South Wales (NSW) coastline, approximately 180 km south of Sydney and approximately 115 km^2 in area (Figure 1). Jervis Bay appears to be an important resting ground for substock E1 (East Australian population) humpback whales on their southern migration from the Great Barrier Reef to Antarctic feeding grounds. October and November are the peak months of humpback whales, specifically mothers and calves, entering and resting in Jervis Bay (Sheehan & Blewitt, 2013; Bruce et al., 2014). During October and November, the average water temperature in the Bay is ~18°C and ~19°C, respectively. The Point Perpendicular headland (75 m elevation), at the northern end of Jervis Bay provides an optimal vantage point to observe whales travelling south and entering or bypassing the Bay. Due to the combination of reliable whale numbers resting on or near the water surface and calm weather conditions Jervis Bay is a suitable site for evaluating the use of UAV-borne sensors for detecting humpback whales.

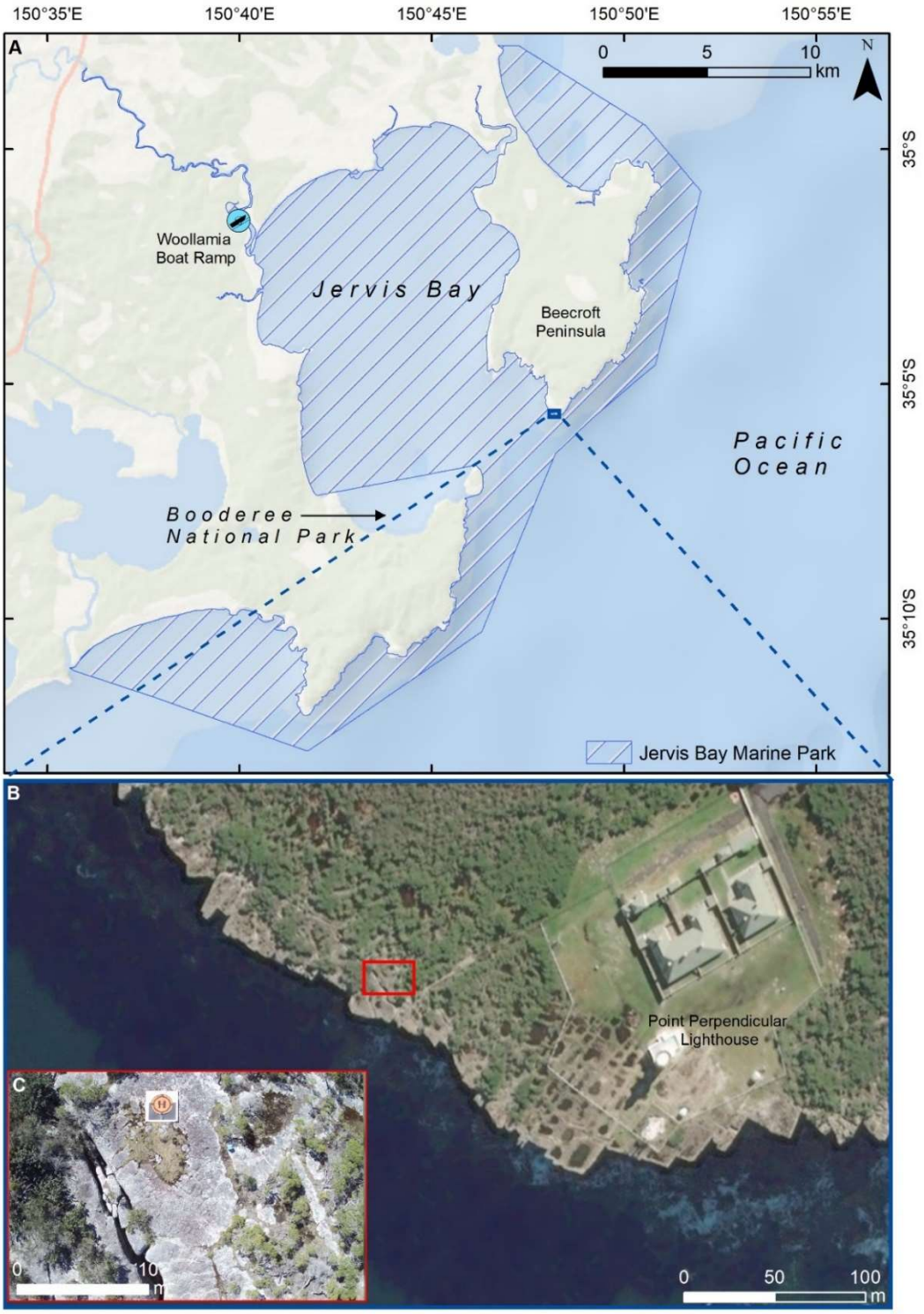

Figure 1. A) Study area highlighting the Jervis Bay Marine Park and UAV launch site; B) The UAV launch site in relation to the Point Perpendicular Lighthouse; C) Aerial image of launch site taken with UAV landing pad

4.3.2 UAV data capture

The visible (RGB) and thermal imaging capabilities for detecting humpback whale cues were evaluated using three UAV platforms: the DJI Matrice 600 Pro (M600 Pro), the DJI Mavic 2 Enterprise Dual (M2ED), and the DJI Mavic 2 Enterprise Advanced (M2EA). All three thermal cameras were uncooled micro-bolometer imaging sensors but differed in resolution (Table 1).

Jervis Bay is a restricted airspace and UAV flights are only approved during times the airspace are not in military use. This restricted the window of survey opportunity to weekends and specified one-two hour time blocks during weekdays often approved at short notice.

UAV surveys were flown in October 2019 using the M600 Pro (Figure 2, Table 1) equipped with a DJI infrared Zenmuse XT2 sensor (FLIR® Tau 2 Thermal, radiometric). The M600 Pro was launched from a portable wooden pad on a flat section of the headland away from the cliff edge and vegetation in accordance with environment and heritage permits and fire safety requirements (Figure 1). A headland launch site was chosen to capture whales travelling into Jervis Bay following the coastline. This behaviour had been observed in a previous survey (Jones, 2019), and the location was optimal for ensuring the highest probability of capturing imagery over whales whilst complying with UAV operational restrictions. This includes the UAV remaining within a one-kilometre radius from the launch site and within the pilot's visual line-of-sight.

The UAV was launched once whales were in line of sight from the headland launch site with the assistance of trained observers surveying from the Point Perpendicular Lighthouse (130 metres from the launch site). The UAV was flown at an altitude of 100 m above sea level until whales were spotted by the UAV pilot using the live video feed. The altitude was then lowered to a height at or above 50 m during the observation leg of the flight. The FLIR thermal imaging sensor captured video (RGB and thermal infrared) for the entire flight duration. The remote video feed captured from the FLIR thermal sensor was used by the operator to maintain real-time sight of the whales.

Figure 2. The DJI Matrice 600 Pro with mounted DJI infrared Zenmuse XT2 sensor shown on the launch pad (left) and in flight (right).

To compare the thermal and visible capabilities of small, boat-deployed UAV's, the M2ED and M2EA were launched from and landed on a 5.9 metre research boat within Jervis Bay in 2019 and 2021, respectively (see Table 1 for dates). Both UAV models had an integrated dual camera and gimbal system and were the most suitable light-weight UAV options for launching and landing on a small boat. The M2EA was released by DJI in 2020 and provided improved pixel resolution for both thermal and RGB sensors (Table 1). The Bay was visually scanned by researchers on the vessel. Following a confirmed whale sighting, the whale's behaviour and direction of travel were observed for five minutes from the boat at a distance >300 m before an approach was made to a distance >100 m from the whale(s).

The UAVs were launched and landed using a portable wooden platform at the stern of the boat (Figure 3). The initial launch altitude was 55 m to provide sufficient sensor field of view for identifying the whale. The UAV pilot viewed the live feed (visible mode) throughout the flight and lowered the altitude to ≥ 25 m once the whales were visible on the controller screen. As soon as whales were no longer visible in the live feed, the UAV was raised to an altitude >50 m. The vessel remained at a distance >100 m from the whales during the flights to provide a clear line of sight to the UAV and facilitate positioning over the whales. Still images and videos were captured throughout the flight and GPS location timestamped.

During all survey days, environmental conditions were favourable for sighting whales. Surveys were conducted when there was no rain, visibility was >5 km with clear skies, and sea state at or below Beaufort force 2.

Figure 3. The DJI Mavic 2 Enterprise Dual on the launch pad at the stern of the boat (left) and in flight (right).

Table 1. Summary of the survey dates and sensor resolution of the three UAV models, flown over humpback whales in Jervis Bay.

UAV model	Sensors	Sensor Resolution	Thermal accuracy	Dates flown	No. of flights/total flight duration (nearest min.)
Matrice 600 Pro	Zenmuse XT2 thermal (7.5-13.5 µm), true radiometric	640×512 @ 30Hz	Not stated	18 – 20, 25 – 27 Oct 2019	8 flights, 104 minutes
	Zenmuse XT 2 visual RGB	1/1.7" CMOS Effective Pixels: 12 M			
Mavic 2 Enterprise Dual	Thermal (8 – 14 µm)	160×120	± 5%	31 Oct, 3 Nov 2019	8 flights, 47 minutes
	Visual RGB, non radiometric, Uncooled VOx Microbolometer	1/2.3" CMOS ; Effective pixels:12 M			
Mavic 2 Enterprise Advanced	Thermal (8 – 14 µm)	640×512 @ 30Hz	± 2°C or 2% (whichever is greatest)	23, 28 Oct 2021	21 flights, 76 minutes
	Visual RGB, non radiometric, Uncooled VOx Microbolometer	1/2" CMOS, Effective Pixels: 48 M			

4.3.3 Thermal image processing

Thermal videos taken from the DJI infrared Zenmuse XT2 sensor on the DJI Matrice 600 Pro were reviewed using the FLIR Tools® software. The videos were scanned using the FLIR 'ironbow' false colour palette which is effective for quick manual identification of thermal anomalies. For each video, the temperature scale was adjusted for optimal image

brightness and contrast to maximise the thermal gradients of small brighter objects (i.e. whales and boats). Whale cues detected in the thermal video were verified with the RGB videos and theodolite observations. Thermal videos and images taken from the DJI M2ED were not radiometric and consequently could not be scaled using FLIR Tools®. Thermal videos were manually reviewed for the presence of thermal anomalies. In sequences where anomalies were evident, the corresponding RGB video was reviewed. For both the thermal and RGB video, the sequences were extracted to static image files at an interval (e.g., three seconds) determined most appropriate to highlight the movement in the video. The thermal images taken from the DJI M2EA were analysed using DJI Thermal Analysis Tools 2.1 ©, compatible with the M2EA. Videos were not recognised by this software. Although advertised as producing radiometric images, the images and videos were not recognised as radiance images by FLIR Tools ®. Images were reviewed using the 'Iron Red' false colour palette to highlight nuanced differences in heat signatures and was the closest match to 'ironbow' for comparison with footage from the Zenmuse XT sensor. Videos from the M2EA were processed following the same methods as videos from the M2ED. A sample of two images or sequences were selected from each UAV to demonstrate their respective detection capabilities.

4.3.4 Permit statement

Fieldwork activities were compliant with guidelines and regulatory requirements under permits authorization by the University of Sydney Animal Ethic Committee (permit 2019/1592), the Department of Primary Industries Marine Parks (permit MEAA19/179) and the Department of Planning, Industry and Environment, New South Wales (SL102287). Compliant with the Australian Civil Aviation Authority (CASA) all UAV flights were within visual line of sight. UAV flight approval within the Restricted Airspaces (R421A Nowra and R452 Beecroft Head) overlapping the Jervis Bay study site was obtained from the Australian Department of Defence.

4.4 RESULTS

Whales were detected in the video images taken from both thermal and RGB sensors of the Zenmuse XT2 (DJI Matrice 600 Pro) (Figure 4). The sea surface temperature (SST) was ~18°C and atmospheric temperature was ~17.5°C at time of image capture.

The oblique images in Figure 4A were captured at 1113 AEDT, at an altitude of 92 m, when the solar azimuth was 41.72 ° and solar elevation was 54.89 °. The visible and thermal signature of a whale on the surface and boats were detected at a distance of 478 m. The oblique images in Figure 4B were captured at 1821 AEDT, at an altitude of 86 m, when the solar azimuth was 267.53 ° and solar elevation was 8.71 °. The visible and thermal footprint of a whale breaching was detected at a distance of 548 m.

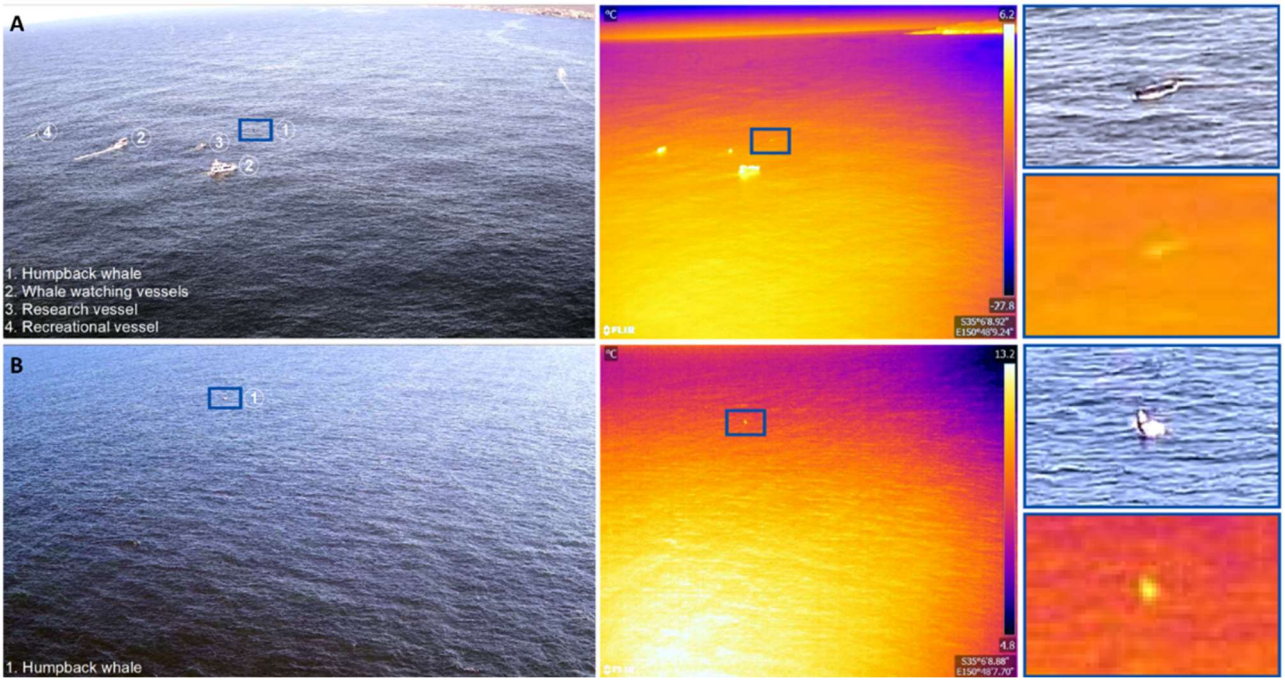

Figure 4. Humpback whale detected in RGB (left) and thermal (right) sensors at distances of A) 478 m and B) 548 m.

In the images captured by the DJI Mavic 2 Enterprise Dual (M2ED) thermal sensor, the thermal signature of colder water upwelled by the whale fluke when diving (Figure 5) or swimming (Figure 6) was observed. The SST was ~19°C and atmospheric temperatures were ~17.5°C and ~21°C at time of image capture for Figures 5 and 6, respectively. In both figures the whale's footprints, shown by the smooth surface of the water in the visual (RGB) images, are captured as a distinct surface temperature gradient in the thermal images. In Figure 6, the thermal signature of the whale's footprint was evident after the visual footprint had dissipated. The thermal signature of a whale on the surface was not detected in any of the thermal footage taken from the M2ED.

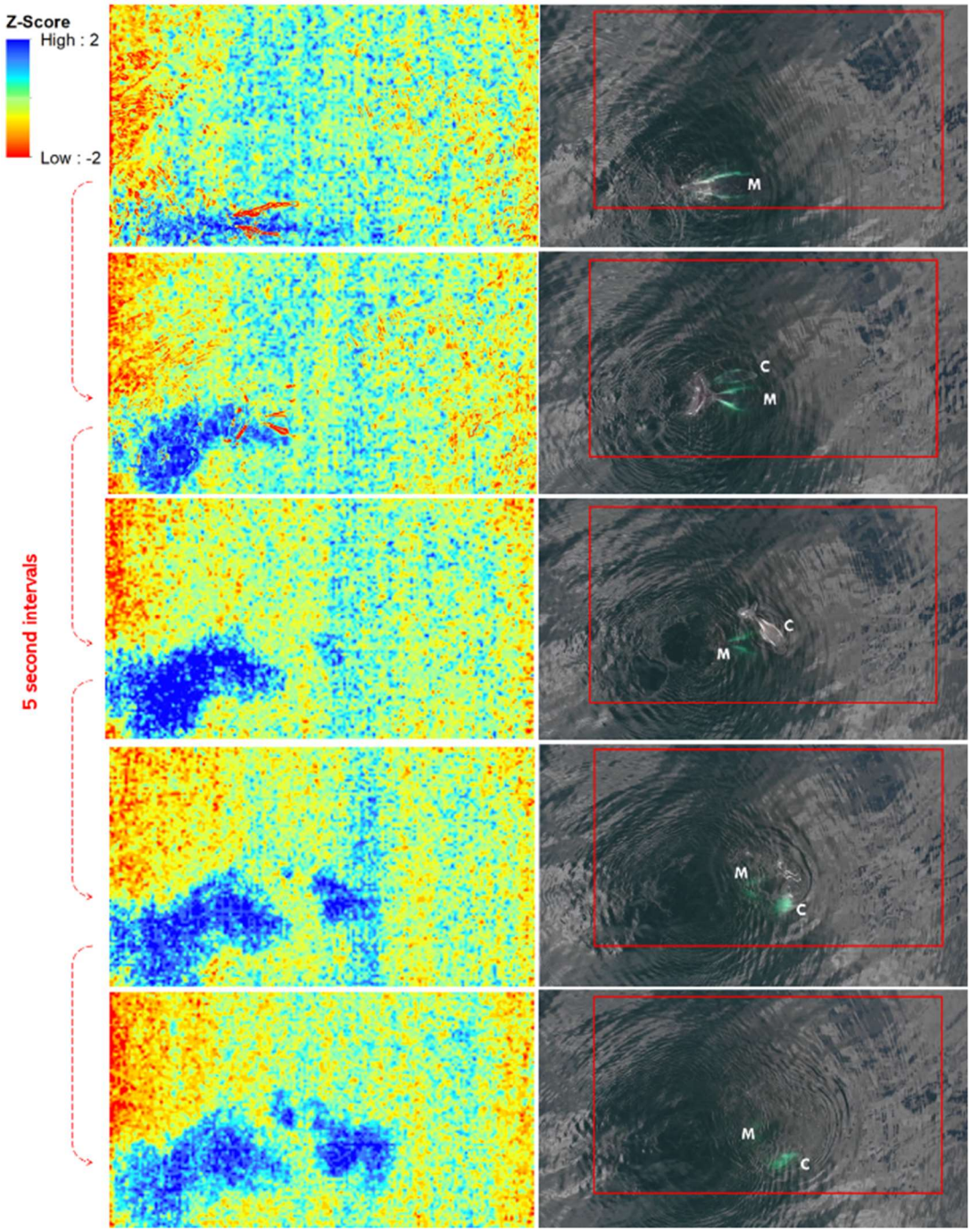

Figure 5. A comparison of synchronous thermal (left) and visual (RGB, right) images taken of a whale's footprint. The whale's outline, visible in the top two thermal images, was enhanced in the FLIR MSX® (Multi-Spectral Dynamic Imaging) product, which adds visible light details to thermal images. To represent deviation from the mean, the thermal images are represented as anomalies. The red outline illustrates the extent of the thermal image within the visual RGB image. M and C denote the mother (M) and calf (C) humpback whale. Image sequence capture began at 1108 AEDT.

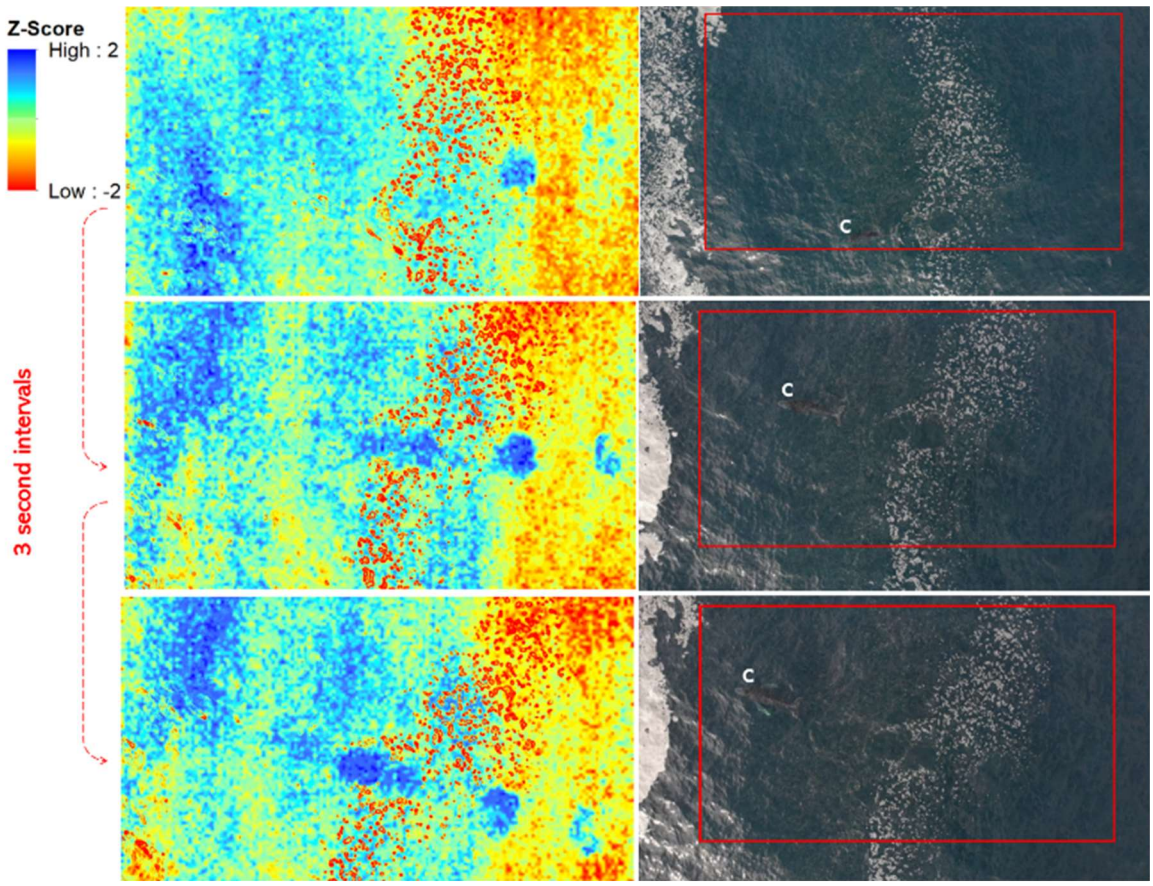

Figure 6. A comparison of synchronous thermal (left) and visual (RGB, right) images taken of a whale's footprint. To represent deviation from the mean, the thermal images are represented as anomalies and coloured in ArcGIS. The red outline illustrates the extend of the thermal image compared to the visual RGB image. C denotes the calf humpback whale. Image sequence was taken on 3 November 2019. Capture began at 0824 AEDT.

Similarly, the thermal sensor on DJI Mavic 2 Enterprise Advanced (M2EA), was able to detect the thermal gradient of the whale's footprint (Figure 7A). In the corresponding RGB image, the footprint is also evident as a smooth slick on the water surface. The observed temperature difference between footprint and surrounding water was 1.3°C. This sensor was also able to detect the thermal signature of whales on the surface (Figure 7B). The calf's blowhole was the warmest detected feature in the image (23.4°C ± 2°C). The calculated temperature difference between the whale and adjacent water was of 1.3°C. The sea surface temperature was ~18°C and atmospheric temperature was ~18°C at time of image capture.

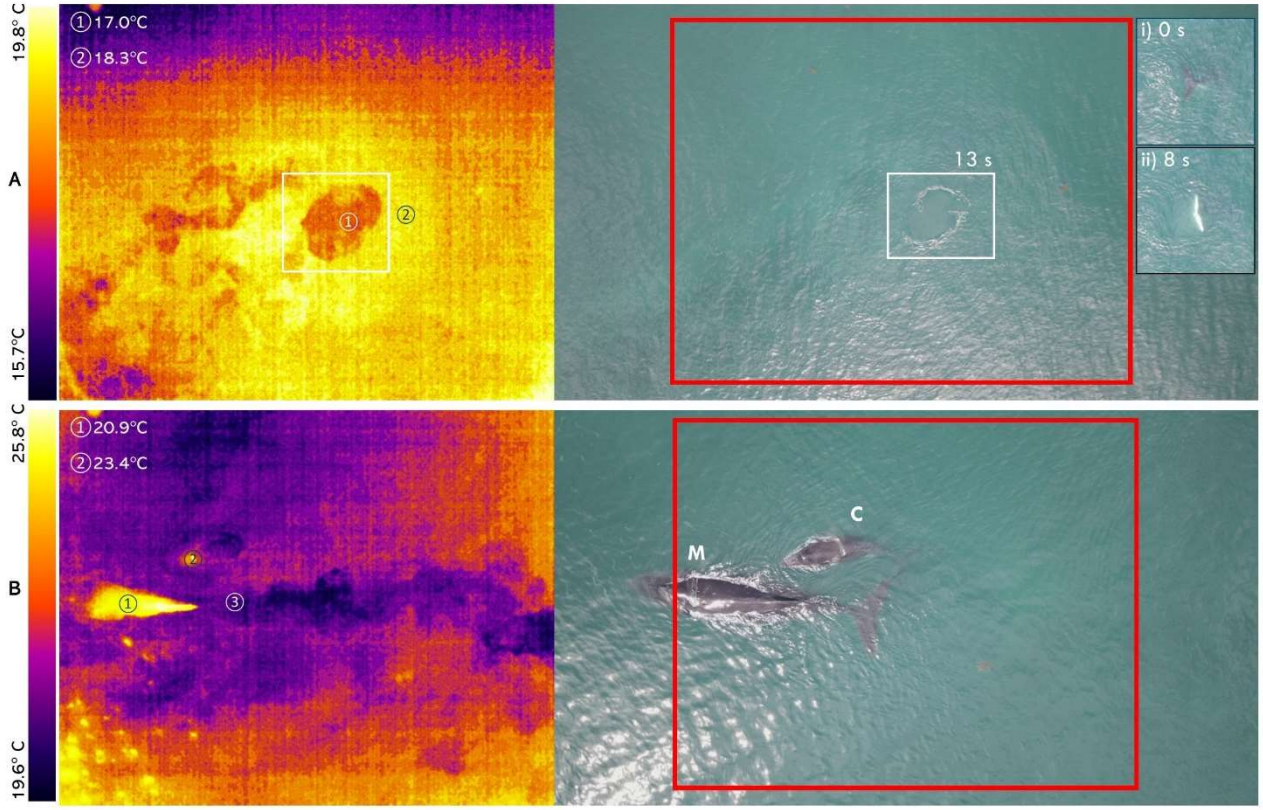

Figure 7. A) A comparison of synchronous thermal (left) and visual (RGB, right) images taken of a whale's footprint (A) and mother and calf humpback whale on the surface (B). A) Images were taken on 28 October 2021 at A) 1035 AEDT, at an altitude of 55 m, and B) at 1038 AEDT, at an altitude of 42 m. Inset images (i) and (ii) are clipped to illustrate the formation of the footprint with images (ii) and A taken 8 and 13 seconds after image (i), respectively. The red outline illustrates the extent of the thermal image compared to the visual RGB image. The white outline highlights the footprint in the image. M denotes the mother humpback whale, and C denotes the calf.

4.5 DISCUSSION

UAV thermal sensing methods can be used to detect whales based on thermal signatures characteristic of both direct (body on the surface) and indirect (footprint) cues. The efficacy of these methods is influenced by sensor resolution (microbolometer sensitivity) and focal length, sea state conditions and emissivity effects. Whales were detected in images acquired from all three UAV-borne thermal sensors but differences in thermographic accuracy between sensors impacted the types of cues observed. Previous studies on surface water temperature differentials generated by whale movements have been restricted to colder waters (Churnside et al., 2009; Florko et al., 2021; Lonati et al.,

2022). Findings from this study demonstrated the abilty to detect these thermal contrasts in temperate waters (~19°C SST).

Synchronous capture of thermal and visual (RGB) imagery highlighted the benefits of utilising thermal imagery to complement visual (RGB) imagery. Direct whale were cues detected from the higher resolution sensors (Zenmuse XT2 and M2ED), however, these were limited to detecting whale(s) for brief periods (<5 seconds) when they were surfacing. This is not comparable with the increased observation capacity of submerged whales provided by UAV-borne visual (RGB) sensors (Torres et al., 2018). However, our results highlight the advantage of the thermal detection of indirect cues. The temperature differential associated with a whale's footprint persisted beyond the period the whale was visible at the surface, increasing observation time. Florko et al. (2021) reported that of 29 narwhals detected using thermal sensors from a piloted aerial survey, 100% left footprints that were detected in a thermal sensor. This highlights the potential for these methods to be used to track whale movments. However, the flight altitude (e.g., altitude of 300 m and 305 m in Churnside et al., 2009 and Florko et al., 2021, respectively) and continuous flight time afforded by piloted aerial surveys, or fixed wing UAV models (Hodgson et al., 2017), are likely necessary to track movements. In comparison, smaller UAV models, as flown in this research, have flight times limited ~30 minutes (Table 2). Even with the benefits of thermal sensors for detection of indirect whale cues, visual (RGB) sensors are required to provide information on species, size of the whale(s), and counts of individuals (Florko et al., 2021).

Emisivity defines the efficiency with which an object radiates energy compared to a blackbody (Handcock et al., 2012). Due to lower levels of background emisivity in data recorded from thermal sensors operating horizontally from the surface, they have previously been considered more effective in detecting cetacean blows than sensors recording on the nadir (Churnside et al., 2009). Ocean surface roughness, refractive index, and the zenith angle from which the surface is being observed (Masuda et al., 1988) will influence the noise associated with emissivity in UAV captured thermal imagery. Depending on the angle of capture, emissivity associated with rough ocean water could mask whale cues, but this physical property can also be adventagous. We found that thermal image captured on an oblique geometric angle can generate greater IR signal

contrast as a whale breaks the water surface due to emissivity effects. An increased view geometry achieved from an elevated UAV platform can result in stronger thermal contrast.

The thermal gradient associated with the footprints were still observable after the footprint had dissipated in the visual images, prolonging the availability of the whale for detection. The temperature gradient between footprint and surrounding waters was 1.3˚C, highlighting the thermal stratification in Jervis Bay, as modelled by Liao and Wang (2018). Comparing our detection of footprints in temperate waters, with comparable results in Arctic (Florko et al., 2021) and subarctic waters (Churnside et al., 2009), it is apparent that absolute temperature does not impact the contrast, however, a temperature gradient between the surface and subsurface layer is required (Lonati et al., 2022). Further research is needed to assess how environmental conditions (e.g. sea surface temperature and sea state) and an animal's behaviour influence detectability from an aerial viewpoint.

The distinguishable circular shapes of whale footprints is evident in Figures 6 and 7A and more so in Churnside et al. (2009) who detected the thermal footprints of north Atlantic right whales (*Eubalaena glacialis*) and humpback whales using a thermal infrared camera mounted on a piloted aircraft. The ability to detect whales using the thermal gradient of footprints without visual confirmation requires further investigation, however these results demonstrate a novel use for thermal sensor capabilities and potential for enhanced machine learning techniques for whale detection.

4.5.1 Thermal sensor comparison

Although simultaneous thermal and visual (RGB) imagery was captured directly above a humpback whale mother-calf group using both the M2ED and M2EA, the M2ED had limited capability for detecting thermal signature gradients associated with the presence of a whale on the water surface. However, both these non-radiometric thermal sensors, were able to detect thermal footprints (Figures 5, 6, and 7A). The clear advantage of the Zenmuse XT2 sensor was the long-distance thermal gradient detection capability with whales detected on the surface at 478 m and a whale breach detected at 548 m (Figure 4). Potential issues in the application of UAV-borne thermal infrared sensors include; the

distance between the camera and target object, emissivity of the target object, humidity, temperature of surrounding objects, atmospheric attenuation, sensitivity of the sensor which can detect thermal radiation from the camera interior, and the non-uniformity correction (NUC) which offsets temperature change which is affected by wind and sudden temperature changes (Kelly et al., 2019). Here we assess the trade-offs between UAV platform/payload, subsequent launch/landing site options and thermographic accuracy (Table 2).

In determining an optimal UAV payload and platform for thermal detection of whales, compromises are reached between price, flexibility in flight mission, thermal sensor resolution, and radiometric calibration. Sensor sensitivity and accuracy increases with cost with a significance price difference between the true radiometric thermal Zenmuse XT2 sensor and the non-radiometrically calibrated inbuilt thermal sensor on the M2ED (Table 2) which only provides relative temperature differences (Kelly et al., 2019). Cost and smaller payloads are the only advantage of the non-radiometric thermal sensors over higher-end radiometric thermal sensors for detecting temperature gradients or anomalies (Horton et al., 2019). Studies involving accurate recordings of body temperature will require radiometric calibration, however, for detection purposes directly above the whale (temperature gradients and anomalies) non-radiometric thermal data is sufficient.

The advantage of the radiometric Zenmuse XT2 thermal sensor is that it captures temperature data in every pixel within the image providing accurate relative measurements of surface temperature. However, the distance between the sensor and whale target, and atmospheric conditions, may reduce the detectability of the gradient between the surface temperature of the whale and the background (i.e., water and atmosphere). This study demonstrated that surfacing humpback whales can be detected on the oblique at distances >500 metres in images acquired from the Zenmuse XT2. The threshold performance of high-end radiometric thermal sensors for the detection of whales at distance would need to be systematically assessed both during daylight and low light conditions to determine their potential detection capability within management areas that have regulated distances such as whale impact zones.

The larger payload of the Zenmuse XT2 meant it was unsuited to launch and recovery from a small research vessel. There were logistical difficulties associated with surveying fast moving animals from a static point on land. The flexibility of boat launch and recovery afforded by the M2ED/M2EA eliminated many of the issues encountered launching a UAV from land. Once the humpback whales had been located launching the UAV and positioning it directly above the whales was relatively simple for a trained UAV operator providing the UAV settings are updated for safe landing on a boat. These will depend on UAV model but include updating the home point during flight and turning off obstacle avoidance sensors and landing protection to allow UAV landing on a moving object. It is necessary to sight the target whales through the visual (RGB) live feed during the flight (Horton et al., 2019), a UAV model that allows for thermal capture using a visible display mode should be prioritised, as was possible with the M2EA but not the M2ED.

The Zenmuse XT2 sensor on the M600 Pro and the inbuilt thermal sensors on the M2ED and M2EA have demonstrated that simultaneous thermal image capture from multiple sensors is possible. Dual sensor UAV payloads eliminate the need for multiple flights to capture images from different sensors, an issue identified by Horton et al. (2019) when collecting biometrical thermal data. Surveys involving fast moving animals, such as whales, that rely on multiple consecutive flight missions to capture data from different UAV platforms will present logistical constraints due to the likelihood that the target whale/s will be out of range within a short timeframe.

Table 2. Summary of the trade-offs between the three UAV platforms and sensors used in this study. Using the same Zenmuse XT sensor, Horton et al. (2019) detected the thermal signature of whales on the surface. *Advertised as radiometric but images/videos captured were not true radiometric.

	Matrice 600 Pro with XT2 sensor	**Mavic 2 Enterprise Dual**	**Mavic 2 Enterprise Advanced**
Radiometric	Yes	No*	No*
Price (approx. AUD)	UAV: $7,500 Zenmuse XT2: $20,000	$4,500 off the shelf	$10,000 off the shelf
Multiple payloads	Yes - 6 kg payload capacity	No	No
Flight time (approx. minutes)	18 (with payload) 35 (no payload)	30	31
Dimensions (LxWxH mm)	1668×1518×727	322×242×84	322×242×84
Max takeoff weight (kg)	15.5	1.1	1.1
Thermal detection of whales on the surface	Yes[1]	No	Yes

4.6 CONCLUSIONS

Here we demonstrated that a high resolution, radiometrically calibrated sensor (Zenmuse XT2) was able to detect the direct cues of whales above the water surface at distances > 500 metres. Synchronous visual (RGB) and thermal capture showed that footprints were detectable in the thermal sensors after they were no longer evident in the visual RGB sensor images, extending whale observation time. This demonstrated the thermal footprint of a whale signature could be detected in temperate waters by low resolution thermal sensors. These results highlight that UAV-borne thermal sensors can be used to complement data captured from visual sensors to enhance whale detection rates but are not a viable option to replace visual sensors for daytime detection in marine environments.

4.7 REFERENCES

Anderson, K., & Gaston, K. J. (2013). Lightweight unmanned aerial vehicles will revolutionize spatial ecology. *Frontiers in Ecology and the Environment, 11*(3), 138-146. doi:https://doi.org/10.1890/120150

Bejder, L., Videsen, S., Hermannsen, L., Simon, M., Hanf, D., & Madsen, P. T. (2019). Low energy expenditure and resting behaviour of humpback whale mother-calf pairs highlights conservation importance of sheltered breeding areas. *Scientific Reports, 9*(1), 771. doi: https://doi.org/10.1038/s41598-018-36870-7

Bruce, E., Albright, L., Sheehan, S., & Blewitt, M. (2014). Distribution patterns of migrating humpback whales (*Megaptera novaeangliae*) in Jervis Bay, Australia: A spatial analysis using geographical citizen science data. *Applied Geography, 54*, 83-95. doi:https://doi.org/10.1016/j.apgeog.2014.06.014

Burke, C., Rashman, M., Wich, S., Symons, A., Theron, C., & Longmore, S. (2019). Optimizing observing strategies for monitoring animals using drone-mounted thermal infrared cameras. *International Journal of Remote Sensing, 40*(2), 439-467. doi:10.1080/01431161.2018.1558372

Christiansen, F., Dujon, A. M., Sprogis, K. R., Arnould, J. P., & Bejder, L. (2016). Noninvasive unmanned aerial vehicle provides estimates of the energetic cost of reproduction in humpback whales. *Ecosphere, 7*(10), e01468. doi: https://doi.org/10.1002/ecs2.1468

Christie, K. S., Gilbert, S. L., Brown, C. L., Hatfield, M., & Hanson, L. (2016). Unmanned aircraft systems in wildlife research: current and future applications of a transformative technology. *Frontiers in Ecology and the Environment, 14*(5), 241-251. doi:10.1002/fee.1281

Christman, C. L., London, J. M., Conn, P. B., Hardy, S. K., Brady, G. M., Dahle, S. P., . . . Ziel, H. L. (2022). Evaluating the use of thermal imagery to count harbor seals in aerial surveys. *Mammalian Biology*. doi:10.1007/s42991-021-00191-6

Churnside, J., Ostrovsky, L., & Veenstra, T. (2009). Thermal Footprints of Whales. *Oceanography, 22*(1), 206-209. doi:10.5670/oceanog.2009.20

Dunlop, R. A., Noad, M. J., McCauley, R. D., Scott-Hayward, L., Kniest, E., Slade, R., . . . Cato, D. H. (2017). Determining the behavioural dose–response relationship of marine

mammals to air gun noise and source proximity. *Journal of Experimental Biology, 220*(16), 2878-2886.

Favilla, A. B., Horning, M., & Costa, D. P. (2022). Advances in thermal physiology of diving marine mammals: The dual role of peripheral perfusion. *Temperature, 9*(1), 46-66.

Florko, K. R. N., Carlyle, C. G., Young, B. G., Yurkowski, D. J., Michel, C., & Ferguson, S. H. (2021). Narwhal (*Monodon monoceros*) detection by infrared flukeprints from aerial survey imagery. *Ecosphere, 12*(8). doi:10.1002/ecs2.3698

Gooday, O. J., Key, N., Goldstien, S., & Zawar-Reza, P. (2018). An assessment of thermal-image acquisition with an unmanned aerial vehicle (UAV) for direct counts of coastal marine mammals ashore. *Journal of Unmanned Vehicle Systems, 6*(2), 100-108. doi:10.1139/juvs-2016-0029

Handcock, R. N., Torgersen, C. E., Cherkauer, K. A., Gillespie, A. R., Tockner, K., Faux, R. N., & Tan, J. (2012). Thermal infrared remote sensing of water temperature in riverine landscapes. *Fluvial remote sensing for science and management*, 85-113.

Hinke, J. T., Giuseffi, L. M., Hermanson, V. R., Woodman, S. M., & Krause, D. J. (2022). Evaluating Thermal and Color Sensors for Automating Detection of Penguins and Pinnipeds in Images Collected with an Unoccupied Aerial System. *Drones, 6*(9), 255.

Hodgson, A., Kelly, N., & Peel, D. (2013). Unmanned aerial vehicles (UAVs) for surveying marine fauna: a dugong case study. *PLoS One, 8*(11), e79556. doi:10.1371/journal.pone.0079556

Hodgson, A., Peel, D., & Kelly, N. (2017). Unmanned aerial vehicles for surveying marine fauna: assessing detection probability. *Ecological Applications, 27*(4), 1253-1267. doi:https://doi.org/10.1002/eap.1519

Horton, T. W., Hauser, N., Cassel, S., Klaus, K. F., Fettermann, T., & Key, N. (2019). Doctor Drone: Non-invasive Measurement of Humpback Whale Vital Signs Using Unoccupied Aerial System Infrared Thermography. *Frontiers in Marine Science, 6*. doi:10.3389/fmars.2019.00466

Hughey, L. F., Hein, A. M., Strandburg-Peshkin, A., & Jensen, F. H. (2018). Challenges and solutions for studying collective animal behaviour in the wild. *Philosophical Transactions of Royal Society B Biological Science, 373*(1746). doi:10.1098/rstb.2017.0005

Iwata, T., Biuw, M., Aoki, K., Miller, P. J. O. M., & Sato, K. J. B. p. (2021). Using an omnidirectional video logger to observe the underwater life of marine animals: Humpback whale resting behaviour. *Behavioural processes, 186*, 104369.

Jones, A., Bruce, E., Cato, D., Davies, K. (2019). *Tracking of humpback whales by theodolite from Point Perpendicular, Jervis Bay: Fieldwork Report 2018*. unpublished report University of Sydney. *unpublished report*.

Kays, R., Sheppard, J., McLean, K., Welch, C., Paunescu, C., Wang, V., . . . Crofoot, M. (2018). Hot monkey, cold reality: surveying rainforest canopy mammals using drone-mounted thermal infrared sensors. *International Journal of Remote Sensing, 40*(2), 407-419. doi:10.1080/01431161.2018.1523580

Kelly, J., Kljun, N., Olsson, P.-O., Mihai, L., Liljeblad, B., Weslien, P., . . . Eklundh, L. (2019). Challenges and Best Practices for Deriving Temperature Data from an Uncalibrated UAV Thermal Infrared Camera. *Remote Sensing, 11*(5). doi:10.3390/rs11050567

Kniest, E. Visual and Acoustic Detection and Ranging at Sea (VADAR) (Version 2.0). University of Newcastle.

Liao, F., & Wang, X. H. (2018). A numerical study of coastal-trapped waves in Jervis Bay, Australia. *Journal of Physical Oceanography, 48*(11), 2555-2569.

Lonati, G. L., Zitterbart, D. P., Miller, C. A., Corkeron, P., Murphy, C. T., & Moore, M. J. (2022). Investigating the thermal physiology of Critically Endangered North Atlantic right whales *Eubalaena glacialis* via aerial infrared thermography. *Endangered Species Research, 48*, 139-154.

Masuda, K., Takashima, T., & Takayama, Y. J. R. S. o. E. (1988). Emissivity of pure and sea waters for the model sea surface in the infrared window regions. *24*(2), 313-329.

McCarthy, E. D., Martin, J. M., Boer, M. M., & Welbergen, J. A. (2022). Ground-based counting methods underestimate true numbers of a threatened colonial mammal: an evaluation using drone-based thermal surveys as a reference. *Wildlife Research*.

McKellar, A. E., Shephard, N. G., & Chabot, D. (2021). Dual visible-thermal camera approach facilitates drone surveys of colonial marshbirds. *Remote Sensing in Ecology and Conservation, 7*(2), 214-226.

Nex, F., Armenakis, C., Cramer, M., Cucci, D. A., Gerke, M., Honkavaara, E., . . . Skaloud, J. (2022). UAV in the advent of the twenties: Where we stand and what is next. *ISPRS Journal of photogrammetry and remote sensing, 184*, 215-242.

Noad, M. J., Kniest, E., & Dunlop, R. A. (2019). Boom to bust? Implications for the continued rapid growth of the eastern Australian humpback whale population despite recovery. *Population Ecology, 61*(2), 198-209. doi:10.1002/1438-390x.1014

Nowacek, D. P., Christiansen, F., Bejder, L., Goldbogen, J. A., & Friedlaender, A. S. (2016). Studying cetacean behaviour: new technological approaches and conservation applications. *Animal Behaviour, 120*, 235-244. doi:10.1016/j.anbehav.2016.07.019

Schofield, G., Esteban, N., Katselidis, K. A., & Hays, G. C. (2019). Drones for research on sea turtles and other marine vertebrates – A review. *Biological Conservation, 238*. doi:https://doi.org/10.1016/j.biocon.2019.108214

Seymour, A. C., Dale, J., Hammill, M., Halpin, P. N., & Johnston, D. W. (2017). Automated detection and enumeration of marine wildlife using unmanned aircraft systems (UAS) and thermal imagery. *Sci Rep, 7*, 45127. doi:10.1038/srep45127

Sheehan, S., & Blewitt, M. (2013). *Jervis Bay: an Area of Significance for Southward Migrating Humpback Whale Cow/Calf Pairs?* Paper presented at the Australian Marine Science Association (AMSA), Gold Coast, Queensland, Australia.

Smith, T. S., Amstrup, S. C., Kirschhoffer, B., & York, G. (2020). Efficacy of aerial forward-looking infrared surveys for detecting polar bear maternal dens. *PLoS One, 15*(2), e0222744.

Torres, L. G., Nieukirk, S. L., Lemos, L., & Chandler, T. E. (2018). Drone Up! Quantifying Whale Behavior From a New Perspective Improves Observational Capacity. *Frontiers in Marine Science, 5*. doi:https://doi.org/10.3389/fmars.2018.00319

Turner, D., Lucieer, A., Malenovský, Z., King, D. H., & Robinson, S. A. (2014). Spatial co-registration of ultra-high resolution visible, multispectral and thermal images acquired with a micro-UAV over Antarctic moss beds. *Remote Sensing, 6*(5), 4003-4024.

Verfuss, U. K., Gillespie, D., Gordon, J., Marques, T. A., Miller, B., Plunkett, R., . . . Thomas, L. (2018). Comparing methods suitable for monitoring marine mammals in low

visibility conditions during seismic surveys. *Marine Pollution Bulletin, 126*, 1-18. doi:10.1016/j.marpolbul.2017.10.034

Wedekin, L. L., Engel, M. H., Andriolo, A., Prado, P. I., Zerbini, A. N., Marcondes, M. M. C., . . . Simões-Lopes, P. C. (2017). Running fast in the slow lane: rapid population growth of humpback whales after exploitation. *Marine Ecology Progress Series, 575*, 195-206. doi:10.3354/meps12211

Witt, R. R., Beranek, C. T., Howell, L. G., Ryan, S. A., Clulow, J., Jordan, N. R., . . . Roff, A. (2020). Real-time drone derived thermal imagery outperforms traditional survey methods for an arboreal forest mammal. *PLoS One, 15*(11), e0242204. doi:10.1371/journal.pone.0242204

Young, B. G., Yurkowski, D. J., Dunn, J. B., & Ferguson, S. H. (2019). Comparing infrared imagery to traditional methods for estimating ringed seal density. *Wildlife Society Bulletin, 43*(1), 121-130.

5 OPTIMISING THE USE OF THERMAL INFRARED IMAGERY FOR MITIGATING IMPACTS OF CETACEANS AND HUMAN INTERACTIONS: A REVIEW AND CASE STUDY

5.1 ABSTRACT

With increasing potential for anthropogenic impact on cetacean species there is a need to improve current methods, reliant on visual detection, to increase detection rates. Thermal imaging systems have been proposed as a solution to provide effective, round the clock detection of cetaceans. However, there has been limited evaluation of how thermal sensor configuration may influence detection rates. Here we tested the thermal capabilities of three sensors that differed in sensor resolution, detector temperature, and spectral range, for the detection of bottlenose dolphins. Additionally, we present a review of how cetacean cues and environmental factors will influence the effectiveness of automated detection systems. All three sensors sufficiently detected dolphins at distances of ~1km, however, the cooled high resolution sensor provided enhanced clarity of dolphin cues at greater distances. Six research studies that have used thermal imaging systems for the detection of whales from ship or shore platforms were identified. These studies highlighted that current automated detection methods are unable to detect cetaceans to a species level and high rates of false detections are delaying potential use for mitigation. There is a need to evaluate the efficiency of innovative thermal sensor platforms for improved detection rates and low levels of false detections.

5.2 INTRODUCTION

Expansion of the 'blue economy' and associated investment in ocean development and infrastructure including offshore renewable energy (Dolman et al., 2003), shipping, commercial fishing (Davies & Brillant, 2019), mining (Thompson et al., 2023), and naval operations is projected to increase risk of human interactions potentially harmful to whales. Simultaneously, growth in humpback whale populations globally, particularly in the Southern Hemisphere (Wedekin et al., 2017; Noad et al., 2019), could further increase exposure to vessel disturbances and anthropogenic noise pollution. High levels of acoustic energy, especially from naval and seismic vessels, have the potential to interfere with whale behavioural patterns that may influence their longer-term survival (Dolman & Jasny, 2015). Concern about the potential impacts of marine activities on cetaceans has led to many nations regulating the conduct of activities to manage the impacts, for example the Environmental Protection and Biodiversity Act (EPBC, Department of the Environment, 2008) in Australia. There is a clear need for robust and deployable methods for improving the detection of whales and other cetaceans in seascapes exposed to increasing levels of human interaction.

Regulated measures to mitigate the effects of maritime activities producing high noise levels (e.g., seismic arrays and naval sonar) include the shut-down of acoustic sources when cetaceans are in exclusion zones based on minimum acceptable distance from the source. This requires constant observation of marine mammals by observers who systematically scan the ocean's surface with the naked eye and binoculars for cetacean sighting cues, including blows (exhalations), body parts above the ocean's surface (dorsal fins or flukes), and easily identified surface behaviours (e.g. pectoral slapping and breaching). Compton et al. (2008) estimated that MMOs detect 70% of animals in daylight and optimal survey conditions (clear and calm). However, this survey method is limited to daylight hours, subject to operator fatigue, and visual sighting rates are reduced in weather conditions such as fog, rain, high sea states, and glare. Additionally, visual detection is often subjective, and sightings may be difficult to confirm (Verfuss et al., 2018). Human based observation methods are also not viable for longer term sources of disturbance such as pile driving in construction of offshore infrastructure for wind farms. Existing research has demonstrated the effectiveness of thermal infrared (TIR) imaging systems for improving visual detection of cetaceans over traditional human observation

methods (Smith et al., 2020). Additionally, TIR systems have been proposed as additional measures to complement speed limit regulations and routing of ships to minimise vessel strikes (Cates et al., 2017). However, there has been limited assessment of different thermal sensor configurations for optimising long-range detection rates of cetaceans.

Thermal imaging sensors capture infrared radiation (heat) emitted from an object (Sarawade & Charniya, 2018). They are designed to operate in two specific wavelength bands in the infrared portion of the electromagnetic spectrum: 3–5 μm or mid-wave infrared (MWIR), and 8 - 12 μm or longwave infrared (LWIR). Thermal infrared sensors are effective for detecting animals, notably endothermic mammals, in environments where the animal's surface temperature is warmer than the surrounding environment (Kays et al., 2018; Witczuk et al., 2018; Witt et al., 2020; McCarthy et al., 2022). Compared to visual detection by eyesight or visual red-green-blue (RGB) sensors, TIR can potentially reduce image complexity and improve target detectability, irrespective of light levels (Hinke et al., 2022). These benefits have been demonstrated in terrestrial environments where thermal imaging systems have outperformed traditional, ground-based survey methods for the detection of arboreal mammals (e.g., Witt et al., 2020; McCarthy et al., 2022). For marine mammal species that come ashore, specifically pinnipeds and marine fissipeds, thermal methods have also proved effective for detection from aerial surveys in open habitats, such as rocky substrates (Seymour et al., 2017; Gooday et al., 2018; Young et al., 2019; Christman et al., 2022) and in snow (Conn et al., 2021). However, thermal methods are less effective in the marine environment, due to the rapid attenuation of infrared radiation with depth in the water column. The insulation capacity of cetacean species also reduces the thermal contrast between the animal and surrounds, and surfacing animals are covered by a thin layer of water which partially or completely masks skin temperature. Thermal imaging to detect cetaceans has primarily focused on detecting their warm exhalations or blows (Zitterbart et al., 2013; Smith et al., 2020; Zitterbart et al., 2020).

Previous studies that use TIR systems to detect cetaceans can be grouped into three main platforms (1) hand-held systems (Horton et al., 2017); (2) aerial methods (Churnside et al., 2009; Florko et al., 2021) and; (3) ship- or shore-based systems (Zitterbart et al., 2013; Sullivan et al., 2020). Although previous studies have compared the detection performance between visual, acoustic, and thermal imaging methods (Smith et al., 2020),

there has been limited review of thermal sensor configuration for optimising detection rates of cetaceans and the implications of improved thermal image quality for automated detection methods. This requires a detailed understanding of: (i) the characteristics of cetacean cues (surface exposure and exhalations) that will influence the training of automated detection models and, (ii) the impact of environmental conditions, including sea surface temperature, humidity, sea state, wind, and visibility, on detection rates. The intent of this paper is to provide an evaluation of how TIR sensor configuration will influence detection rates and the reliability of automated detection models. Here we review the current literature related to the use of thermal imaging for the long-range detection of cetaceans and present a case study comparing the capabilities of three thermal infrared sensors for detecting bottlenose dolphins (*Tursiops aduncus*). Because bottlenose dolphins have a smaller thermal signature than most cetaceans this provided an opportunity to evaluate sensor sensitivity on more challenging smaller sized cetacean targets.

5.3 METHODS

5.3.1 Literature Review

A quantitative scoping review of academic literature was conducted to synthesise emerging approaches for detection of cetaceans using thermal sensors, automated detection, and identify evidence for informing optimal sensor configuration. Original peer reviewed publications and conference proceedings in the English language were accessed from electronic database searches the *Web of Science* (Core Collection) and *Google Scholar* February 2021 to February 2023. Keywords used in the searches were 'thermal imaging', 'thermal infrared', 'whales', 'cetaceans', 'automated', 'detection' were applied to search these databases. Reference lists of articles found in the initial search were also reviewed. For research focused on whale detection, only studies that detected whales at distances greater than 500 metres, the minimum required radius for the shut-down zone in many mitigation guidelines, were included. Studies focused on automated detection were reviewed separately.

For each publication that matched the above criterion, the specifications of the thermal imaging system(s), detector type, study location and respective sea surface temperature,

system height, automated detection capability, species detected, and the maximum distance of detection were noted. The compiled database of papers was analysed to identify trends in thermal sensor configuration, artificial intelligence (AI) methods and impact of environmental conditions.

5.3.2 Field Data Collection

The research platform was the commercial whale watching vessel *Dolphin Watch Cruises* (17m length, 5m height above the water line). The detection capabilities of three different Forward Looking Infrared (FLIR) thermal sensors of varying resolution and detector types, were assessed on 18 February (mean monthly SST = 22.6°C) and 1 April 2021 (mean monthly SST = 21.3°C) (sensor specifications are shown in Table 1). Survey conditions were clear and calm on both survey days. The Indo-Pacific bottlenose dolphin (*Tursiops aduncus*) in Jervis Bay, on the east coast of Australia was selected as the target object for sensor comparison due to smaller target size, site accessibility and consistent presence of a resident population. The FLIR Boson, a low resolution uncooled sensor, and x8400sc, a very high resolution cooled sensor, were handheld. The x8400sc sensor remained on the bottom platform (1.6 m) due to weight (> 5kg) and size and the Boson sensor, connected to a tablet for real time visual monitoring, recorded from the upper deck (4.2 m). The uncooled FLIR Tau 2 was mounted to the top of the vessel (4.2 m) within a rotating system (RobotEye) and controlled remotely from inside the boat (Figure 1). The surveys were not systematic, and the direction and movement of the boat was determined based on common sighting locations. Once a pod of dolphins was sighted by trained observers, the three sensors simultaneously focused on the pod. Six videos from the Boson sensor were captured, and five videos were captured from both the Tau 2 and x8400sc sensors.

Table 1. Summary of thermal sensors tested on bottlenose dolphins in Jervis Bay

Imager	Detector Type	Resolution	Frame rate	Spectral Range
FLIR Boson	Uncooled VOx microbolometer	320 x 256 6.3 mm (focal length)	<9 Hz	8 – 14 µm (LWIR)
FLIR Tau 2	Uncooled VOx microbolometer	640 x 512	30 – 60 Hz	7.5 - 13.5 µm (LWIR)
FLIR x8400sc	Cooled InSb detector	1280 x 1024	106 Hz	1.5 – 5.1 µm (MWIR)

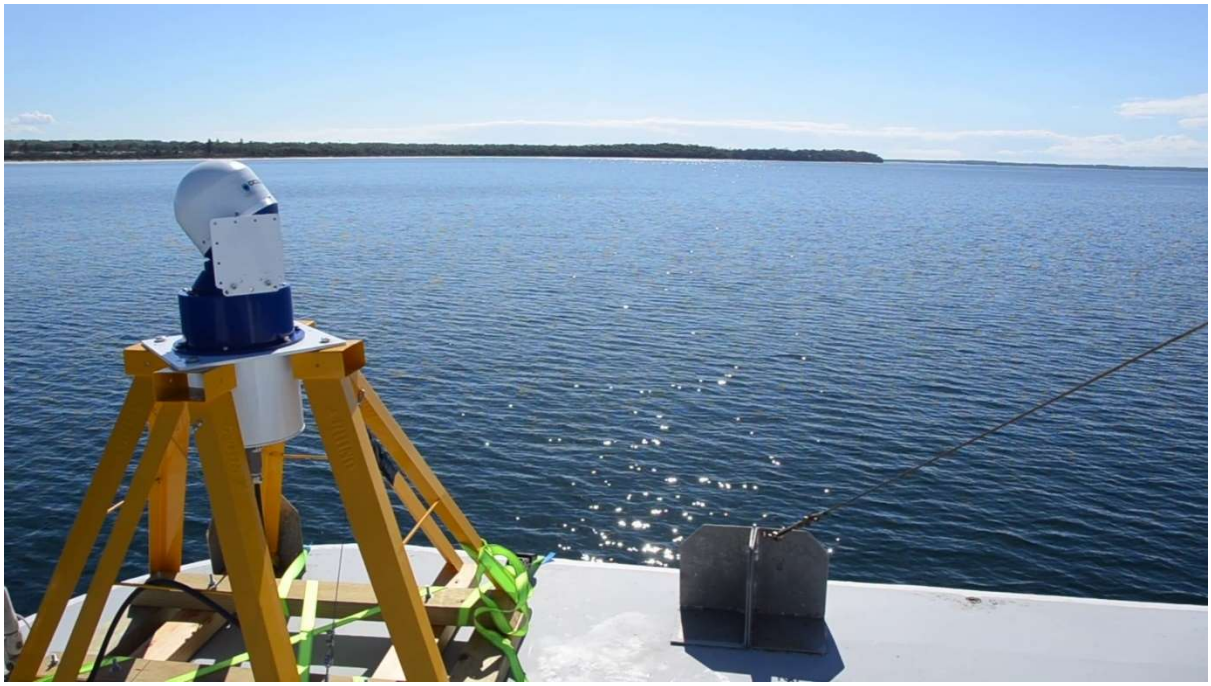

Figure 1. Setup of the Tau 2 integrated into the RobotEye on the top platform of a vessel operated by *Dolphin Watch Cruises*

5.3.3 Field Data Analysis

Individual images were extracted from the videos at one frame per second using VLC media player and grouped by sensor. All processing steps below were performed in ENVI™ 5.5.3. Videos from the Tau 2 sensor were captured in grey scale, providing a single

band for analysis. Footage from the Boson and x8400 sensors were captured using a colour gradient and exported as RGB three band images, and were transformed into a single, grey-scale band using equation 1 (Stokes, 1996), where R, G, and B represent bands red, green and blue, respectively.

$$Y_{linear} = 0.2126R_{linear} + 0.7152G_{linear} + 0.0722B_{linear} \quad (1)$$

The greyscale images were used for comparison across each sensor type. The thermal contrast (anomaly) between the target animal and the surrounding background was compared between sensors by converting pixels into a Z-Score, using the mean and standard deviation of all pixels in the image (equation 2).

$$Z = \frac{[pixel\ value - mea\ ]}{standard\ deviation} \quad (2)$$

A horizontal profile was extracted across at least one dolphin cue in each image to quantify the anomaly peak of the target animal(s). For each sensor, four images were selected to evaluate sensor effectiveness in detecting dolphin targets at different distances. Given the absence of a true horizon inside Jervis Bay, accurate distance estimates were not possible.

5.3 RESULTS

5.3.1 Literature Review

The literature search identified six research studies, published between 1999 and 2020, using thermal imaging systems for the detection of whales at a distance > 500 m from ship or shore (summarised in Table 2). Three of the studies utilised the same rotating system (FIRST-Navy), testing the system both from land and vessel under a range of environmental conditions, with sea surface temperature (SST) ranging from -1.8°C to ~25°C. The remaining three studies tested systems from land only. All systems detected whales at distances > 5km using their exhalations. Four of these studies used automated detection algorithms with varying levels of accuracy (Table 3).

Table 2. Summary of six research studies identified that used thermal imaging systems to detect whales at distances >500m

Study	Imaging System	Specs	Detector	Study location	SST (°C , mean± SD)	System height (m, MSL)	Species detected with IR/ number of detections	Max. distance detected (km)
Zitterbart et al. (2013)	FIRST-Navy	Scans 360° horizontal x 8° vertical, 5	Cooled, LWIR	Vessel survey: Arctic and Southern Oceans	-1.8 to +22.7°C (min – max)	28.5	Humpback whales, minke whales, fin whales, 4500+ blow detections	5.5
Smith et al. (2020)	FIRST-Navy	As above	Cooled, LWIR	Vessel survey: Nova Scotia and Newfoundland	18.23 ±0.71	7.8	2 baleen sp., 7 toothed sp. 952 blow detections	> 5
Zitterbart et al. (2020) All land surveys	FIRST-Navy	As above	Cooled, LWIR	North Stradbroke Island, QLD	21.84 ±0.94	51.3	Humpback whales Detections: 1560 whale blows, 137 detections from whale backs, 162 slaps, 241 breaches	10
				Cape Race, Newfoundland	14.32 ±1.55	26.0		5
				Poipu Shores, Hawaii	25.72 ±0.41	16.0		6
				Princeville, Hawaii	24.98 ±0.2	49.8		6
Guazzo et al. (2019)	FLIR F-606	640x480 video stream, 30 Hz (not rotating), 7.5 – 13.5	Uncooled, LWIR	Land surveys: Big Sur, California, USA	Not reported Monthly average 13	28.1	Gray whales 1472 blow detections	5.8
Sullivan et al. (2020)	FLIR F-606, FLIR F-610	As above	Uncooled, LWIR	Land surveys: Big Sur, California, USA	Not reported Monthly average 12.9	28.1	Gray whales, 1170 blow detection	~ 5
Perryman et al. (1999)	AN/KAS-1A		Cooled, LWIR	Land surveys: California, USA	Not reported Monthly average 13	22	Gray whales, no. not stated	5.4

Table 3. Computer vision methods used in IR-based automatic detection of whales.

Detection and classification method	Automation	Training/validation data sets	Detection accuracy	Study
Combined adaptive thresholding and neural networks	Automated	5 video hours 96 visual detections	85-90.0%	Santhaseelan et al. (2012)
Support vector machine models. Change in contrast in multi-scale, sliding windows used for detection. Classification combined Eigenimage approach and Support-Vector-Machine model.	Events manually annotated	120 validated blow signatures (true event) 1400 non-blow signatures (false event)	82% within 5km	Zitterbart et al. (2013)
Heuristic rule based using customised software Tashtego	Automated, observers checked detections to verify sightings and record false positives	Not stated	Not stated. Mean false positive rates 8-13 fp/h (location dependent)	Zitterbart et al., (2020)
			True positive detection 15.5%, false positive 84.5%	Smith et al., (2020)
State vector involving a mixed continuous-discrete state	Semi-automated, output reviewed by humans	Not stated	85%	Sullivan et al. (2020)

5.3.2 Field data

The horizontal profiles extracted from the images captured by each sensor exhibited a dominant peak in Z-score across all dolphin cues captured at various distances (Figure 2). The maximum Z-score (Z = 10.99; Fig 2i) was caused by sun glint reflection from the back of the dolphin. This Z-score was substantially higher than any other dolphin cue profile. Sun glint was present in several images, both visually and on the respective horizontal profiles (Figures 2a, b, e, i, j). In these images, the dolphins were closer to the sensor that in other images. At distances further from the sensor, sharper detection peaks were apparent for all three sensors, demonstrating improved contrast between a dolphin and the surrounding water. Although, Z-scores did not greatly differ between sensors, image detail and shape definition of dolphin cues improved with increasing sensor resolution. This comparison is illustrated in the images nearest to the sensor (Fig 2.a, e, i).

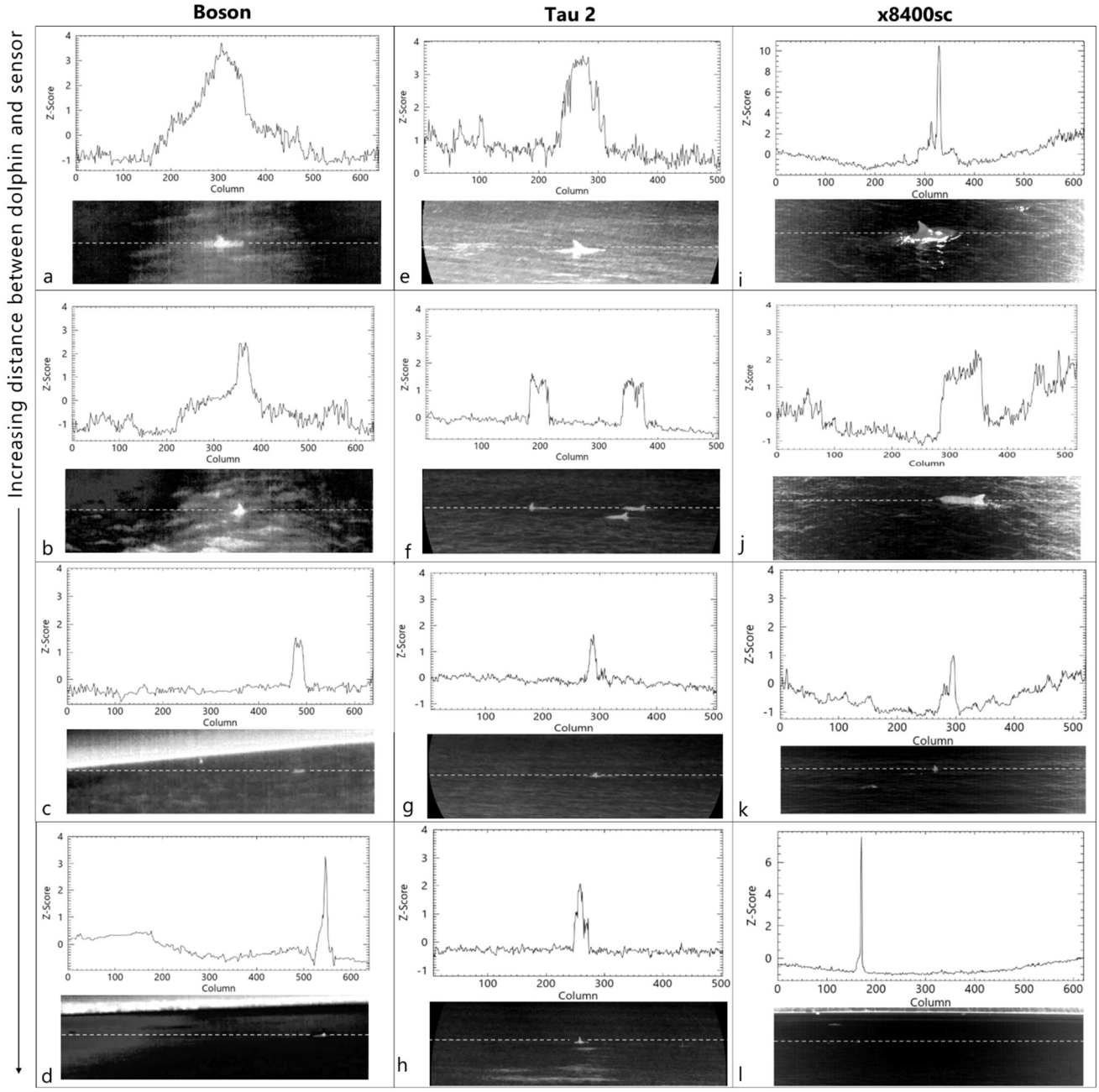

Figure 2. Visual results and horizontal profiles of anomaly detections taken from FLIR thermal sensors: Boson (a-d), Tau2 (e-h), x8400sc (i-l). Images have been clipped to highlight the location of the horizontal profile within the image (white dotted line). A break in the line has been left across the dolphin(s) for easier visualisation. For all except, except i and l, the y column ranges from 0 – 4. Images i and l had greater peaks, thus their maximum values are shown. Full images are presented in Figure S1.

5.4 DISCUSSION

5.4.1 Sensor configuration

The Boson (uncooled low resolution), Tau 2 (uncooled high resolution) and x8400sc (cooled very high resolution) all detected the thermal signature of bottlenose dolphins on the water surface. The case study demonstrated that a low-resolution, uncooled sensor (Boson) will be sufficient for detecting dolphins at a ~1km distance. The small thermal signature of dolphins provided an opportunity to test sensor sensitivity on a small target, recognising the thermal signature will differ to that of a larger whale exhalation cue. The calm sea state conditions at the time of survey also limits the translation of these results to whale exhalation cues in open ocean conditions. However, consideration of sensor resolution, detector temperature, and spectral range is important for improving detection results. Sensor resolution is important when detecting small objects at significant distances. In our results, there was no clear difference between detection capabilities of the sensors, however at distances >1km it is expected the sensors with increased resolution (i.e., x8400sc) will provide greater detection capabilities at further distances. However, Guazzo et al. (2019) and Sullivan et al. (2020) were able to detect the exhalations of gray whales at distances > 5km, using an uncooled sensor of 640 x 480 resolution.

A key distinguishing factor of thermal systems is the use of cryogenically cooled sensors, operating within 60-100 K (-213 to -173°C) range, or uncooled sensors, operating at ambient temperature. The thermal sensitivity of a cooled sensor typically increases by a factor of 3 to 5 compared to uncooled sensors, resulting in improved detection probabilities (Verfuss et al., 2018). Increased image clarity, provided by a cooled sensor, required for enhanced delineation of cue shape is evident in the x8400 sensor (Fig. 2i-l). This improved sensitivity is critical for cetacean detection at distance. For example, the warm thermal signature of a whale blow at a distance >3 km can be as little as four pixels in an image or video stream for a sensor of 640x480 resolution (Sullivan et al., 2020). Representation of a cetacean cue by only a small number of image pixels results in a high proportion of image pixels not contributing to the object of interest. Optimising the signature response of these pixels is also relevant for improving the accuracy of automated detection models as discussed further in section 5.4.2. However, cryogenically

cooled sensors do have disadvantages which include the significantly higher cost, slower start up times that limits their agility for rapid response, greater fragility in marine field environments and increased maintenance requirements (every ~10,000 hours of operation) (Hristov et al., 2008).

The limited range of survey conditions encountered during our field collection restricted evaluation of the influence of atmospheric conditions, however, these conditions will have the greatest influence on the choice of MWIR or LWIR systems. MWIR sensor will perform better in warm, humid climates, and for longer ranges than LWIR. In contrast LWIR will perform better in cooler atmospheres and if smoke, fog, or haze is present (Havens & Sharp, 2015). For example, in category II fog and a temperature gradient of 10°C between target and background, FLIR (2013) reported that LWIR sensors will have a detection range of 2.4km compared to 0.5km for a MWIR system. Havens and Sharp (2015) propose surveys should be undertaken when atmospheric conditions are optimised. This is not viable for whale mitigation purposes, however, the climatic and weather conditions of the location of operations, may influence decisions for the spectral range of the sensor. Furthermore, the atmospheric conditions alone are not sufficient in determining detection range. The size of the target, temperature contrast, and spatial resolution will have an impact. For long range detection, cooled sensors will be more effective, irrespective of atmospheric conditions or spectral resolution.

5.4.2 Automated detection

Applications in which cetacean detection requires continuous observations, for extended periods of time (weeks to months), such as monitoring migration movements or determining cetacean presence within high disturbance zones (windfarm construction sites and shipping lanes), may rely on automated methods. Automated detection methods using thermal image input are effective in terrestrial mammal applications, due to the steep thermal gradient between the target and their surrounds (Seymour et al., 2017). Previous studies involving automated or semi-automated systems demonstrated that thermographic imaging provided comparable results with the performance of human observers using eyesight and binoculars during daylight hours at distances of several kilometres (Sullivan et al., 2020; Zitterbart et al., 2020). Consistent and reproduceable temperature anomalies were used to identify quantitative constraints that

can inform transient temperature anomaly detection algorithms (Sullivan et al., 2020). However, reliability of automated detection methods is impacted by high false-alarm rates associated with the thermal detection of other visual stimuli (e.g. white caps, small vessels and birds), and obstruction by sea spray and large waves when surveying near-horizontal (Smith et al., 2020). Due to the situational complexity and confounding variables in thermal images captured at sea, data driven machine learning models with adequate detection and classification accuracy require a higher standard of thermal image quality. Sensors with high thermal sensitivity that are cryogenically cooled and/or have sufficiently large focal length required for detection at distances >1-2km are expensive and less manoeuvrable. Poor stabilisation of the thermal sensor platform has been identified as the key determinant for high positive rates (Smith et al., 2020).

A high contrast between an animal and their surroundings is particularly important for automated methods (Chabot & Francis, 2016; Hollings et al., 2018). This is where thermal imaging is particularly beneficial, particularly for cetacean species of lighter colouration that may appear similar in colour to surrounding waters in RGB imagery (Cubaynes et al., 2018). The clear contrast between a dolphin and surrounding waters is demonstrated in our results, particularly at greater distances.

5.4.3 Factors influencing detection reliability

The six research studies identified using thermal imaging systems for the horizontal detection of whales at a distance >500m (Tables 2, 3), provide insight into how characteristic cetacean cues can influence automated detection models and the impact of environmental conditions on detection rates.

(i) Blow characteristics

TIR imaging for the detection of marine mammals relies on the thermal contrast between a marine mammal cue, either their body on the surface or their blow, and the surrounding colder ocean. These surveys do not require absolute temperature measurements. Whale blows, observed as bright, transient features, are the most common cue and have been the focus of studies utilising thermal detection methods (Zitterbart et al., 2013; Guazzo et al., 2019; Sullivan et al., 2020). Consistency in the characteristics of these features have potential to facilitate the development of automated detection algorithms. For example,

blow heights will vary in response to species, wind strength, the volume of sea water in the blow hole at exhalation, the whale's position relative to the ocean surface when exhaling, and whale size (i.e. the blow from a calf vs an adult) (Horton et al., 2017). The growth of a blow is predictable (Santhaseelan et al., 2012) and there will be a linear decay of detectability with increased distance from sensor. Horton et al. (2017) analysed the blows of 174 humpback whales surveyed in the Cook Islands and Alaska and found that all blows reached a maximum blow height in less than 1.2 seconds. The same study estimated that at 0.4 seconds after exhalation, blow heights ranged from 1 to 3.3 metres, with an average of 2.2 metres. Using sensor resolution, blow heights and distance measurements, it is possible to determine how many bright pixels should be present in the image at a set distance from a blow. Sullivan et al. (2020) used the blow characteristics of gray whales (*Eschrichtius robustus*) to train an automated detection system. For example, if the whale is within one kilometre to the sensor, the blow should comprise 49 pixels in the frame (25 pixels if >1 km, < 2 km etc.) and each blow must persist for at least 0.4 seconds but no longer than six seconds. Blow characteristics will also differ between species, for example southern right whales (*Eubalaena australis*) have a distinctive V-shaped blow, but the capability of thermal sensors and automated systems to differentiate between species based on blows has not been studied.

(ii) Environmental conditions

Thermal detection systems over water are subject to environmental conditions, wind, sea surface temperature, sea state and visibility (sun glint, rain, fog) which can mask whale cues and impact both visual and thermal detection methods.

Sun glint, or glare, from specular reflection of sunlight off the water surface, visualised as a bright reflection, can both obscure features and be visually confused with the body of a whale on the surface (Araújo et al., 2022) and glint contamination (warm contrast) can reduce the likelihood of detecting a whale cue. However, thermal images have a narrower field of glare than visual detectors as the thermal sensor only captures the local contrast of each frame (Zitterbart et al., 2013). Thermal sensors are typically more effective at night due to the decrease in reflected radiation from the sun (Verfuss et al., 2018).

Fog and rain can significantly reduce the range of thermal imaging and detection accuracy as the scattering of light by water droplets diminishes the thermal signal. Zitterbart et al.

(2020) found that in “hazy or misty conditions”, LWIR thermal sensors still had a greater detection distance than MMOs, as infrared radiation can penetrate better than visible bands. In dense fog conditions, thermal systems and observers will be equally affected (Beier et al., 2004; Zitterbart et al., 2020). The impact of rain on system performance is understudied but it is likely to be reduced as thermal infrared imaging cannot penetrate water.

With increased sea state, an exponential decline in detection probability is expected. Using visual line-transect surveys, Barlow (2015), determined that detection probability decreased to 0.6 in Beaufort 6 conditions for humpback whales (*Megaptera novaeangliae*). All other species (small and large baleen species, sperm whales *Physeter macrocephalus* and delphinids) had lower detection probabilities in the same environmental conditions. Zitterbart et al. (2020) found that at Beaufort states ~3-4, detection probabilities started to significantly reduce. Sea state also impacts rates of false positives. In larger swell, birds and small vessels disappearing behind waves and then reappearing for a short time period (2-3 seconds), mimics the same thermal pattern of a whale blow (Zitterbart et al., 2020). Floating blocks of ice follow this same pattern (Zitterbart et al., 2013). Breaking waves and white caps are another key source for false positives. In automated thermal detection, white caps increase the contrast across an image, increasing overall noise and thus reducing the signal to noise ratio for whale cues (Zitterbart et al., 2020).

Although it could be expected that colder sea surface temperature (SST) will provide a greater temperature contrast, Zitterbart et al. (2020) successfully detected whale cues up to 10 kilometres in subtropical waters (SST >20°C) off Queensland, Australia, using a rotating, cooled sensor. Similarly, using a handheld uncooled thermal sensor Horton et al. (2017), found a constant thermal anomaly of ~3°C warmer for whale blows compared to the adjacent 8°C and 24°C ocean waters in Alaska and the Cook Islands, respectively. These warmer water detections demonstrate that the efficacy of thermal imaging techniques for capturing cetacean exhalations is not restricted to higher latitude waters.

5.4.4 Species Identification

The dynamic movement of thermal anomalies can potentially be used to develop automated detection models for species identification with sufficiently large visible and

thermal image datasets to characterise blow velocity and geometry (Horton et al., 2017). However, species-level identification requires high sensitivity and pixel cover which is limited by distance and direction of image capture. Previous studies demonstrating automated detection of whale blows at distances up to ~5 km (Table 2) have used sightings by visual observers to confirm detected species but there has been no attempt to automate species identification using either visual or thermal images. Machine learning has been used to discriminate between species relatively successfully for terrestrial animals of different sizes and body shapes. For example, Ulhaq et al. (2021) successfully trained an automated detection system to identify rabbits, pigs, and kangaroos using thermal aerial imagery. However, there are additional logistical challenges in collecting a sufficient number of verified images (1000+) to train automated models from animals that are highly mobile and often in remote locations. Furthermore, species identification based on transient features that are not always characteristic of the species, e.g. V-shaped humpback whale blow (characteristic for a right whale) (see Fig. S2 in Zitterbart et al., 2013), adds significant complexity. In addition to variations in whale blows, environmental conditions (e.g. wind and glare) may alter the appearance of the blow. Smith et al. (2020) reported that experienced MMOs were only able to identify ~50% of species at distances greater than 500 m, using visual observations. Retrospective assessment of 1427 thermal cetacean detections demonstrated that only four could be identified confidently as sperm whales (Smith et al., 2020). Despite the potential of high resolution thermal sensors for discriminating species cues in low light conditions, these findings demonstrate current limitations in accurate species identification beyond 500 m in low light conditions.

5.4.5 Thermal sensor platforms

Due to the sensitivity of thermal sensors, platform stability and design will influence image quality and is an important consideration when using cryogenically cooled sensors. In this study, the uncooled Tau 2 sensor was integrated on a RobotEye (developed and manufactured by Ocular Robotics) a rapidly rotating 360° system that uses an autonomously-controlled lens-mirror system and point and feeds images to stationary cameras. The low inertia unit that delivers captured light to an imaging array avoids the complexity associated with current technology, such as rotating cameras (FIRST-Navy system from Zitterbart et al. (2013), Smith et al. (2020), and Zitterbart et al. (2020)) or

multiple fixed cameras (e.g., Sullivan et al., 2020). The system has extremely high acceleration rates ($60{,}000^0/s^2$), aperture speeds ($4{,}000^0/s$) and pointing precision (0.00055^0) which allowed clear thermal image capture of dolphins (Tau 2 sensor in Figure 2). The ability of the RobotEye to automatically zoom in on detected objects enables maximization of the number of pixels covered by the object for classification as cetacean or non-cetacean (Figure 3). A high pixel count is essential since even state-of-the-art artificial intelligence (AI) methods are limited by the quality of the images. Further research is required to evaluate the efficacy of improved thermal sensor platform design on detection rates.

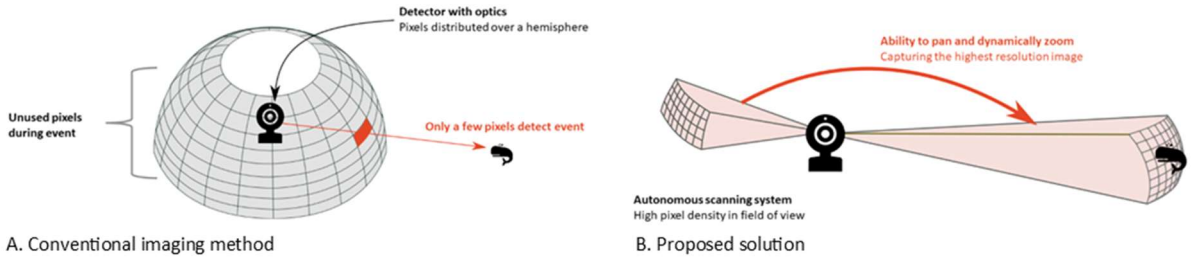

Figure 3. Comparison of A) conventional methods to scan for whales using an imaging array that projects pixel values over an entire hemisphere resulting in a low resolved region where only a few pixels contribute a whale event ultimately reducing detection accuracy B) robotically controlled automatic zoom within the RobotEye captures a high-resolution image of the object ensuring every pixel on the detector is maximised for target identification.

5.4.6 Research limitations

Here we demonstrated that all three thermal sensors were able to detect dolphin cues in clear and calm survey conditions. Sun glint can be problematic for automated methods due to decreased noise, and was evident in our results, appearing as a bright anomaly feature (Verfuss et al., 2018). Although glint is not problematic for night time detections, it cannot be avoided during the day, and detection for mitigating human activities on cetaceans may be required at any time of day. Research is needed to investigate the potential for deep learning methods to assist in improving the discrimination between a cetacean cue and sun glint (Giles et al., 2021) to reduce false positives in automated systems (Smith et al., 2020). Our results were limited in only testing the sensors in clear

and calm conditions. As outlined above, sensor effectiveness will depend on environmental conditions and may influence sensor selection (e.g., LWIR vs MWIR, cooled vs uncooled). In addition to reviewing how sensor resolution, detector temperature, and spectral range may impact on the detection rate of cetacean cues, we recognise there are several other factors that would impact sensor effectiveness. These include, but are not limited to, sensor field of view, thermal sensitivity, and focal length, however these were outside the scope of this research.

5.5 CONCLUSIONS

An understanding of how thermal sensor configuration will influence cetacean detection accuracy and the reliability of automated detection methods is critical for optimising detection rates to mitigate the impacts of anthropogenic interactions, particularly at night. Here we demonstrated the effectiveness of three thermal sensors for detecting dolphin cues within one kilometre of the sensor and in calm conditions. We highlighted how characteristic cetacean cues, particularly whale exhalations, and environmental factors may help inform automated detection methods. Despite advances in computer vision detection and classification techniques, current automated systems still have high levels of false detections, hindering potential use for mitigation.

5.6 REFERENCES

Araújo, V. M., Shukla, A., Chion, C., Gambs, S., & Michaud, R. (2022). Machine-learning approach for automatic detection of wild Beluga Whales from hand-held camera pictures. *Sensors, 22*(11), 4107.

Barlow, J. (2015). Inferring trackline detection probabilities, g(0), for cetaceans from apparent densities in different survey conditions. *Marine Mammal Science, 31*(3), 923-943. doi:10.1111/mms.12205

Beier, K., Gemperlein, H. J. A. s., & technology. (2004). Simulation of infrared detection range at fog conditions for enhanced vision systems in civil aviation. *Aerospace science and technology*, *8*(1), 63-71.

Cates, K., DeMaster, D., Brownell Jr, R., Silber, G., Gende, S., Leaper, R., . . . Panigada, S. (2017). Strategic plan to mitigate the impacts of ship strikes on cetacean populations: 2017-2020. *IWC*.

Chabot, D., & Francis, C. M. (2016). Computer-automated bird detection and counts in high-resolution aerial images: a review. *Journal of Field Ornithology, 87*(4), 343-359.

Christman, C. L., London, J. M., Conn, P. B., Hardy, S. K., Brady, G. M., Dahle, S. P., . . . Ziel, H. L. (2022). Evaluating the use of thermal imagery to count harbor seals in aerial surveys. *Mammalian Biology*. doi:10.1007/s42991-021-00191-6

Churnside, J., Ostrovsky, L., & Veenstra, T. (2009). Thermal Footprints of Whales. *Oceanography, 22*(1), 206-209. doi:10.5670/oceanog.2009.20

Compton, R., Goodwin, L., Handy, R., & Abbott, V. J. M. P. (2008). A critical examination of worldwide guidelines for minimising the disturbance to marine mammals during seismic surveys. *Marine Policy, 32*(3), 255-262.

Conn, P. B., Chernook, V. I., Moreland, E. E., Trukhanova, I. S., Regehr, E. V., Vasiliev, A. N., . . . Boveng, P. L. (2021). Aerial survey estimates of polar bears and their tracks in the Chukchi Sea. *PLoS One, 16*(5), e0251130.

Cubaynes, H. C., Fretwell, P. T., Bamford, C., Gerrish, L., & Jackson, J. A. (2018). Whales from space: Four mysticete species described using new VHR satellite imagery. *Marine Mammal Science, 35*(2), 466-491. doi:10.1111/mms.12544

Davies, K. T., & Brillant, S. W. (2019). Mass human-caused mortality spurs federal action to protect endangered North Atlantic right whales in Canada. *Marine Policy, 104*, 157-162.

Department of the Environment, W., Heritage and the Arts. (2008). *EPBC Act Policy Statement 2.1–Interaction between offshore seismic exploration and whales*.

Dolman, S. J., & Jasny, M. (2015). Evolution of marine noise pollution management. *Aquatic Mammals, 41*(4), 357.

Dolman, S. J., Simmonds, M. P., & Keith, S. (2003). *Marine wind farms and cetaceans*: Whale and Dolphin Conservation Society.

FLIR. (2013). *Seeing through fog and rain with a thermal imagin';[pg camera.* Retrieved from Retrieved from: http://www.flirmedia.com/MMC/CVS/Tech_Notes/TN_0001_EN.pdf.:

Florko, K. R. N., Carlyle, C. G., Young, B. G., Yurkowski, D. J., Michel, C., & Ferguson, S. H. (2021). Narwhal (*Monodon monoceros*) detection by infrared flukeprints from aerial survey imagery. *Ecosphere, 12*(8). doi:10.1002/ecs2.3698

Giles, A. B., Davies, J. E., Ren, K., & Kelaher, B. (2021). A deep learning algorithm to detect and classify sun glint from high-resolution aerial imagery over shallow marine environments. *ISPRS Journal of photogrammetry and remote sensing, 181*, 20-26.

Gooday, O. J., Key, N., Goldstien, S., & Zawar-Reza, P. (2018). An assessment of thermal-image acquisition with an unmanned aerial vehicle (UAV) for direct counts of coastal marine mammals ashore. *Journal of Unmanned Vehicle Systems, 6*(2), 100-108. doi:10.1139/juvs-2016-0029

Guazzo, R. A., Weller, D. W., Europe, H. M., Durban, J. W., D'Spain, G. L., & Hildebrand, J. A. (2019). Migrating eastern North Pacific gray whale call and blow rates estimated from acoustic recordings, infrared camera video, and visual sightings. *Sci Rep, 9*(1), 12617. doi:10.1038/s41598-019-49115-y

Havens, K. J., & Sharp, E. J. (2015). Thermal imaging techniques to survey and monitor animals in the wild: a methodology. Academic Press. 121 – 141.

Hinke, J. T., Giuseffi, L. M., Hermanson, V. R., Woodman, S. M., & Krause, D. J. (2022). Evaluating Thermal and Color Sensors for Automating Detection of Penguins and Pinnipeds in Images Collected with an Unoccupied Aerial System. *Drones, 6*(9), 255.

Hollings, T., Burgman, M., van Andel, M., Gilbert, M., Robinson, T., Robinson, A., & McPherson, J. (2018). How do you find the green sheep? A critical review of the use of remotely sensed imagery to detect and count animals. *Methods in Ecology and Evolution, 9*(4), 881-892. doi:10.1111/2041-210x.12973

Horton, T. W., Oline, A., Hauser, N., Khan, T. M., Laute, A., Stoller, A., . . . Zawar-Reza, P. (2017). Thermal Imaging and Biometrical Thermography of Humpback Whales. *Frontiers in Marine Science, 4*. doi:10.3389/fmars.2017.00424

Hristov, N. I., Betke, M., & Kunz, T. H. (2008). Applications of thermal infrared imaging for research in aeroecology. *Integregative Comparative Biology, 48*(1), 50-59. doi:10.1093/icb/icn053

Kays, R., Sheppard, J., McLean, K., Welch, C., Paunescu, C., Wang, V., . . . Crofoot, M. (2018). Hot monkey, cold reality: surveying rainforest canopy mammals using drone-mounted thermal infrared sensors. *International Journal of Remote Sensing, 40*(2), 407-419. doi:10.1080/01431161.2018.1523580

McCarthy, E. D., Martin, J. M., Boer, M. M., & Welbergen, J. A. (2022). Ground-based counting methods underestimate true numbers of a threatened colonial mammal: an evaluation using drone-based thermal surveys as a reference. *Wildlife Research*.

Noad, M. J., Kniest, E., & Dunlop, R. A. (2019). Boom to bust? Implications for the continued rapid growth of the eastern Australian humpback whale population despite recovery. *Population Ecology, 61*(2), 198-209. doi:10.1002/1438-390x.1014

Perryman, W. L., Donahue, M. A., Laake, J. L., & Martin, T. E. (1999). Diel variation in migration rates of eastern Pacific gray whales measured with thermal imaging sensors. *Marine Mammal Science, 15*(2), 426-445.

Santhaseelan, V., Arigela, S., & Asari, V. K. (2012). *Neural network based methodology for automatic detection of whale blows in infrared video.* Paper presented at the International Symposium on Visual Computing.

Sarawade, A. A., & Charniya, N. N. (2018). *Infrared thermography and its applications: a review.* Paper presented at the 2018 3rd International conference on communication and electronics systems (ICCES).

Seymour, A. C., Dale, J., Hammill, M., Halpin, P. N., & Johnston, D. W. (2017). Automated detection and enumeration of marine wildlife using unmanned aircraft systems (UAS) and thermal imagery. *Scientific Reports, 7*, 45127. doi:10.1038/srep45127

Smith, H. R., Zitterbart, D. P., Norris, T. F., Flau, M., Ferguson, E. L., Jones, C. G., . . . Moulton, V. D. (2020). A field comparison of marine mammal detections via visual, acoustic, and infrared (IR) imaging methods offshore Atlantic Canada. *Marine Pollution Bulletin, 154*, 111026. doi:10.1016/j.marpolbul.2020.111026

Stokes, M. (1996). A standard default color space for the internet-srgb. *http://www. w3. org/Graphics/Color/sRGB. html*.

Sullivan, K., Fennell, M., Perryman, W., Weller, D., Oswald-Tranta, B., & Zalameda, J. N. (2020). *Automated detection, tracking, and counting of gray whales*. Paper presented at the Thermosense: Thermal Infrared Applications XLII.

Thompson, K. F., Miller, K. A., Wacker, J., Derville, S., Laing, C., Santillo, D., & Johnston, P. (2023). Urgent assessment needed to evaluate potential impacts on cetaceans from deep seabed mining. *Frontiers in Marine Science, 10*, 166.

Ulhaq, A., Adams, P., Cox, T. E., Khan, A., Low, T., & Paul, M. (2021). Automated Detection of Animals in Low-Resolution Airborne Thermal Imagery. *Remote Sensing, 13*(16), 3276.

Verfuss, U. K., Gillespie, D., Gordon, J., Marques, T. A., Miller, B., Plunkett, R., . . . Thomas, L. (2018). Comparing methods suitable for monitoring marine mammals in low visibility conditions during seismic surveys. *Marine Pollution Bulletin, 126*, 1-18. doi:10.1016/j.marpolbul.2017.10.034

Wedekin, L. L., Engel, M. H., Andriolo, A., Prado, P. I., Zerbini, A. N., Marcondes, M. M. C., . . . Simões-Lopes, P. C. (2017). Running fast in the slow lane: rapid population growth of humpback whales after exploitation. *Marine Ecology Progress Series, 575*, 195-206. doi:10.3354/meps12211

Witczuk, J., Pagacz, S., Zmarz, A., & Cypel, M. (2018). Exploring the feasibility of unmanned aerial vehicles and thermal imaging for ungulate surveys in forests-preliminary results. *International Journal of Remote Sensing, 39*(15-16), 5504-5521.

Witt, R. R., Beranek, C. T., Howell, L. G., Ryan, S. A., Clulow, J., Jordan, N. R., . . . Roff, A. (2020). Real-time drone derived thermal imagery outperforms traditional survey methods for an arboreal forest mammal. *PLoS One, 15*(11), e0242204. doi:10.1371/journal.pone.0242204

Young, B. G., Yurkowski, D. J., Dunn, J. B., & Ferguson, S. H. (2019). Comparing infrared imagery to traditional methods for estimating ringed seal density. *Wildlife Society Bulletin, 43*(1), 121-130.

Zitterbart, D. P., Kindermann, L., Burkhardt, E., & Boebel, O. (2013). Automatic round-the-clock detection of whales for mitigation from underwater noise impacts. *PLoS One, 8*(8), e71217. doi:10.1371/journal.pone.0071217

Zitterbart, D. P., Smith, H. R., Flau, M., Richter, S., Burkhardt, E., Beland, J., . . . Boebel, O. (2020). Scaling the Laws of Thermal Imaging–Based Whale Detection. *Journal of Atmospheric and Oceanic Technology, 37*(5), 807-824. doi:10.1175/jtech-d-19-0054.1

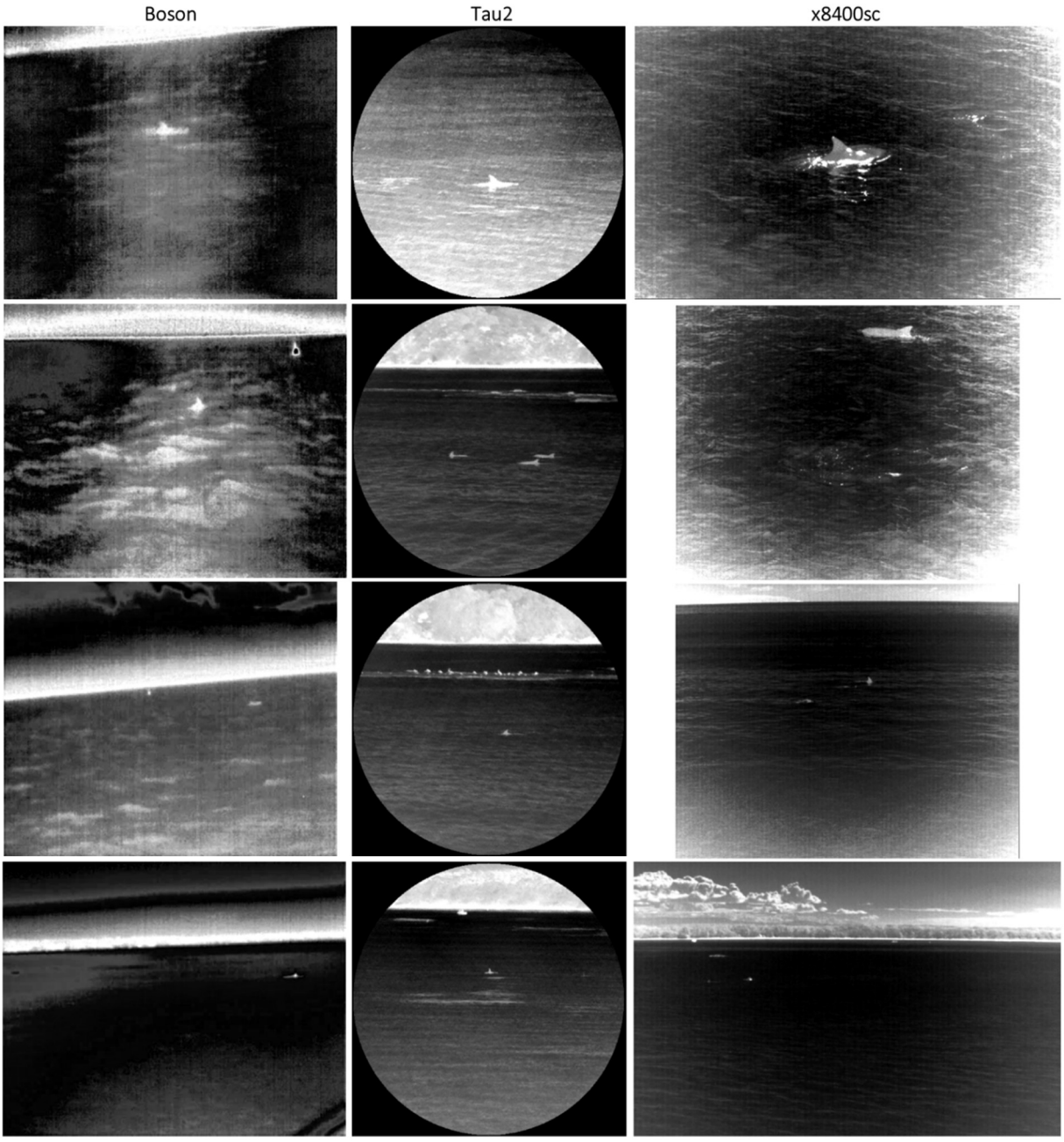

Figure S1. Unclipped images corresponding to thermal image results presented in Figure 2

6 GENERAL DISCUSSION

Humpback whale populations that migrate along the Australian east (subpopulation E1) and west coast (subpopulation D) each year have recovered at a remarkable rate since modern whaling ceased in 1963 (Noad et al., 2019; Hedley et al., 2020). Larger populations have been associated with increased numbers of humpbacks in coastal embayments where there is potential for disturbance from anthropogenic activities. This highlights the need to understand the importance of coastal areas long the migratory route and methods for monitoring the movement patterns of humpback whales in multi-use marine environments. The outcomes of this research were twofold. First, the research provided key insight into the use of Jervis Bay, on Australia's east coast, for-mother calf humpback whale groups and characterised resting patterns and second, the feasibility of novel methods for optimising whale detection was assessed.

Systematic land-based surveys, boat-based photo identification methods, and UAV surveys were utilised to provide the first detailed observation of humpback whales in Jervis Bay (Chapter 2). Unlike other areas where resting behaviour has been observed, including Hervey Bay, Queensland, (Franklin et al., 2011) and the Exmouth Gulf, Western Australia, (Bejder et al., 2019; Ejrnæs & Sprogis, 2021), Jervis Bay is considerably further in distance from recognised breeding grounds (~1,500 km) and whales must divert from the main migratory corridor to enter the Bay. Results demonstrated that of the groups entering Jervis Bay, a very high proportion contained a calf and these groups travelled at significantly slower speeds with less directed travel than groups migrating offshore. Furthermore, UAV surveys enabled clear observation of resting and nurturing behaviour. Findings from these multiple survey methods indicate that Jervis Bay is a resting ground for mother-calf groups. This research also highlighted the need to systematically quantify resting behaviour. Prior to this work, resting behaviour had predominantly been established through individual methods. This included boat-based surveys that are limited to observations on the water surface (McCulloch et al., 2021), UAV observations that are unable to provide continuous observations (Fiori et al., 2019a), or DTAGs that are able to quantify fine-scale behaviour, but are costly and limited to small sample sizes

and short windows of observation (average 10 hours in Bejder et al., 2019). Land surveys allowed for continuous observation (during daylight hours) and allowed a direct comparison with whales migrating offshore. This enabled quantitative analysis of the differences in whale movement inside a sheltered embayment compared with offshore which has not previously been presented in the literature.

The benefits of traditional survey methods, particularly, land-based surveys for comprehensive detection and observation of humpback whales during daylight hours were demonstrated in this research. There has been a rapid increase in the uptake of new technologies and methodologies, particularly UAVs (Schofield et al., 2019), thermal sensors that enable round-the-clock detection, and automated detection methods (Rodofili et al., 2022). There is an immediate need to evaluate other methods that leverage these emergent technologies to optimise cetacean detection (Chapters 3 – 5).

Environmental conditions (e.g. water turbidity) associated with aerial imagery are recognised as limiting factors in the detection of submerged objects (Aniceto et al., 2018; Colefax et al., 2018). In Chapter 3 a method for compensating for water attenuation through simple post-processing of UAV-captured images was applied. Using a modified version of Lyzenga's (1978; 1981) water column correction (Mumby et al., 1998; Hamylton, 2011) image enhancement improved detection of whales on the surface, and submerged below. The results showed that post-processed band pairs improved the contrast and definition of the whale in all images compared to the visual red-green-blue (RGB) images. Increasing the contrast between the whale and surrounding waters, demonstrated the potential for increasing the confidence of machine learning and automated detection methods that are reliant on a clear contrast between an animal and their surrounds (Laliberte & Ripple, 2003).

Although RGB imagery is most commonly used for animal detection, it is subject to light levels, contrast of the target animal compared to their environment, and shadows that may mask targets (Hinke et al., 2022). In Chapter 4 the effectiveness of UAV-borne thermal sensors to improve whale detection methods was assessed by testing three UAV platforms with synchronous capture capability. The higher resolution thermal sensors (640 x 512) detected both direct (e.g., body on the surface) and indirect (e.g., footprint) thermal whale cues from nadir and oblique angles. Previous studies have identified surface water temperature differentials for indirect thermal cues in colder waters

(Churnside et al., 2009; Florko et al., 2021; Lonati et al., 2022). However, the results presented here highlighted that a thermal contrast can be observed between a whale footprint and surrounding temperate waters (SST ~19°). Synchronous capture also showed that footprints were detectable in the thermal sensors after they were no longer evident in the visual RGB sensor images. Importantly, these results established that although thermal sensors are not a viable option to replace visual sensors for the daytime detection of whales, they complement RGB sensors and extend whale observation time.

Previous research has demonstrated that thermal sensors deployed from horizontal platforms (i.e., from ship or shore) provide detection rates comparable to visual sightings during good visibility conditions (Smith et al., 2020). Although, they have been deployed to improve continuous, round-the-clock detection methods required for regulatory purposes (e.g., during seismic surveys or naval activity) (Zitterbart et al., 2013; Smith et al., 2020), the importance of thermal sensor properties have received limited attention in the literature. In Chapter 5 the current state of knowledge was reviewed and the detection capabilities of three sensors were tested. Each sensor differed in sensor resolution, detector temperature, and spectral range to increase understanding of how thermal sensor configuration, cetacean cues, and environmental conditions will influence animal detection and the reliability of automated detection models. Although these field results applied to clear, calm conditions that cannot translate directly to open ocean conditions, the highest resolution cooled sensors demonstrated improved enhanced clarity of dolphin cues at distances of ~ 1km. The rapid rotating RobotEye system, that can be trained to automatically zoom into objects of interest (acceleration rates of $60{,}000^{0}/s^{2}$), such as cetacean cues, was proposed to improve current limitations in existing automated thermal detection systems.

6.1 MANAGEMENT IMPLICATIONS

The humpback whale groups using Jervis Bay on their southern migration are disproportionately mother-calf groups which were observed demonstrating resting and nurturing behaviour. The peak time for mother-calf groups in the Bay from late September to early November, coincides with both naval activity and commercial whale watching and recently introduced swim-with-whale activities that rely on close encounters with these animals. The importance of this stage for calves undertaking their

first southern migration highlights the need to monitor and manage the potential impacts of these activities.

The potentially invasive nature of swim-with-whale activities are of particular concern from a management perspective, not only for the wellbeing of the whales but also participants swimming. Due to their reliable seasonal occurrence and preference for calm, shallow waters, humpback whales are the most common large cetacean species targeted for swim-with-whale tourism. There is increasing evidence to highlight short-term behavioural effects associated with these activities. Fiori et al. (2020) used UAV methods to assess humpback whale response to swim-with activities in Tonga, demonstrating that for groups with a calf, surface-active behaviours reduced significantly in the presence of swimmers. Additionally, nurturing behaviour decreased almost five-fold and the time spent travelling almost doubled compared to behaviour in the absence of swimmers. Similarly, southern right southern right whales (*Eubalaena australis*) were found to significantly reduce their resting and socialising behaviours, whilst increasing travel in the presence of swimmers (Lundquist et al., 2013). Although not as invasive as swim-with activities, commercial whale watching activities still have the potential for disturbance. Sprogis et al. (2023) used UAV methods to find a significant reduction in resting of southern right whale mothers and calves during whale watching activities off the South Australian coastline. However, they found no significant effect on maternal swim speed, nursing rate or respiration rate, at the 300 m regulation distance. Disturbance to resting behaviour can have significant energetic costs to the calf if they are required to allocate energy to travelling. Additionally, the energy reserves of lactating females may decrease if whales are required to increase their travel speed or add distance to their migration, resulting in reduced calf growth (Braithwaite et al., 2015). Larger calf size provides the calf an energetic advantage during the subsequent migration and increases the probability of surviving a predation attempt (Videsen et al., 2017).

In Jervis Bay swimming with a whale group is prohibited if a calf is present, under requirements of the Australian National Guidelines for Whale and Dolphin Watching 2017. However, enforcing these activities is difficult and resource intensive. Sprogis et al. (2017) observed nine whale watching vessels that participated in swim-with-whale activities within the Ningaloo Marine Park, Western Australia, and reviewed the effectiveness of regulations. Overall, swimmers were placed in the water with calves

during 19.6% of observations. Low levels of compliance appear to be frequently observed for swim-with-whale activities involving humpback whales elsewhere (Tonga; Fiori et al., 2019b; Reunion Island; Hoarau et al., 2020). Sprogis et al. (2017) highlighted that the initial definition of a "calf" as "half the length or less of adult individuals of its species" was inadequate for encompassing all year-of-young calves. However, they still observed non-compliance during 33% of observations following a revised definition of "a young whale, paler in colour than adults of its species and/or less than 8 metres in length and/or less than two thirds of the adult it is in association with". Commercial operator confusion over the definition of a calf and ability to distinguish a calf from a juvenile highlight that to provide adequate protection for calves during their first migration, swim-with-activities should not be permitted during the southern migration.

The importance of Jervis Bay as a nursing/resting area for fasting, lactating females and their calves, underscores the need to minimise disturbance from naval, commercial whale-watching and swim-with-whale activities. Given the high likelihood of a calf being present in all observed whale groups during October, management regulations, such as enforcing the 300 m caution zone within which vessels must not enter should be prioritised.

6.2 FUTURE RESEARCH DIRECTIONS

This research provided a comprehensive analysis of the movement patterns of mother-calf humpback whales in Jervis Bay compared to whales migrating offshore. However, there is a need for longitudinal research to further explore residency time and site fidelity. Photo-identification methods in Jervis Bay were limited to two consecutive field seasons in 2018 and 2019, due to COVID-19 lockdown and social distancing restrictions in 2020 and 2021, respectively, prohibiting opportunity for data capture during successive migrations to investigate potential for maternal site fidelity. Sheehan and Blewitt (2013) demonstrated on one occasion that a mother entered the Bay two years apart with two different calves. Additional dedicated photo-identification methods are required to accurately determine extended residency in the Bay (beyond 1-2 days). Sheehan and Blewitt (2013) observed one mother-calf group stayed in the Bay for eight days. Understanding residency time and site fidelity is particularly important when assessing the impact of anthropogenic activity in the Bay and will help inform management decisions, particularly regarding commercial whale interactions.

Marine wildlife surveys to date have predominantly employed visual (RGB) sensors. However, there is a need to evaluate the role of multispectral sensors, including the near infrared (NIR) band (700 – 1,500 nm wavelength), for potential to mitigate the effects of sun glint contamination. Sun glint causes high brightness in visual images, reduces the signal-to-noise ratio, and reduces the accuracy of remotely sensed observation data (Muslim et al., 2019). Influenced by sun position, viewing angle and sea surface state (Kay et al., 2009), the effects of sun glint can be avoided by selectively choosing to survey in the early morning or later afternoon. Whilst this can be effective for static objects, including the mapping of nearshore benthos, this is not always feasible for moving and wide-ranging marine vertebrates. In the absence of flexibility in survey timing, there are robust methods to remove sun glint contamination from multispectral images (Hedley et al., 2005; Martin et al., 2016). Whilst these techniques are effective for multi-spectral images containing a NIR band, they are not suitable for images containing only red, green and blue (RGB) bands. Additionally, Colefax et al. (2021) found NIR bands effective for detecting submerged fauna in highly turbid conditions. As multispectral sensors become smaller, lighter, and more affordable there is a need to test the benefits of removing the effects of sun glint to enhance whale detection, particularly in UAV surveys. However, to date, most of this research has been in clearer coastal waters (Colefax et al., 2021) and further investigation is required on how the water body characteristics (Colefax et al., 2018), for example turbidity, and whale depth would influence these results.

In this thesis the thermal infrared imaging from nadir, oblique, and near-horizontal angles was demonstrated. There is a need to further explore how the angles at which thermal imaging is captured will influence the detection of thermal signatures. For example, Horton et al. (2017) found capturing thermal images from a near-horizontal platform resulted in similar thermal brightness anomalies for humpback whale blows and their bodies on the surface, at two locations that had a 16°C difference in sea surface temperature. This was attributed to emissivity effects. Due to lower levels of background emissivity captured from near-horizontal platforms they are considered more effective in detecting whale exhalations than sensors capturing at a nadir angle (Churnside et al., 2009). Depending on the angle of capture, emissivity associated with rough ocean water could mask whale cues, but this physical property can also be advantageous for detecting thermal signatures at a distance on oblique angles from a UAV (demonstrated in Chapter

4). Understanding how the angle of the thermal sensor will influence whale detectability is particularly important during UAV surveys if the sensor is on a rotating gimbal.

6.3 CONCLUSION

This thesis provided the first scientific survey of humpback whales in Jervis Bay and demonstrated resting and nurturing behaviours by mother-calf groups within the Bay. Jervis Bay is a multi-use marine park, supporting a breadth of activities. The temporal and geographical overlap of these activities within Jervis Bay highlights the need for effective monitoring and management. This research established the benefits of using multiple survey methods to observe movement patterns. Combining land-based surveys, boat-based surveys, and UAV methods allowed validation across different data sets providing evidence of low energy expenditure, or resting behaviour, within Jervis Bay. Finally, these research findings highlight the need to understand and monitor for potential impacts of increased anthropogenic activity and development of our oceans, including offshore mining, shipping, and naval operations, and consequently the need for novel, accurate and resource effective whale detection methods.

6.4 REFERENCES

Aniceto, A. S., Biuw, M., Lindstrøm, U., Solbø, S. A., Broms, F., & Carroll, J. (2018). Monitoring marine mammals using unmanned aerial vehicles: quantifying detection certainty. *Ecosphere, 9*(3), e02122.

Bejder, L., Videsen, S., Hermannsen, L., Simon, M., Hanf, D., & Madsen, P. T. (2019). Low energy expenditure and resting behaviour of humpback whale mother-calf pairs highlights conservation importance of sheltered breeding areas. *Scientific Reports, 9*(1), 771. doi:10.1038/s41598-018-36870-7

Braithwaite, J. E., Meeuwig, J. J., & Hipsey, M. R. (2015). Optimal migration energetics of humpback whales and the implications of disturbance. *Conservation Physiology, 3*(1), cov001. doi:10.1093/conphys/cov001

Churnside, J., Ostrovsky, L., & Veenstra, T. (2009). Thermal Footprints of Whales. *Oceanography, 22*(1), 206-209. doi:10.5670/oceanog.2009.20

Colefax, A. P., Butcher, P. A., Kelaher, B. P., & Browman, H. (2018). The potential for unmanned aerial vehicles (UAVs) to conduct marine fauna surveys in place of manned aircraft. *ICES Journal of Marine Science, 75*(1), 1-8. doi:10.1093/icesjms/fsx100

Colefax, A. P., Kelaher, B. P., Walsh, A. J., Purcell, C. R., Pagendam, D. E., Cagnazzi, D., & Butcher, P. A. (2021). Identifying optimal wavelengths to maximise the detection rates of marine fauna from aerial surveys. *Biological Conservation, 257*, 109102.

Ejrnæs, D. D., & Sprogis, K. R. (2021). Ontogenetic changes in energy expenditure and resting behaviour of humpback whale mother–calf pairs examined using unmanned aerial vehicles. *Wildlife Research, 49*(1), 34-45.

Fiori, L., Martinez, E., Bader, M. K. F., Orams, M. B., & Bollard, B. (2019a). Insights into the use of an unmanned aerial vehicle (UAV) to investigate the behavior of humpback whales (*Megaptera novaeangliae*) in Vava'u, Kingdom of Tonga. *Marine Mammal Science, 36*(1), 209-223. doi:10.1111/mms.12637

Fiori, L., Martinez, E., Orams, M. B., & Bollard, B. (2019b). Effects of whale-based tourism in Vava'u, Kingdom of Tonga: Behavioural responses of humpback whales to vessel and swimming tourism activities. *PLoS One, 14*(7), e0219364. doi:10.1371/journal.pone.0219364

Fiori, L., Martinez, E., Orams, M. B., & Bollard, B. (2020). Using Unmanned Aerial Vehicles (UAVs) to assess humpback whale behavioral responses to swim-with interactions in Vava'u, Kingdom of Tonga. *Journal of Sustainable Tourism, 28*(11), 1743-1761.

Florko, K. R. N., Carlyle, C. G., Young, B. G., Yurkowski, D. J., Michel, C., & Ferguson, S. H. (2021). Narwhal (*Monodon monoceros*) detection by infrared flukeprints from aerial survey imagery. *Ecosphere, 12*(8). doi:10.1002/ecs2.3698

Franklin, T., Franklin, W., Brooks, L., Harrison, P., Baverstock, P., & Clapham, P. (2011). Seasonal changes in pod characteristics of eastern Australian humpback whales (*Megaptera novaeangliae*), Hervey Bay 1992-2005. *Marine Mammal Science, 27*(3), E134-E152. doi:10.1111/j.1748-7692.2010.00430.x

Hamylton, S. (2011). An evaluation of waveband pairs for water column correction using band ratio methods for seabed mapping in the Seychelles. *International Journal of Remote Sensing, 32*(24), 9185-9195. doi:10.1080/01431161.2010.550648

Hedley, J. D., Harborne, A. R., & Mumby, P. J. (2005). Technical note: Simple and robust removal of sun glint for mapping shallow-water benthos. *International Journal of Remote Sensing, 26*(10), 2107-2112. doi:10.1080/01431160500034086

Hedley, S. L., Bannister, J. L., & Dunlop, R. A. (2020). Abundance estimates of Southern Hemisphere Breeding Stock 'D'humpback whales from aerial and land-based surveys off Shark Bay, Western Australia, 2008. *J. Cetacean Res. Manage.*, 209-221.

Hinke, J. T., Giuseffi, L. M., Hermanson, V. R., Woodman, S. M., & Krause, D. J. (2022). Evaluating Thermal and Color Sensors for Automating Detection of Penguins and Pinnipeds in Images Collected with an Unoccupied Aerial System. *Drones, 6*(9), 255.

Hoarau, L., Dalleau, M., Delaspre, S., Barra, T., & Landes, A.-E. (2020). Assessing and mitigating humpback whale (*Megaptera novaeangliae*) disturbance of whale-watching activities in Reunion Island. *Tourism in Marine Environments, 15*(3-4), 173-189.

Horton, T. W., Oline, A., Hauser, N., Khan, T. M., Laute, A., Stoller, A., . . . Zawar-Reza, P. (2017). Thermal Imaging and Biometrical Thermography of Humpback Whales. *Frontiers in Marine Science, 4*. doi:10.3389/fmars.2017.00424

Kay, S., Hedley, J. D., & Lavender, S. (2009). Sun glint correction of high and low spatial resolution images of aquatic scenes: a review of methods for visible and near-infrared wavelengths. *Remote Sensing, 1*(4), 697-730.

Laliberte, A. S., & Ripple, W. J. J. W. S. B. (2003). Automated wildlife counts from remotely sensed imagery. 362-371.

Lonati, G. L., Zitterbart, D. P., Miller, C. A., Corkeron, P., Murphy, C. T., & Moore, M. J. (2022). Investigating the thermal physiology of Critically Endangered North Atlantic right whales *Eubalaena glacialis* via aerial infrared thermography. *Endangered Species Research, 48*, 139-154.

Lundquist, D., Sironi, M., Würsig, B., Rowntree, V., Martino, J., & Lundquist, L. (2013). Response of southern right whales to simulated swim-with-whale tourism at Península Valdés, Argentina. *Marine Mammal Science, 29*(2), E24-E45.

Lyzenga, D. R. (1978). Passive remote sensing techniques for mapping water depth and bottom features. *Applied Optics, 17*(3), 379-383.

Lyzenga, D. R. (1981). Remote sensing of bottom reflectance and water attenuation parameters in shallow water using aircraft and Landsat data. *International Journal of Remote Sensing, 2*(1), 71-82.

Martin, J., Eugenio, F., Marcello, J., & Medina, A. (2016). Automatic Sun Glint Removal of Multispectral High-Resolution Worldview-2 Imagery for Retrieving Coastal Shallow Water Parameters. *Remote Sensing, 8*(1). doi:10.3390/rs8010037

McCulloch, S., Meynecke, J.-O., Franklin, T., Franklin, W., Chauvenet, A. J. M., & Research, F. (2021). Humpback whale (*Megaptera novaeangliae*) behaviour determines habitat use in two Australian bays.

Mumby, P., Clark, C., Green, E., & Edwards, A. (1998). Benefits of water column correction and contextual editing for mapping coral reefs. *International Journal of Remote Sensing, 19*(1), 203-210.

Muslim, A. M., Chong, W. S., Safuan, C. D. M., Khalil, I., & Hossain, M. S. (2019). Coral Reef Mapping of UAV: A Comparison of Sun Glint Correction Methods. *Remote Sensing, 11*(20), 2422.

Noad, M. J., Kniest, E., & Dunlop, R. A. (2019). Boom to bust? Implications for the continued rapid growth of the eastern Australian humpback whale population despite recovery. *Population Ecology, 61*(2), 198-209. doi:10.1002/1438-390x.1014

Rodofili, E. N., Lecours, V., & LaRue, M. (2022). Remote sensing techniques for automated marine mammals detection: a review of methods and current challenges. *PeerJ, 10*, e13540.

Schofield, G., Esteban, N., Katselidis, K. A., & Hays, G. C. (2019). Drones for research on sea turtles and other marine vertebrates – A review. *Biological Conservation, 238*. doi:10.1016/j.biocon.2019.108214

Sheehan, S., & Blewitt, M. (2013). *Jervis Bay: an Area of Significance for Southward Migrating Humpback Whale Cow/Calf Pairs?* Paper presented at the Australian Marine Science Association (AMSA), Gold Coast, Queensland, Australia.

Smith, H. R., Zitterbart, D. P., Norris, T. F., Flau, M., Ferguson, E. L., Jones, C. G., . . . Moulton, V. D. (2020). A field comparison of marine mammal detections via visual, acoustic, and infrared (IR) imaging methods offshore Atlantic Canada. *Marine Pollution Bulletin, 154*, 111026. doi:10.1016/j.marpolbul.2020.111026

Sprogis, K. R., Bejder, L., & Christiansen, F. (2017). Swim-with-whale tourism trial in the Ningaloo Marine Park, Western Australia. *Report to the Department of Parks and Wildlife, Western Australia. Murdoch University, Murdoch, WA*.

Sprogis, K. R., Holman, D., Arranz, P., & Christiansen, F. (2023). Effects of whale-watching activities on southern right whales in Encounter Bay, South Australia. *Marine Policy, 150*, 105525.

Videsen, S. K. A., Bejder, L., Johnson, M., Madsen, P. T., & Goldbogen, J. (2017). High suckling rates and acoustic crypsis of humpback whale neonates maximise potential for mother-calf energy transfer. *Functional Ecology, 31*(8), 1561-1573. doi:10.1111/1365-2435.12871

Zitterbart, D. P., Kindermann, L., Burkhardt, E., & Boebel, O. (2013). Automatic round-the-clock detection of whales for mitigation from underwater noise impacts. *PLoS One, 8*(8), e71217. doi:10.1371/journal.pone.0071217

APPENDIX A | PUBLISHED NOTE RELATING TO CHAPTER 3

Jones, A., Bruce, E., Davies, K. P., Cato, D. H. (2022). Enhancing UAV images to improve the observation of submerged whales using a water column correction method. *Marine Mammal Science*. https://doi.org/10.1111/mms.12994

Received: 22 March 2022 | Accepted: 23 November 2022

DOI: 10.1111/mms.12994

NOTE

Marine Mammal Science

Enhancing UAV images to improve the observation of submerged whales using a water column correction method

Alexandra Jones [1,2] | Eleanor Bruce [1,2] | Kevin P. Davies [1,2] | Douglas H. Cato [1,2]

[1]School of Geosciences, University of Sydney, Sydney, Australia

[2]Marine Studies Institute, University of Sydney, Sydney, Australia

Correspondence
Alexandra Jones, Madsen Building F09, Camperdown, NSW 2006, Australia.
Email: alexandra.jones1@sydney.edu.au

Funding information
Defence Science and Technology Group (Maritime Division) through the ARC Training Centre for Cubesats, UAVs and Their Applications (CUAVA), Grant/Award Number: ICI70100023

Ultra-high spatial resolution sensors made available by advancements in the miniaturization of instruments deployable on uncrewed aerial vehicle (UAVs),[1] present new and innovative opportunities for remote detection of marine wildlife. The spatio-temporal resolution and survey responsiveness afforded by these low-cost platforms enables the collection of data that can provide insights on the spatio-temporal dynamics of individual marine animals at close range (Anderson & Gaston, 2013). In the last decade there has been an increase in marine studies utilizing UAVs (Schofield et al., 2019), which allows for novel insights on the abundance (Hodgson et al., 2017), behavior (Fiori et al., 2020; Torres et al., 2018), and body condition (Christiansen et al., 2016; Hodgson et al., 2020) of marine wildlife. Importantly, UAV-based image capture has the potential to increase the duration of visible observation through detection of animals below the water surface (Torres et al., 2018). This has significant ramifications for the study of mother-calf humpback whale groups that rest in shallow protected embayments (Bruce et al., 2014; McCulloch et al., 2021), spending high proportions of time resting at depths of <5 m (Bejder et al., 2019; Iwata et al., 2021). However, the use of remotely sensed data in coastal environments is challenged by the optical complexity of the water column (Figure 1). Research until now has focused primarily on image detection based on the visual spectrum with limited evaluation of conventional remote sensing methods for enhancing observation of whales. Processing techniques are commonly used in remote sensing research to enhance or enable the detection of underwater features, including benthic habitat (Hedley et al., 2016; Mumby et al., 1998; Zoffoli et al., 2014). Similar techniques, including water column correction, can be applied to UAV-captured images to enhance visibility of animals below the water surface, which may be missed in manual counts or automated deep-learning based classifications

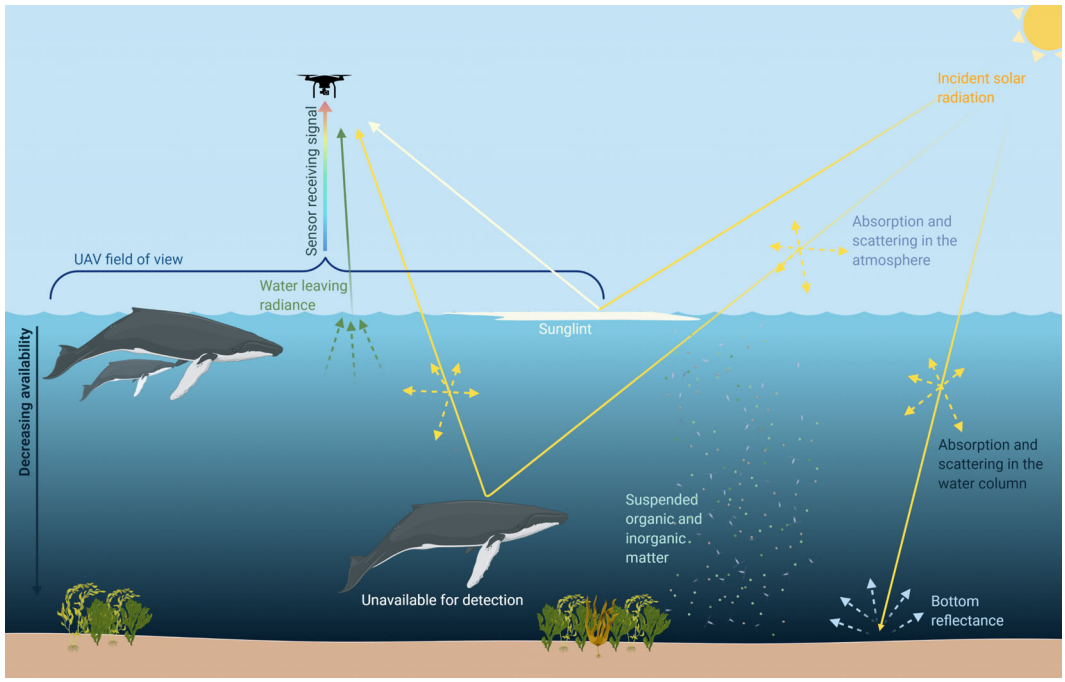

FIGURE 1 Diagram illustrating the various processes contributing to complexities in surveying large marine species from a UAV platform. Created with BioRender (https://biorender.com/).

(Gray et al., 2019). This paper presents remote sensing-based methods for enhancing UAV-acquired visual image data to improve the contrast of whales on the water surface and submerged near the surface. Application of these methods has the potential to reduce perception error (Colefax et al., 2018) and subsequently improve detection rates. The Jervis Bay Marine Park study site on the eastern Australian coastline is frequented by humpback whale (*Megaptera novaeangliae*) mother-calf groups during the southern migration from the breeding grounds (Bruce et al., 2014; Jones, 2019).

The visible RGB imaging capabilities of sensors for detecting whales were evaluated using a DJI Mavic 2 Enterprise Dual (M2ED) launched from a small boat in Jervis Bay. Following a confirmed whale sighting, the whale's behavior and direction of travel were observed for 5 min from the boat at a distance >300 m before an approach was made to a distance >100 m from the whale. The UAV was launched to an initial altitude of 55 m to provide sufficient sensor field of view for whale identification and lowered to ≥25 m once whale(s) were visible on the controller screen. The boat remained at a distance >100 m from the whales during the flights to provide a visual line of sight to the UAV and facilitate positioning over the whales. Still images and videos were captured throughout each flight.

Lyzenga's water column correction (Lyzenga, 1981) as modified by Mumby et al. (1998) and Hamylton (2011) was applied to three UAV images containing humpback whales (steps summarized in Figure 2). To enhance the spectral signature of the whale, radiance values were taken from transects along and across the whale's body surface to account for the fusiform shape of the whale (Step 3, Figure 2). This method, suitable for high clarity water, produces a depth-invariant band based on each pair of spectral (wavelength) bands (Mumby et al., 1998). This generated three depth invariant bands from the available spectral band pairs (red/green, red/blue, green/blue). To allow for comparison between the original image and processed images, all pixels were converted into *Z*-scores ($Z = [\text{pixel value} - \text{mean}]/\text{standard deviation}$), enabling detection of anomalies. The performance of the applied image processing methods was assessed visually (Figure 3), and quantitively by evaluating the mean *Z*-score values (Table 1) extracted across the whale's surface for the original RGB images and the three resulting band pairs.

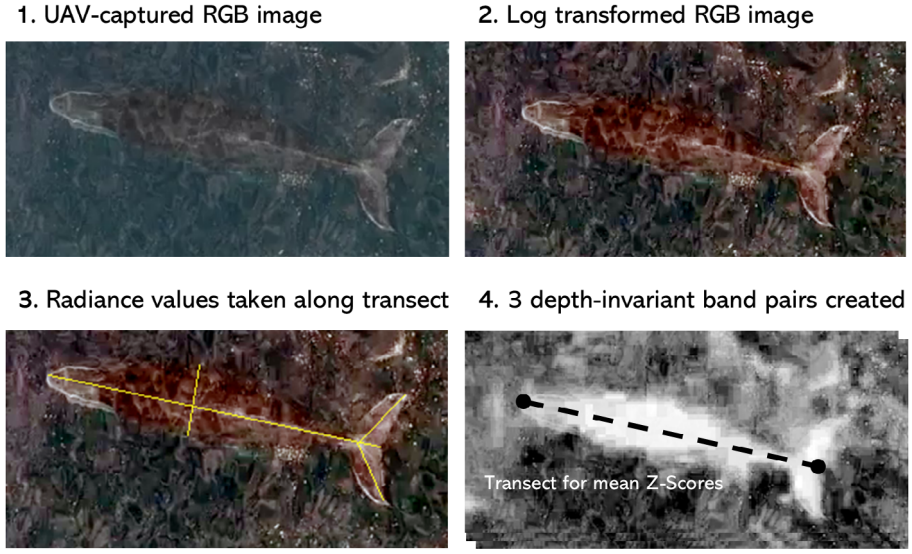

FIGURE 2 Overview of processing steps applied in the depth invariant analysis. In Step 3, the yellow transect outlines where the radiance values were extracted for inclusion in the correction. The correction process resulted in three depth-invariant band pairs. These images were then converted into *Z*-scores and transects (black dotted line, Step 4) were extracted along the length of the whale to determine average values for each image.

Application of Lyzenga's water column correction enhanced the contrast and edge definition between whales and surrounding water in the three UAV-captured images presented here. For whales on or just below the surface, the red/green and red/blue depth-invariant band pairs were the most effective band pair combination for enhancing contrast between the whale and surrounding waters, both visually (Figure 3A and C) and resulting in the highest anomaly values (Table 1). The effectiveness of the red band for animals on or near the surface is consistent with findings from Colefax et al. (2021), who demonstrated the red band produced the greatest spectral contrast for detecting dolphins, sharks, and other marine fauna from a UAV. At increasing depths, the green/blue band pair produced a stronger visual contrast and highest anomaly result (Figure 3B; Table 1) owing to the red waveband becoming attenuated at greater depth.

The depth of the target animal(s) will influence the optimal band pairing and subsequent object enhancement within the image. The red band (610–700 nm), and other bands with wavelengths approaching the red end of the spectrum (e.g., red edge and near infrared), will become fully attenuated around 2–3 m depth (Hamylton, 2011; Mishra et al., 2005). Thus, the effectiveness of band pairs using the red band will be substantially reduced at this depth. However, in turbid waters, where sightability below the surface is limited, longer wavelength bands may be optimal for increasing the contrast of animals just below the surface (Colefax et al., 2021). Image enhancement methods for improving whale detection rates even in optically shallow waters (<2–3 m) has important implications for studies reliant on whale visibility, such as estimating abundance (e.g., Hodgson et al., 2017). This is key for research conducted on breeding/resting grounds, with lactating females and their calves spending over 50% of time within 3 m of the surface (Bejder et al., 2019).

The methods presented here have the potential to increase the confidence of machine learning and automated detection models. Machine learning techniques for automated detection of whales are increasingly being applied to UAV-collected data sets providing an efficient way to process large amounts of data. Studies using machine learning to detect individual animals or plants rely on the detection of target objects against mostly homogenous backgrounds which typically rely on a clear contrast to reliably discriminate animals from their surrounding environment (Laliberte & Ripple, 2003). The use of machine learning for detecting marine vertebrates is further complicated by

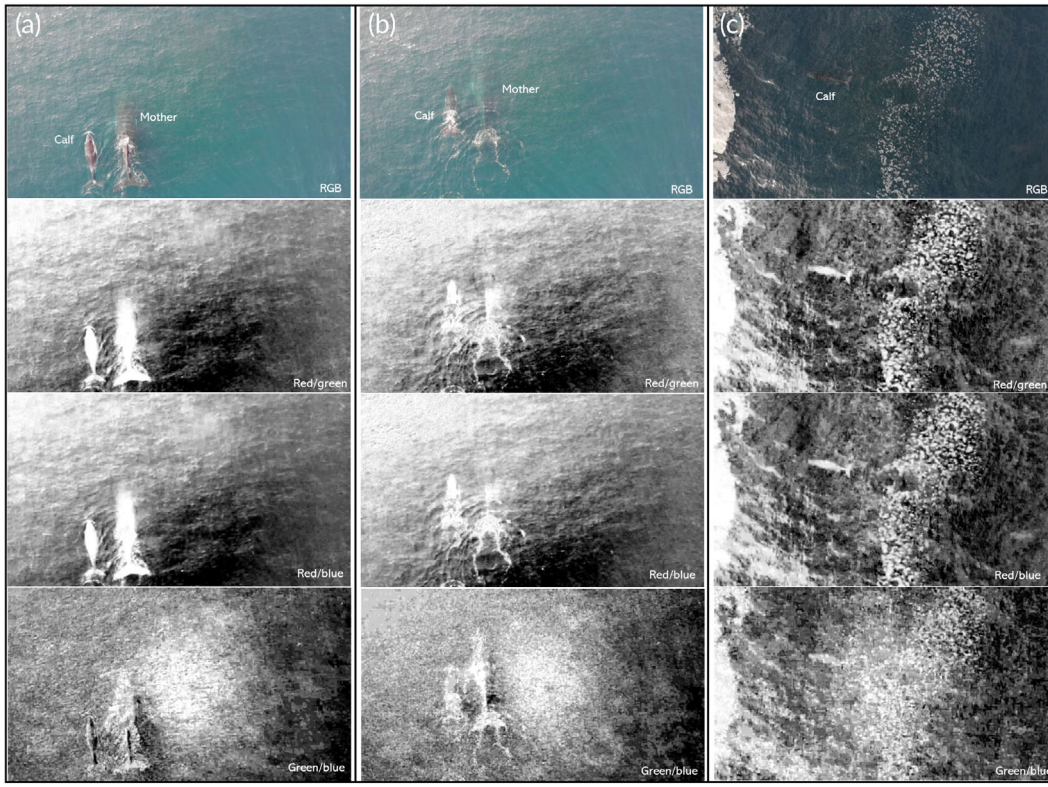

FIGURE 3 Results of depth-invariant processing for three UAV images. (A) Shows a partially submerged humpback whale mother and calf at the surface, (B) shows the same mother calf group now fully submerged, taken 5 s after Image A, and (C) shows a submerged humpback whale calf. The four panels, from top to bottom present: the raw red, green, and blue (RGB) images, depth-invariant red/green band pairs, depth-invariant red/blue band pairs, depth-invariant green/blue band pairs.

TABLE 1 Mean *Z*-scores extracted across the whales in the three images from Figure 3, presenting results from the RGB image and three depth-invariant band pairs. The results from the RGB image are presented as individual red, green, and blue bands. The highest value for each image is shown in bold.

	Mean *Z*-scores Image A	Image B	Image C
Red	1.00	0.85	0.40
Green	−0.28	0.90	0.07
Blue	−0.45	0.54	−0.08
Red/green	**2.21**	0.67	1.85
Red/blue	2.11	1.05	**1.88**
Green/blue	0.32	**1.64**	1.25

coloration similarities between some species and the surrounding water (e.g., blue whales; Gray et al., 2019) and non-uniform backgrounds that are subject to varying environmental conditions. In ecological studies, object-based image analysis (OBIA) is the most commonly used machine learning method (Dujon & Schofield, 2019). It provides versatility for detecting objects in varied backgrounds with confounding features, objects that vary in size and shape, and may be sparsely distributed in the image data set (Chabot et al., 2018), making it ideal for abundance and distribution

studies. Importantly, even with increased flexibility over other machine learning methods, OBIA is still reliant on the object(s) of interest in the image being localized from surrounding pixels through a local brightness contrast, either as a relatively brighter or relatively darker group of image pixels (Groom et al., 2013). For whale detection, increasing the anomaly (Z-score) of the whale object, as demonstrated here, could potentially improve OBIA-derived results and increase detection availability.

Here we have demonstrated that water column correction techniques can enhance the visual outline and anomaly signal over the body of whales on the surface and submerged at shallow depths. However, we recognize constraints associated with the limited spectral resolution provided when working with three bands (i.e., red, green, and blue) within the visible range (wavelength 400–700 nm). Employing multispectral or hyperspectral sensors and customizing or selecting bands configured to focus on wavelength bands optimal for the spectral characteristics of the water body, such as the coastal band (Fretwell et al., 2014), and target species may further reduce perception bias and subsequently improve animal availability at depth compared to standard RGB sensors (Colefax et al., 2018). Additionally, obtaining a larger image data set is critical for understanding the effectiveness of depth invariant indices derived from possible band pairs, and whether these differ with the whale depth and environmental factors (e.g., turbidity). Ultimately, an understanding of the role of water column attenuation correction is critical for accurate detection of whales and is particularly relevant with the increasing use of low-cost UAV platforms and machine learning techniques for achieving estimates of population abundance and monitoring movement patterns of marine wildlife in shallow coastal habitats.

AUTHOR CONTRIBUTIONS

Alexandra Jones: Conceptualization; formal analysis; investigation; methodology; project administration; writing – original draft; writing – review and editing. **Eleanor Bruce:** Conceptualization; investigation; methodology; project administration; supervision; writing – review and editing. **Kevin Davies:** Conceptualization; formal analysis; methodology; supervision; writing – review and editing. **Douglas Cato:** Methodology; project administration; supervision; writing – review and editing.

ACKNOWLEDGMENTS

Thank you to Scott Sheehan for assistance in conducting the UAV surveys. VADAR software was designed by Eric Kniest who customized it for this research. And to Nathan Angelakis, Natasha Garner, Gabrielle Genty, Kennadie Haigh, Evie Hyland, David Lorieux, Lisa McComb, and Euan Smith for support in the field.

This research was conducted under authorization by the University of Sydney Animal Ethic Committee (permit 2019/1592) and permits from the Department of Primary Industries Marine Parks (permit MEAA19/179) and the Department of Planning, Industry and Environment, New South Wales (SL102287). Under restrictions from the Australian Civil Aviation Authority (CASA) all UAV flights were within visual line of sight. Approval was obtained from the Department of Defence to fly UAVs in the Restricted Airspaces (R421A Nowra and R452 Beecroft Head) covering Jervis Bay. Open access publishing facilitated by The University of Sydney, as part of the Wiley - The University of Sydney agreement via the Council of Australian University Librarians.

ORCID

Alexandra Jones https://orcid.org/0000-0002-5565-6109

ENDNOTE

[1] Also commonly referred to as drones, unmanned, unoccupied aerial vehicles, or remotely piloted aircraft system.

REFERENCES

Anderson, K., & Gaston, K. J. (2013). Lightweight unmanned aerial vehicles will revolutionize spatial ecology. *Frontiers in Ecology and the Environment*, *11*, 138–146. https://doi.org/10.1890/120150

Bejder, L., Videsen, S., Hermannsen, L., Simon, M., Hanf, D., & Madsen, P. T. (2019). Low energy expenditure and resting behaviour of humpback whale mother-calf pairs highlights conservation importance of sheltered breeding areas. *Scientific Reports*, *9*, Article 771. https://doi.org/10.1038/s41598-018-36870-7

Bruce, E., Albright, L., Sheehan, S., & Blewitt, M. (2014). Distribution patterns of migrating humpback whales (*Megaptera novaeangliae*) in Jervis Bay, Australia: A spatial analysis using geographical citizen science data. *Applied Geography*, *54*, 83–95. https://doi.org/10.1016/j.apgeog.2014.06.014

Chabot, D., Dillon, C., & Francis, C. (2018). An approach for using off-the-shelf object-based image analysis software to detect and count birds in large volumes of aerial imagery. *Avian Conservation and Ecology*, *13*(1), Article 15. https://doi.org/10.5751/ACE-01205-130115

Christiansen, F., Dujon, A. M., Sprogis, K. R., Arnould, J. P., & Bejder, L. (2016). Noninvasive unmanned aerial vehicle provides estimates of the energetic cost of reproduction in humpback whales. *Ecosphere*, *7*(10), Article e01468. https://doi.org/10.1002/ecs2.1468

Colefax, A. P., Butcher, P. A., Kelaher, B. P., & Browman, H. (2018). The potential for unmanned aerial vehicles (UAVs) to conduct marine fauna surveys in place of manned aircraft. *ICES Journal of Marine Science*, *75*(1), 1–8. https://doi.org/10.1093/icesjms/fsx100

Colefax, A. P., Kelaher, B. P., Walsh, A. J., Purcell, C. R., Pagendam, D. E., Cagnazzi, D., & Butcher, P. A. (2021). Identifying optimal wavelengths to maximise the detection rates of marine fauna from aerial surveys. *Biological Conservation*, *257*, Article 109102. https://doi.org/10.1016/j.biocon.2021.109102

Dujon, A. M., & Schofield, G. (2019). Importance of machine learning for enhancing ecological studies using information-rich imagery. *Endangered Species Research*, *39*, 91–104. https://doi.org/10.3354/esr00958

Fiori, L., Martinez, E., Bader, M. K. F., Orams, M. B., & Bollard, B. (2020). Insights into the use of an unmanned aerial vehicle (UAV) to investigate the behavior of humpback whales (*Megaptera novaeangliae*) in Vava'u, Kingdom of Tonga. *Marine Mammal Science*, *36*(1), 209–223. https://doi.org/10.1111/mms.12637

Fretwell, P. T., Staniland, I. J., & Forcada, J. (2014). Whales from space: counting southern right whales by satellite. *PLoS ONE*, *9*(2), Article e88655. https://doi.org/10.1371/journal.pone.0088655

Gray, P. C., Bierlich, K. C., Mantell, S. A., Friedlaender, A. S., Goldbogen, J. A., Johnston, D. W., & Ye, H. (2019). Drones and convolutional neural networks facilitate automated and accurate cetacean species identification and photogrammetry. *Methods in Ecology and Evolution*, *10*(9), 1490–1500. https://doi.org/10.1111/2041-210X.13246

Groom, G., Stjernholm, M., Nielsen, R. D., Fleetwood, A., & Petersen, I. K. (2013). Remote sensing image data and automated analysis to describe marine bird distributions and abundances. *Ecological Informatics*, *14*, 2–8. https://doi.org/10.1016/j.ecoinf.2012.12.001

Hamylton, S. (2011). An evaluation of waveband pairs for water column correction using band ratio methods for seabed mapping in the Seychelles. *International Journal of Remote Sensing*, *32*(24), 9185–9195. https://doi.org/10.1080/01431161.2010.550648

Hedley, J. D., Roelfsema, C. M., Chollett, I., Harborne, A. R., Heron, S. F., Weeks, S., Skirving, W. J., Strong, A. E., Eakin, C. M., & Christensen, T. R. (2016). Remote sensing of coral reefs for monitoring and management: a review. *Remote Sensing*, *8*(2), Article 118. https://doi.org/10.3390/rs8020118

Hodgson, J. C., Holman, D., Terauds, A., Koh, L. P., & Goldsworthy, S. D. (2020). Rapid condition monitoring of an endangered marine vertebrate using precise, non-invasive morphometrics. *Biological Conservation*, *242*, Article 108402. https://doi.org/10.1016/j.biocon.2019.108402

Hodgson, A., Peel, D., & Kelly, N. (2017). Unmanned aerial vehicles for surveying marine fauna: assessing detection probability. *Ecological Applications*, *27*(4), 1253–1267. https://doi.org/10.1002/eap.1519

Iwata, T., Biuw, M., Aoki, K., Miller, P. J. O. M., & Sato, K. (2021). Using an omnidirectional video logger to observe the underwater life of marine animals: humpback whale resting behaviour. *Behavioural Processes*, *186*, Article 104369. https://doi.org/10.1016/j.beproc.2021.104369

Jones, A., Bruce, E., Cato, D., & Davies, K. (2019). *Tracking of humpback whales by theodolite from Point Perpendicular, Jervis Bay* (Fieldwork Report 2018). University of Sydney.

Laliberte, A. S., & Ripple, W. J. (2003). Automated wildlife counts from remotely sensed imagery. *Wildlife Society Bulletin*, *31*(2), 362–371. https://doi.org/10.2307/3784314

Lyzenga, D. R. (1981). Remote sensing of bottom reflectance and water attenuation parameters in shallow water using aircraft and Landsat data. *International Journal of Remote Sensing*, *2*(1), 71–82. https://doi.org/10.1080/01431168108948342

McCulloch, S., Meynecke, J.-O., Franklin, T., Franklin, W., & Chauvenet, A. (2021). Humpback whale (*Megaptera novaeangliae*) behaviour determines habitat use in two Australian bays. *Marine and Freshwater Research*, *72*, 1251–1267. https://doi.org/10.1071/MF21065

Mishra, D. R., Narumalani, S., Rundquist, D., & Lawson, M. (2005). Characterizing the vertical diffuse attenuation coefficient for downwelling irradiance in coastal waters: Implications for water penetration by high resolution satellite data. *ISPRS Journal of Photogrammetry and Remote Sensing*, *60*(1), 48–64. https://doi.org/10.1016/j.isprsjprs.2005.09.003

Mumby, P., Clark, C., Green, E., & Edwards, A. (1998). Benefits of water column correction and contextual editing for mapping coral reefs. *International Journal of Remote Sensing*, *19*(1), 203–210. https://doi.org/10.1080/014311698216521

Schofield, G., Esteban, N., Katselidis, K. A., & Hays, G. C. (2019). Drones for research on sea turtles and other marine vertebrates – A review. *Biological Conservation*, *238*, Article 108214. https://doi.org/10.1016/j.biocon.2019.108214

Torres, L. G., Nieukirk, S. L., Lemos, L., & Chandler, T. E. (2018). Drone up! Quantifying whale behavior from a new perspective improves observational capacity. *Frontiers in Marine Science*, *5*. https://doi.org/10.3389/fmars.2018.00319

Zoffoli, M. L., Frouin, R., & Kampel, M. (2014). Water column correction for coral reef studies by remote sensing. *Sensors*, *14*(9), 16881–16931. https://doi.org/10.3390/s140916881

How to cite this article: Jones, A., Bruce, E., Davies, K. P., & Cato, D. H. (2022). Enhancing UAV images to improve the observation of submerged whales using a water column correction method. *Marine Mammal Science*, 1–7. https://doi.org/10.1111/mms.12994

APPENDIX B | SUMMARY OF FIELDWORK EFFORT

Table B.1. Summary of land survey effort and sightings of humpback whale groups observed within Jervis Bay and offshore in 2018, 2019, and 2021

Land surveys				
Date	**Survey start time**	**Survey end time**	**No. whale groups observed inside Jervis Bay**	**No. whale groups observed offshore**
27/09/2018	0800	1715	2	29
28/09/2018	1130	1700	0	20
29/09/2018				
30/09/2018	0800	1700	3	25
01/10/2018	0800	1700	17	87
02/10/2018	0800	1700	4	10
03/10/2018	0800	1240	3	13
04/10/2018				
05/10/2018				
06/10/2018	0800	1715	4	61
07/10/2018			0	0
08/10/2018	0900	1725	2	19
09/10/2018	0810	1700	3	50
10/10/2018				
11/10/2018	0800	1230	2	23
12/10/2018	0800	1700	5	43
13/10/2018	0800	1700	3	60
14/10/2018	0800	1700	7	28
15/10/2018				
16/10/2018	0805	1700	8	19
17/10/2018	0800	1700	6	12
18/10/2018	0800	1700	12	29
19/10/2018	0800	1700	9	24
20/10/2018	0800	1700	20	21
21/10/2018	0800	1700	5	28
22/10/2018	0800	1700	15	39
23/10/2018	0800	1700	9	23
24/10/2018	0800	1700	6	6
25/10/2018	0800	1700	11	20
30/09/2019	0840	1430	0	15
01/10/2019	0800	1700	0	50
02/10/2019	0900	1700	0	14
03/10/2019	0800	1700	8	23
04/10/2019	0800	1700	15	19
05/10/2019	0800	1700	2	9

06/10/2019	0800	1000	3	3
07/10/2019	0800	1700	4	5
08/10/2019	0800	0915	0	0
09/10/2019				
10/10/2019	0800	1700	3	15
11/10/2019				
12/10/2019	1330	1700	0	3
13/10/2019	0800	1730	2	30
14/10/2019	0800	1700	3	16
15/10/2019	0800	1700	4	22
16/10/2019	0800	1700	6	6
17/10/2019	0800	1115	4	9
18/10/2019	0800	1700	3	11
19/10/2019	0800	1700	2	14
20/10/2019	0800	1800	7	19
21/10/2019	0800	1715	3	19
22/10/2019	0830	1700	6	12
23/10/2019	0800	1700	19	19
24/10/2019	0800	1700	2	8
25/10/2019	0900	1730	7	10
26/10/2019	0800	0830	0	4
27/10/2019	0800	1820	1	9
28/10/2019	0800	1700	1	4
29/10/2019	0800	1700	5	4
30/10/2019	0800	1700	2	1
31/10/2019	0800	1200	1	0
01/11/2019				
02/11/2019	0820	1110	1	0
03/11/2019	0745	1700	5	6
04/11/2019	0800	1600	3	0
05/11/2019				
06/11/2019	0800	1700	1	1
06/10/2021	0900	1500	6	4
07/10/2021	0900	1400	5	6
08/10/2021	0900	1500	3	19
09/10/2021	0900	1500	2	16
10/10/2021				
11/10/2021				
12/10/2021	0900	1500	3	11
13/10/2021	0900	1500	3	11
14/10/2021				
15/10/2021				
16/10/2021				
17/10/2021	0900	1500	2	13

18/10/2021	0900	1500	10	7
19/10/2021				
20/10/2021				
21/10/2021	0900	1500	2	2
22/10/2021	0900	1500	4	6
23/10/2021	0800	1115	2	1
24/10/2021				
25/10/2021	0900	1500	4	3
26/10/2021	0800	1500	0	9
27/10/2021	0900	1500	1	4

Table B.2. Summary of UAV survey effort of humpback whale groups in Jervis Bay in 2019 and 2021

UAV model	Date	Flight time start	Time of flight (min.sec)
Matrice 600 Pro	20/10/2019	1454	21.56
	20/10/2019	1720	16.52
	20/10/2019	1750	5.02
	27/10/2019	1100	4.54
	27/10/2019	1112	9.41
	27/10/2019	1418	5.23
	27/10/2019	1425	9.34
	27/10/2019	1810	15.23
Mavic 2 Enterprise Dual	31/10/2019	809	7.43
	31/10/2019	818	3.1
	31/10/2019	820	6.17
	31/10/2019	829	8.31
	3/11/2019	817	5.52
	3/11/2019	833	14.01
	3/11/2019	1107	1.5
	3/11/2019	1110	3.38
Mavic 2 Enterprise Advanced	23/10/2021	811	8.2
	23/10/2021	824	1.31
	23/10/2021	836	4.51
	23/10/2021	838	1.47
	23/10/2021	840	1.5
	23/10/2021	845	4.51
	23/10/2021	846	1.16
	23/10/2021	847	1.23
	23/10/2021	900	1.29
	23/10/2021	902	8.11
	23/10/2021	917	3.08

	23/10/2021	1208	3.27
	23/10/2021	1445	10.41
	28/10/2021	1004	2.13
	28/10/2021	1030	1.58
	28/10/2021	1033	3.46
	28/10/2021	1040	3.02
	28/10/2021	1045	0.15
	28/10/2021	1106	3.14
	28/10/2021	1111	9.34
	28/10/2021	1125	9.00

Table B.3. Summary of survey effort capturing Indo-Pacific bottlenose dolphins in Jervis Bay using thermal imagers in 2021

Date	Imager	Survey period	Duration of footage containing dolphins (min.sec)
18/02/2021	FLIR Boson	1103 - 1139	14.19
01/04/2021	FLIR Boson	950 - 1340	19.47
01/04/2021	FLIR Tau 2	950 - 1340	1.15
01/04/2021	FLIR x8400sc	950 - 1340	13.11